The Role of Biosphere-Atmosphere-Ocean Interactions in Regulating Precipitation Variability over West Africa

by

Luis Tomás Pérez-Prado
B.S., Civil Engineering (1997)
Universidad de Puerto Rico, Recinto Universitario de Mayagüez

Submitted to the Department of Civil and Environmental Engineering
in partial fulfillment of the requirements for the degree of

Master of Science in Civil and Environmental Engineering

at the

MASSACHUSETTS INSTITUTE OF TECHNOLOGY

September 2000

Author .....
Department of Civil and Environmental Engineering
August 11, 2000

Certified by .....
Elfatih A.B. Eltahir
Associate Professor of Civil and Environmental Engineering
Thesis Supervisor

Accepted by .....
Daniele Veneziano
Chairman, Department Committee on Graduate Students

The Role of Biosphere-Atmosphere-Ocean Interactions in Regulating Precipitation Variability over West Africa

by

Luis Tomás Pérez-Prado

Submitted to the Department of Civil and Environmental Engineering
on August 11, 2000, in partial fulfillment of the
requirements for the degree of
Master of Science in Civil and Environmental Engineering

Abstract

Vegetation cover greatly regulates the exchange of energy in its internal, latent and kinetic forms. There is a marked difference between the properties of land (with and without vegetation cover) and oceans that further alters the energy distribution. The circulation of the atmosphere is another essential component of the climate, since it both responds to the energy gradient and regulates it by transporting energy and moisture. Land cover changes and sea surface temperature variations over tropical regions have been the subject of extensive research in the last three decades due to their possible regional and global climate change impact. Eltahir and Gong (1996) provided a comprehensive physical mechanism that describes the dynamics of the West African monsoon in terms of variations of the biosphere and ocean components. Starting with the moist static energy horizontal gradient (a quantity related to the entropy gradient of the atmosphere), they described the zonal wind speed. The strength of the monsoon regulates precipitation variability over the region, which in turn affects the state of the regional vegetation. In addition, Eltahir (1997) states that the amount of energy in the boundary layer regulates the height of the level of free convection. Therefore, the energy in the boundary layer affects both large-scale and micro-scale phenomena regulating precipitation variability. The recent drought conditions together with human-induced deforestation and desertification provided a positive feedback to vegetation degradation and low precipitation rates. In this study we performed an analysis of the inter-annual and intranual variability of different climatic variables (e.g. moist static energy, wind, precipitation, sea surface temperature, radiation components and cloud cover) that confirms the proposed physical theory of biosphere-atmosphere-ocean interactions. It is observed that favorable conditions for high precipitation rates existed in the 1958-1967 period in the biosphere and ocean components. The conditions of the biosphere reversed during the 1968-97 period. The ocean conditions were not favorable for high precipitation rates in the 1974-1990 period. Although the ocean conditions became favorable for high precipitation rates during the last decade of the 20^{th} century, the biosphere conditions remained unfavorable. This is consis-

tent with the low precipitation rates observed. It should be pointed out that the monsoon circulation was also weaker during the 1968-97 period. Future research includes sensitivity experiments on deforestation, desertification and sea surface temperature variations using a state of the art regional climate model. Recent enhancements on the large-scale precipitation scheme, sub-grid spatial variability and the surface-vegetation-atmosphere transfer scheme will be included in these future studies.

Thesis Supervisor: Elfatih A.B. Eltahir
Title: Associate Professor of Civil and Environmental Engineering

Acknowledgments

"... a mighty problem looms before us and we can no longer disregard it. We must apply the equations of theoretical physics not to ideal gases only, but to the actual existing atmospheric conditions as they are revealed by modern observation. These equations contain the laws according to which subsequent atmospheric conditions develop from those that precede them. It is for us to discover a method of practically utilizing the knowledge contained in the equations."

Vihelm Bjerknes (1914)

First of all, I would like to thank the Supreme Creator (which has as many names as cultures) for giving me the opportunity to live and contribute to the life of this world. Secondly, I thank my advisor Elfatih A.B. Eltahir for his support and continuos intellectual challenges even when I couldn't see that he was motivating me to perform better all the time. I want to express my gratitude to my parents, Tomás and Carmen, for supporting me even when I didn't followed their advice. Special thanks to Prof. Ismael Pagan-Trinidad and Prof. Jorge Rivera-Santos for introducing me and guiding my first steps into the exciting world of hydrology. My first race was made possible thanks to Bill and Steve of the United States Army Corps of Engineers (USACE) at the Waterways Experiment Station (WES). I am in debt with my research group for making my life at Parsons Lab less torturous. Thanks to Jeremy Pal and Kirsten Findell for creating an inspiring computer environment. Thanks to Guiling Wang and Pat Yeh for sharing research papers, data and ideas. Thanks to Sonia for trying to keep me happy even when I was sad. Thanks to Michelle Irizarry for helping me to verified what I had learned by guiding her at times of difficulty. Without her, I would have not realized that I was worrying too much about things that prevented me from doing a good job in my research and enjoying life.

There are persons with whom ones shares good times and bad times through our life. Those who celebrate with you the good times and stand by you through the bad times are known as friends. They become part of your family like brothers and sisters. To all my

brothers and sisters through my life, I thank you all and I hope no more than to help you as much as you helped me. I need to start by recognizing the support of my real sisters and favorite psychologists, Esther Mariae and Zinia Mariae. The words of support from Jeremy Pal, Richard Camilli, Enrique Vivoni and Sam Arey arrived at a time I needed them the most. To my emotional confidants, Jessica Vargas, Michelle Irizarry and Clari Barreto, thanks for listening. To my friends in Puerto Rico, Vivian Mendez, Jose Negron, Martin Quinones, Maria Vicente and Madeline Colon, who I only see twice a year but that are with me all the time, thank you for defining remote friendship. To my other puertorrican friends in the US, Jorge & Delma, Juan Carlos & Luz, Efrain, Olga, Gianna and Carlos, thanks for setting a good example.

In any research project, organizations allow the realization of the objectives by providing funding, tools or valuable information. The following organizations made enormous contributions to our research proposal in one of those forms:

- GEM Partnership with Genetics Institute: GEM Fellowship
- National Science Foundation-Atmospheric Science Division: NSF Project 35171095
- Graduate Students Office (GSO): in particular Dean Isaac Colbert and Dean Roy Charles
- United Kingdom Meteorological Office (UKMO): Jim Arnott for providing GISST dataset
- National Oceanic and Atmospheric Administration (NOAA): Eugenia Kalnay for providing the latest NCEP/NCAR Reanalysis dataset; NOAA/PMEL TMAP for developing Ferret
- National Aeronautic and Space Administration (NASA): NASA Langley Research Center EOSDIS Distributed Active Archive Center

Last but not least, I am immensely grateful of uncle Luis and aunt Martha for receiving me at their home when I had no place to stay. Thanks to their children and my cousins, Tito, Ariel and Gabriel for letting me be like a big brother for them.

Contents

List of Figures

List of Tables

Chapter 1

Introduction

1.1 General Background

The Earth's surface is the lower boundary of the atmosphere. The exchange of heat and moisture at the air-surface interface immediately affects the lowest layer of the troposphere known as the boundary layer. The entire troposphere is sensible to these fluxes at longer time scales. We humans have the capacity of changing the surface properties in a global scale by altering the vegetation cover, soil, sea or ice sheet. We can also change Earth's atmosphere chemical composition, heat and moisture fluxes in many direct (e.g. air pollution) and indirect ways (e.g. deforestation). Rapid population growth and technological advances, particularly in the last century, have increased the alteration of Earth's environment to satisfy food and shelter needs. Anthropogenic changes and their possible effects on regional and global climate are subject of controversy and concern (Zheng and Eltahir 1997, Kiang and Eltahir 1999). Among the surface changes receiving attention, tropical deforestation and desertification of savanna regions are of particular significance. Due to the role of vegetation in the carbon, water and energy cycles, it is important to have a precise understanding of the interactions between the biosphere and the atmosphere. The fact that local climate greatly regulates vegetation distribution over a region tells us that the interactions of the system are coupled in nature. The understanding of these interactions is relevant to the issues of climate change, climate predictability and natural variability of the climate system. Data

analysis techniques and numerical models provide the basic tools to study these feedbacks.

Tropical climate is characterized by small seasonal temperature fluctuations, dry/wet seasons of different lengths, strong convective systems and monsoon winds. Another distinctive characteristic of tropical regions is the location of deserts at the border between the tropics and mid-latitude regions. West Africa is perhaps the best example of transition between rainforest ecosystems near the equator, semi-arid conditions in the mid-tropics and desert regions at the tropical boundary. This distribution of vegetation is sensitive to rainfall variability and human activities. One of the most debated questions in climate science is what effect land cover changes (e.g. deforestation and desertification) would have on regional and global climate. More specifically, are the biosphere-atmosphere interactions capable of initiating a drought and/or sustaining it? What mechanisms are involved? These and other questions make the study of climate over tropical regions an interesting and challenging subject.

1.2 Research Objectives

In this study, we aim to gain insight in the interactions of the biosphere-atmosphere-ocean in regulating the climate of a particular region. Our objective is to characterize the climate of the region of interest and the processes regulating its variability. The role of biosphere-atmosphere-ocean feedbacks in generating and/or sustaining drought conditions will be addressed. This study will focus on West Africa since it has undergone significant land cover changes according to various regional studies (FAO, 1981; Myers, 1980, 1994; Bertrand, 1983; Gornitz and NASA, 1985; UNEP, 1999), see figure 1-1. Furthermore, it has the potential of even larger environmental changes of natural (e.g. continuous drought) and anthropogenic origins (e.g. rapid population and urban growth and land use mismanagement).

The interactions of the biosphere-atmosphere-ocean system will be studied based on the theoretical framework presented by Eltahir and Gong (1996). They related the gradient of boundary layer energy between ocean and land to the strength of the monsoon. Since monsoon circulation provides a large-scale forcing to precipitation, rainfall variability should be related to the energy gradient in the boundary layer. Furthermore, vegetation degradation

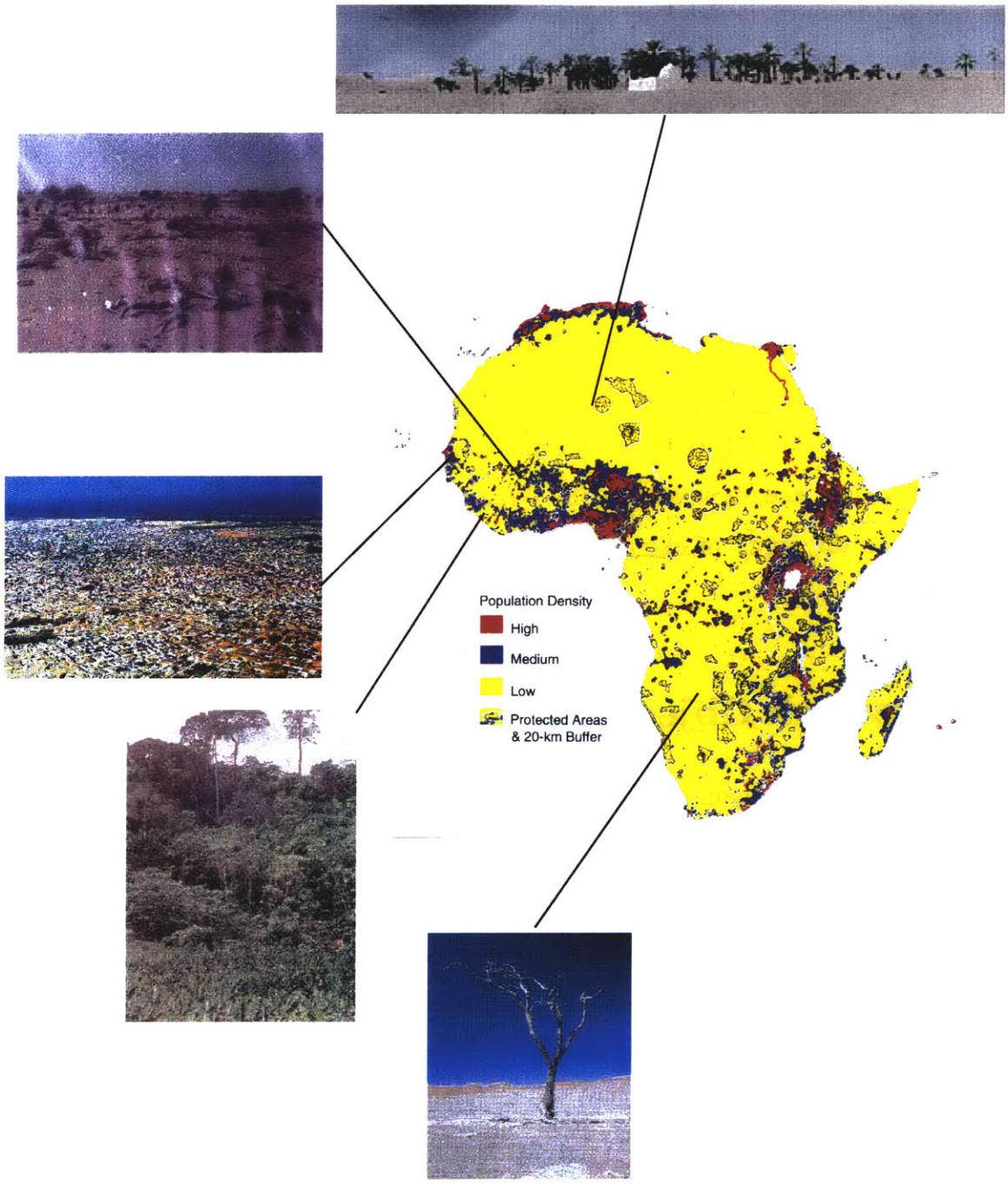

Figure 1-1: Population density superimposed over protected areas and a 20 km buffer perimeter. Legend for population density is red for high density (> 100 persons/km^2), blue for medium ($25 - 100$ persons/km^2) and yellow for low population density (< 25 persons/km^2). Protected areas are identified by black-line polygons with leaf symbol inside. Observe the high population density in West Africa along the coast (Senegal, Gambia, Liberia, Ivory Coast, Ghana, Togo, Benin and Nigeria) and inland at the Sahel (Mali, Burkina Faso, Niger and Nigeria). ©UNEP (1999)

would induce a decrease of Moist Static Energy (MSE) over land. On the other hand, increasing Sea Surface Temperatures (SST) would increase MSE over the ocean. Both of these processes would result in a flatter gradient of energy between ocean and land, which would reduce the strength of the monsoon circulation. The weakening of the monsoon winds would reduce large-scale precipitation. Eltahir (1997) related the amount of moist static energy in the boundary layer to the Level of Free Convection (LFC). An increase of MSE in the boundary layer results in a lower LFC and therefore stronger convection. A decrease in boundary layer moist static enery over land would reduce the frequency and magnitude of convective rainfall further degrading the vegetation over the region. These positive feedbacks could self-sustain drought conditions until a strong enough external forcing provokes an increase in the monsoon strength. If the external forcing, such as a cold SST anomaly, lasted long enough it is possible that the magnitude and frequency of convective events would increase to the point were vegetation is allowed to recover. These two factors would tend to increase the gradient of boundary layer energy, thus providing again a positive feedback. This mechanism could provide a physical explanation of the low frequency variability observed in rainfall over the region. The persistence of the biosphere-atmosphere-ocean system is of great significance for climate predictability. Therefore, it is of primary importance to understand the mechanisms regulating the variability of the regional climate system. The proposed mechanism is compared to observations of the last century in this research study.

1.3 Thesis Outline

Chapter Two presents a general background of the geographical characteristics of the region. It also provides a literature review of rainfall variability and monsoon dynamics. Land cover changes over West Africa are also reviewed in this chapter. Finally, the South Eastern Tropical Atlantic (SETA) region is defined in the last section of the chapter. An introduction of the relevance of this region to the dynamics of the West African monsoon is included. Chapter Three starts by revising the fundamental theoretical background on regional climate physics. A literature review of the land-atmosphere-ocean interactions and the interactions between large-scale motion and local convection is also provided in Chapter Three. The

dynamics of the biosphere-atmosphere-ocean interactions theory based on Eltahit and Gong (1996) is presented at the end of the chapter. Chapter Four provides a description of the datasets used to study the proposed regional climate mechanism. The climatology of the regional variables derived from several sources is discussed in Chapter Five. The data was obtain from the National Center for Environmental Prediction/National Center for Atmospheric Research Reanalysis dataset (NCEP/NCAR Reanalysis), United Kingdom Meteorological Office Global Sea Ice Sea Surface Temperature dataset (UKMO GISST), Prof. Mike Hulme's Global Land Precipitation dataset (HGLP), International Satellite Cloud Climatology Project (ISCCP), Global Precipitation Climatology Project (GPCP) and the Advanced Very High Resolution Radiometer/Normalized Difference Vegetation Index (AVHHR/NDVI) datasets. The regional climatology of West Africa is used as a case study for the biosphere-atmosphere-ocean interactions using the theoretical framework presented in Chapter Three. Chapter Six summarizes the findings of the study and presents future research directions.

Chapter 2

Geographical Information and General Background

2.1 Introduction

The region of interest for this study is West Africa, defined here as the area located between the latitudes of 5°N and 25°N and between the longitudes of 15°W and 15°E (figure 2.1). The total land area is roughly 7.4 million square kilometers. The land area covers the countries of Liberia, Ivory Coast, Ghana, Togo, Benin, Nigeria, Sierra Leon, Guinea, Guinea-Bissau, Senegal, Mali, Burkina-Faso and parts of Cameroon, Niger, Chad and Mauritania. The West Africa region has suffered an almost continuous drought in the last thirty years. The scarcity of water had a significant impact in the life and economy of the countries within the region. Unprecedented low-levels of Lake Chad and significant decline in the flows of Senegal River and Niger River provide record of the drought conditions. The population over West Africa has increased by ninety-five million during the last four decades (3% per year). The population increase exerts great stress on the environment over West Africa and further exacerbates the scarcity of water over the region. Thus, it is imperative to understand the causes of the drought and the persistence mechanisms of the current conditions. The scientific community has studied the precipitation decline over West Africa for more than twenty years. The onset of the current drought has been attributed to natural and/or anthropogenic

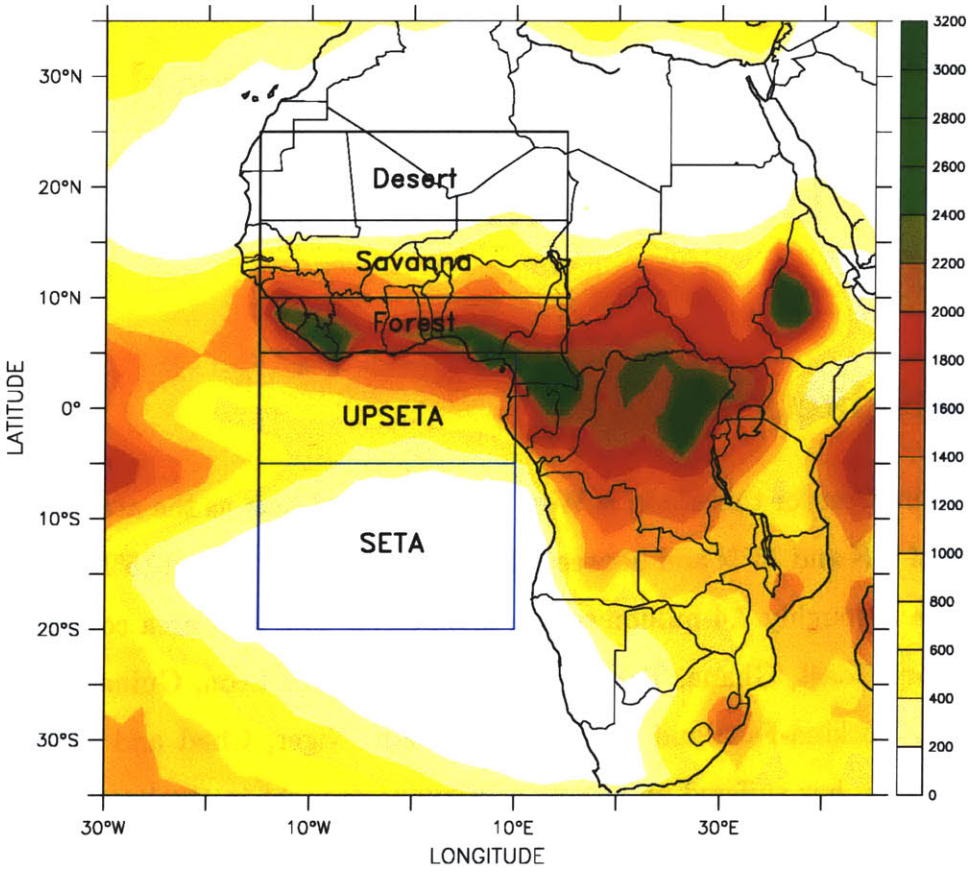

Figure 2-1: Region of study and ecosystem subregions. Climatology of rainfall over the West African region. NCEP/NCAR Reanalysis simulated precipitation (1958-97) [$mm/year$]

causes by different studies. In this study, we will perform theoretical and empirical analysis of the regional climate to gain insight of the factors and mechanisms that triggered and maintained the drought conditions. In the following sections, a literature review of rainfall variability, monsoon circulation, land-cover changes and sea surface temperature fluctuations is presented.

2.2 Rainfall Variability over West Africa

The annual rainfall distribution over West Africa shows a strong meridional gradient ranging from 1500 mm near the coast to 200 mm in the Sahel-Sahara. A slight zonal gradient in the western coast makes the contours parallel to the coast. The rainy season over land also has a meridional gradient lasting 5 months near the coast to one month near the desert border. The peak of the rainy season occurs in the months of June-July in the coastal regions and during August-September over the Sahel. This coincides with the arrival of the West African Monsoon, suggesting a correlation between the atmospheric dynamics and precipitation over the region. The rainy season associated with the monsoon is also characterized by the formation of the African Easterly Jet (AEJ) and the Tropical Easterly Jet (TEJ) in the lower and middle troposphere. The AEJ is centered at 16.5°N and 650-700hPa, while the TEJ is centered at 12.5°N and 200-300hPa during summer. The role of the AEJ over rainfall variability is less understood than the monsoon forcing. Nicholson (1993) found that the August-September rainfall contributes between 20 and 40% of the annual total near the coast and 45-60% inland. The correlation between the August-September rainfall and annual total is in the range of 0.63-0.93 according to the same study. This suggests that most of the interannual variability can be attributed to anomalies during this period. Nevertheless, Nicholson and Entekhabi (1986) showed that the rainfall fluctuations in the Sahel are dominated by low-frequency variability with periods generally longer than 7 years.

The lack of rainfall over the Sahel region has been pointed out by numerous studies (see review in Wang and Eltahir 1999a). During the last thirty years, the region has experienced the most severe drought of the twentieth century. The coastal region has experienced a

similar decline in rainfall, although not as severe as the savanna region. Despite the differences in time and spatial coverage of various studies, there seems to be good agreement between the spatial coherency of the rainfall anomalies over West Africa. Several studies (Rowell et al. 1995; Nicholson and Palao 1993; Janicot 1992; Nicholson 1989) have shown a negative correlation between the savanna and forest regions, particularly during transitions between wet/dry conditions for the annual, June-July and August September rainfall. Still, the main mode of rainfall anomaly is spatially coherent for both regions (Lamb 1978; Folland et al. 1986; Janicot 1992). The spatially coherent mode has dominated the recent drought, particularly the annual and June-July rainfall. Over the late part of the rainy season (August-September), the second spatial mode characterized by contrasting conditions between the coastal forest and inland savanna regions dominates the rainfall variability. In general, both spatial modes are homogenous in the zonal direction, as recognized widely in literature.

Although the statistical characteristics of the rainfall variability over West Africa have been extensively studied and described within the uncertainties of the different data collection methods, the mechanisms producing these patterns are still the subject of debate and active research. There is discrepancy in the role of the EL Niño-Southern Oscillation (ENSO), Sea Surface Temperature (SST) anomalies in the South Eastern Tropical Atlantic (SETA) region, displacement of the Inter-Tropical Convergence Zone (ITCZ), land and vegetation feedbacks, and monsoon circulation over rainfall variability in West Africa. Theories on the relationship of these factors with rainfall variability found in literature are presented in Chapter 3. The role of these and other factors is discussed in more detail in the next chapters.

2.3 West African Monsoon

The West African Monsoon provides a large scale forcing to precipitation over the region. The word monsoon is derived from the Arabic word for season, "mawsim". A monsoon is generally described as a seasonal shift in wind direction that is responsible for summer rainfall and winter dryness over the continent mass. In the classical literature (e.g. Wallace and Hobs 1977), the onset of the monsoon is related to the seasonal land-ocean temperature

difference. During spring, the relatively cool air over the ocean in contrast to the warmer air over land generates a pressure gradient that allows humid air from the oceans to flow inland with the southwesterly low-level winds from the South Eastern Tropical Atlantic (SETA) region. Over land, the air parcels are heated and then rised by convection, increasing the relative humidity of the higher levels of the troposphere. Condensation is then promoted by adiabatic cooling of the rising parcels. This leads to the formation of clouds and subsequent precipitation. As precipitation falls, latent heat is released which promotes the continuation of the rise of air parcels resulting in heavier rainfall. At the top of the clouds, the air parcels return towards the ocean descending over the cooler sea surface. The pressure gradient is reversed during autumn, which allows flow from land towards the ocean. Therefore, the wind direction over land is northeasterly, giving rise to the notion of direction reversal of winds associated to monsoon circulations. The lack of a sufficiently large moisture source over land together with the reversed heating gradient makes the winter a cool-dry season.

Eltahir and Gong (1996) provided a compatible explanation of the dynamics of the monsoon in terms of energy considerations. Boundary layer entropy is used as a measure of energy in the near-surface atmosphere. Entropy is related to moist static energy, a function of temperature and humidity as defined in equation (3.5). During summer, differential heating of land and ocean due to increased solar radiation absorption over land relative to the ocean increases moist static energy over land. The gradient of moist static energy induces a circulation from the ocean towards land. The rotation of the earth deflects the southerly direction of the winds to a southwesterly movement. The low-level flow brings moisture from the ocean further increasing moist static energy over land (figure 2-2). The convergence of this highly energetic moist flow produce a region of strong convection and intense rainfall. As generally described, the release of latent energy by precipitation and the increased sensible and latent energy fluxes from the land surface enhances the rainfall intensity. The tendency towards a radiative-convective quasi-equilibrium results in a uniform distribution of saturation moist static energy in the convective-convergence zone. Dynamically this implies that the troposphere is heated from the boundary layer flow, resulting in negative relative vorticity near the tropopause. A negative relative vorticity with high magnitude is capable of canceling the planetary vorticity (coriolis parameter), resulting in

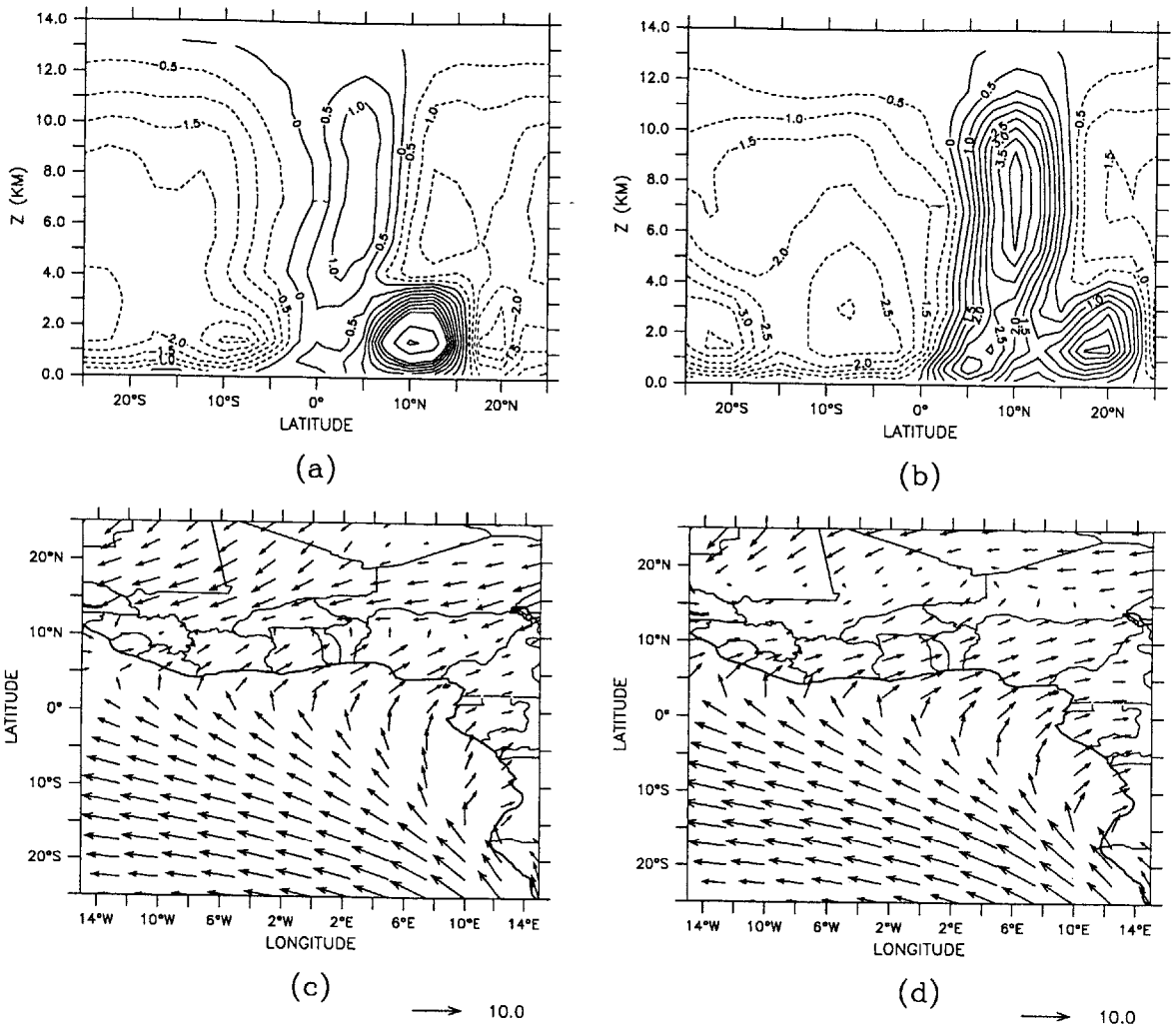

Figure 2-2: West African Monsoon:(a) winter and (b) summer climatology of the vertical velocity field $[mm/s]$; (c) winter and (d) summer low-level winds over the region $[m/s]$. Wind data obtained from NCEP/NCAR Reanalysis for the 1958-97 period.

a near zero absolute vorticity. When such conditions are satisfied, the monsoon circulation is enhanced providing a positive feedback for rainfall. During winter, the land loses energy more rapidly than the ocean; thus, the energy gradient is reversed. In addition, ocean mixed layer circulations warms the sea surface near the coast further altering the energy gradient. Therefore, a reversed circulation is induced, resulting in a flow from land towards the ocean. The northeasterly flow and the location of the convergence zone near the equator inhibit precipitation over the mid-tropics resulting in a dry climate. Figure 2-2 presents the vertical structure of the monsoon circulation and the climatology of the low-level winds derived from the NCEP/NCAR Reanalysis. As presented in the introduction, vegetation affects the exchange of both heat and moisture between the land surface and the atmosphere. Changes in vegetation cover and density could have a significant impact over the climate of a region when their effects are integrated over various time scales. Therefore, it is important to quantify the magnitude of the vegetation changes before reaching any conclusions on the possible effects on the climate of the region. In the next section, we do a literature review on land cover changes over West Africa.

2.4 Land Cover Changes in West Africa

As previously mentioned in the introduction, West Africa has an annual population growth rate of 3%, one of the highest for any region in the world. The International Conference on Population and Development (Cairo, September 1994) stated in their Plan of Action that "population is the largest threat to the world environment" (from UNEP 1999). This point of view about population impact over the environment represents an extreme view. Nevertheless, the needs for food and shelter have altered the Earth's surface since prehistoric times. Technological advances in pursuit of economic progress have enhanced the environmental impact of humans in the last two centuries.

In the 20^{th} century, West Africa has experienced intense land cover changes ranging from desertification at the northern border to deforestation at the coastal border. The definition of desertification has changed over the last twenty years from a completely anthropogenic process to one that is driven by both natural and human factors (Nicholson 1998). The cur-

rent definition states that desertification is the degradation of vegetation and land over arid, semi-arid and dry sub-humid areas under the combined influence of climate variations (e.g. droughts) and human activities (e.g. livestock grazing, primitive agricultural techniques). On the other hand, the definition of deforestation states that it is the clearing of the natural vegetation for agriculture, grazing and/or logging. Deforestation has always been considered an anthropogenic change, in part due to the strong resilience of forest ecosystems. It was generally believed that climatic fluctuations over equatorial forest regions are not strong enough to alter such ecosystem and that any further climate change was induced by the clearing of vegetation. Nevertheless, no scientific evidence of the mechanism initiating and/or sustaining the observed climate change has been produced. Furthermore, there is disagreement in the magnitude of the land cover changes themselves. In addition, scientists do not agree in attributing the observed climate differences to natural climate variations or anthropogenic changes.

Therefore, one of the priorities in addressing the effect of land cover changes on climate must be to determine the extent of these changes. The most comprehensive study on land cover changes over West Africa was performed by V. Gornitz of NASA in 1985. Land cover change estimates range between 0.88×10^6 km^2 from a derived land use map ($\Delta t = 1880-1980$), 1.149×10^6 km^2 from population statistics ($\Delta t = 1910-1980$), and 1.228×10^6 km^2 from forestry data ($\Delta t = 1920 - 1980$). Although the percentage of agricultural population is decreasing, the increase in total population overcomes this decrease resulting in larger agricultural population totals, if the averaged area cultivated per farmer remains constant. The differences in the estimates are principally due to different assumptions to derive the data of the earliest years. The report gives the mean of the three estimates, $(1.086 \pm 0.18) \times 10^6$ km^2, as a reasonable figure of the total land cover change (deforestation and desertification) for the whole period.

According to their study, the tropical forest that remains in West Africa is mostly mature secondary forest. Secondary forest is a new vegetation cover over a once cleared area that was later abandoned. In general, moist tropical forest has been replaced by a combination of tree crops, field crops and secondary regrow. Gornitz (1985) estimated that 468,000 squared kilometers of primary forest had been cleared based on forestry data over the last 60-80

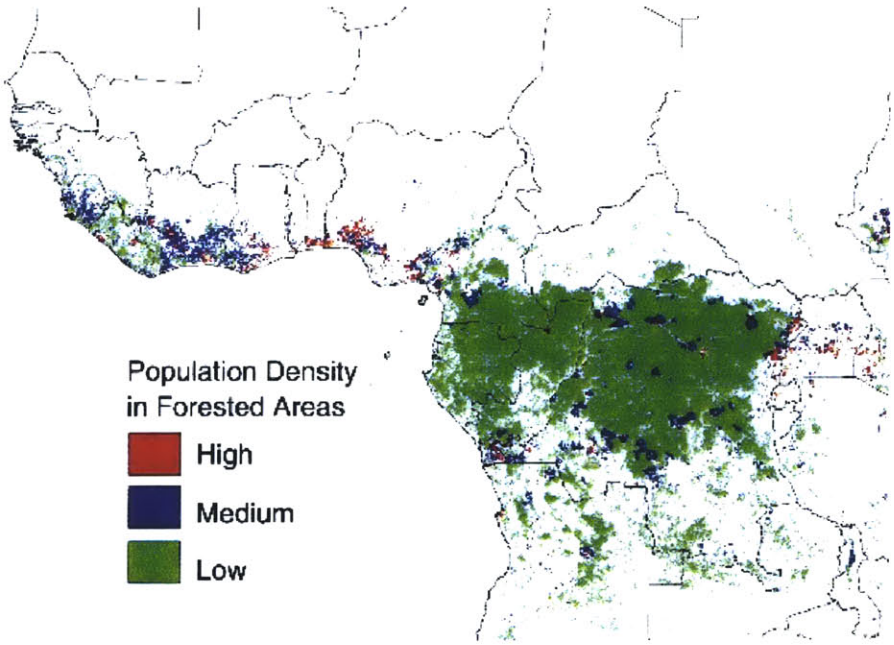

Figure 2-3: Population density over forest regions. Legend for population density is red for high density (> 100 persons/km^2), blue for medium ($25 - 100$ persons/km^2) and yellow for low population density (< 25 persons/km^2). Observe the high population density in West Africa along the coast (Senegal, Gambia, Liberia, Ivory Coast, Ghana, Togo, Benin and Nigeria). ©UNEP (1999)

years. Zheng and Eltahir (1997) estimated the territorial domain of rain forests over West Africa at the beginning of the 20^{th} century to be around 500,000 km^2 using the data reported by Gornitz (1985), Myers (1991) and Aldhous (1993). Based on the rates of deforestation presented in several studies, less than ten percent of the primary rain forest was left by the mid-nineties (Zheng and Eltahir 1997). The population stress over forested areas remained high during the 1980-90 period as illustrated in figure 2-3 from the United Nations Environment Programme (UNEP). The forest regions of Ivory Coast and Nigeria have the highest population densities over the forested areas. There are regions in Sierra Leone and Liberia with medium and high population density as well. It should be noted that over Senegal, less than four squared kilometers show forest regions under population stress. There were approximately 250 km^2 of forest land back in 1985 according to Gornitz (1985). UNEP (1999) reports savanna and grassland as the dominant vegetation cover for Senegal in 1990. This is consistent with a continuous forest clearing over Senegal as stated by Gornitz (1985). There is a marked contrast between the population stress over the forest regions of East Africa and West Africa as can be appreciated in the figure. It coincides with different rainfall anomaly patterns, suggesting that land cover changes may have played a significant role in the decline of rainfall over West Africa. This consistency is further discussed in chapter five.

The role of desertification in the northern border of the Sahel over rainfall variability has been studied in more detail than the role of tropical deforestation (Zheng and Eltahir 1997). This could be due to several reasons including the marked rainfall decline over the Sahel, the total population in semi-arid regions and the ratio of total land cover changed by desertification compared to the deforested area. For the whole continent, approximately 82% of the population currently live in savanna-type regions (UNEP 1999). This ratio should be higher for West Africa based on figure 1-1 and the actual vegetation distribution over the region. The amount of woodland and savanna cleared up to 1980 was estimated to be 760,000 squared kilometers (Gornitz and NASA 1985). Tucker and Nicholson (1999) used a Normalized Difference Vegetation Index (NDVI) derived from several satellite platforms combined with annual precipitation rates based on ground-station data to monitor the movement of the Sahara-Sahel border for the 1980-1997 period. The area considered in the study lies between 16° W and 39° E, and 10° N and 25° N. The combined index used showed a systematic

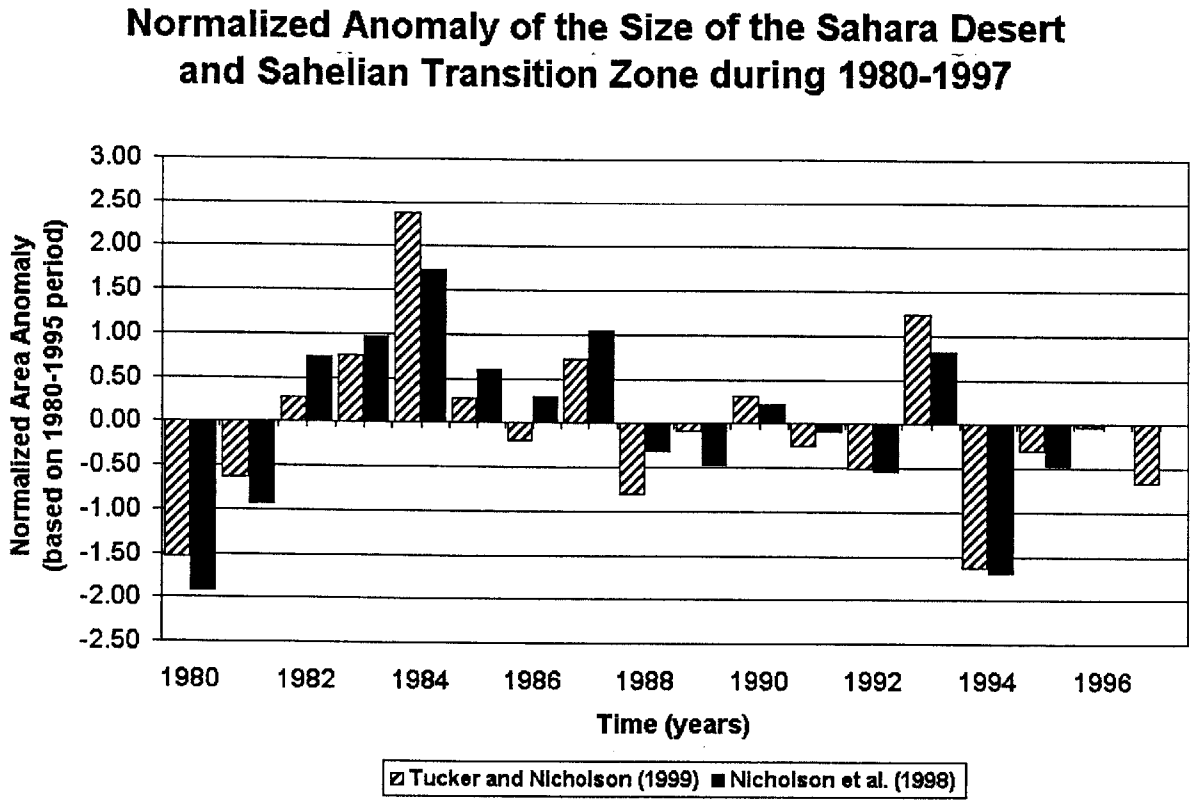

Figure 2-4: Sahara-Sahel transition zone size variations during the last two decades based on Nicholson et al., (1998) and Nicholson (1999). The normalized anomalies where computed using the mean and standard deviation for the 1980-1995 common period.

increase of the Sahara desert and transition zone area from 1980-1984 (one of the driest years in record). After 1984, no systematic increase or decrease in the size of the Sahara Desert was evident according to the authors. Nevertheless, they report significant year-to-year variations (in the order of 85,000-992,000 squared kilometers). These results are not surprising because of the limitations of the method used. First, the correlation between annual precipitation and July-October NDVI is very low for rainfall rates lower than 150 mm/yr. due to limited green vegetation in such regions. This forced the use of the 200-mm/yr. as a proxy for the desert border. Second, the authors recognized that the 200-mm/yr. isoline represents the border of the proper Sahel and the Sahara-Sahelian transition zone rather than the desert border. Therefore, it was expected that the "desert border" defined in their study followed rainfall fluctuations since NDVI in semi-arid regions dominated by bushland/ticket and grassland responds immediately to rainfall (Nicholson et al. 1990). As Nicholson et al. (1998) pointed out in a similar study, desertification in the Sahel has mistakenly been associated with an irreversible degradation of vegetation resulting in a southward expansion of the desert area. From the results of both studies, it can be concluded that the transition zone border is indeed dynamic. The fluctuations of the "desert area" as defined in each study are summarized in figure 2-4. The normalized anomalies where computed using the mean and standard deviation for the 1980-1995 common period. These two studies, as most reports, are compromised in that the period considered have coincided with droughts and long-term decline in rainfall. In addition, anthropogenic changes due to agricultural needs can result in the replacement of indigenous species for plants with higher tolerance to dry conditions. This makes virtually impossible to separate the impact of drought from that of anthropogenic desertification and suggest that both processes could work together (Nicholson et al. 1998). Therefore, when referring to desertification, we consider vegetation degradation in semi-arid regions due to both natural and anthropogenic causes, unless otherwise specified.

2.5 Southeastern Tropical Atlantic (SETA) Region

To the south of West Africa lies the Southeastern Tropical Atlantic (SETA) region. In this study, the SETA region is defined as the area between 5°N and 25°S and 15°W to 10°E as

illustrated in figure 2.1. The Inter-Tropical Convergence Zone (ITCZ) moves between the SETA region and West Africa responding indirectly to the seasonal solar forcing. The wind circulation associated this motion within the studied region is the West African Monsoon (WAM). The West African Monsoon (WAM) is driven by the contrast in conditions between land and ocean as described in section 2.3. The ITCZ and the WAM are defined as thermally driven tropical circulations. These thermally driven circulations are responsible for the low frequency variability of climate, e.g. variations in the seasonal, annual, decade and longer time scales. It is necessary to stress the point that when refering to thermally driven circulations, we depart from the classic definition of heat driven circulations. The term thermally driven is used in the context of equivalent potential temperature (θ_e) gradient. Equivalent potential temperature is related to moist static energy (mse) by the approximate relation $[c_p T d(\ln \theta_e) \approx d(mse)]$. The reader is refer to Holton (1992) and Emanuel (1994) for in-depth discussions of the dynamics of tropical circulations.

During summer months the southwesterly low-level winds bring moist warm air from the SETA region inland. The convergence zone is characterized by heavy rainfall. During winter, the ITCZ is located over the ocean. The seasonal movement of the convergence zone serves as a regulating factor of the rainfall over West Africa. The supply of moisture to West Africa from different regions, including a sector the SETA region, was studied by Gong (1996). She used a modified version of the recycling ratio model based on mass balance that was developed by Eltahir and Bras (1994). Evaporation from the Tropical Atlantic Ocean (between 5°S and 5°N) contributed twenty-three percent of the rainfall over West Africa for the 1992-94 period. The contribution of moisture from the ocean was found higher during the peak of the monsoon (July-August). Nevertheless, the recycling ratio for the moisture advected from the ocean remained the same and sometimes even decreased slightly due to the increase of local evaporation during the monsoon season. The availability of moisture from an ocean surface is strongly regulated by the sea surface temperature as expected from the Clausius-Clapeyron relationship. These characteristics of the SETA region suggest an important role of SST over SETA in the dynamics of the monsoon. Some of the proposed interactions are reviewed in the following chapter.

Chapter 3

Theory of Biosphere-Atmosphere-Ocean Interactions

This chapter provides a literature review of the most important concepts in the biosphere-atmosphere-ocean interaction theory. First, we describe the hydrologic cycle and the energy conservation law. Then, we proceed to review the atmosphere-ocean interactions and the biosphere-atmosphere interactions in a separate discussion as traditionally considered. The biosphere-atmosphere-ocean interactions theory presented by Eltahir and Gong is reviewed in section 3.2.2. The significance of this theory is further discussed in section 3.3, where a review of the current theories of the interactions between large scale motion and convection is presented.

3.1 Fundamental Theoretical Concepts

In any research work, there are certain fundamental concepts upon which we base our assumptions and frame our scientific inquiries. The following sections present the basic definitions used in formulating our research objectives. We start by describing the hydrologic cycle, the foundation of any hydrology thesis. The coupling of the hydrologic and energy

cycles is the core of the biosphere-atmosphere-ocean interactions theory. This coupling is still not completely understood, although the fundamental concepts are straightforward. We will look into the details of the coupled water-energy balance in the following chapters paying special attention to the role of the biosphere and ocean dynamics in modulating the regional climate system.

As previously mentioned, the coupled dynamics of the biosphere-atmosphere-ocean system is of primary interest in this scientific study. We emphasize the importance of a physical mechanism when describing the interactions of the climate system. The Sun provides the initial energy input to the Earth system. Due to the spherical shape of the Earth, the rotation over its own axis, the declination of this axis and the asymmetry of the orbit around the Sun, this input of energy is uneven in time and space and predisposes a gradient of energy in the atmosphere. The exchange of energy in its internal, latent and kinetic forms at the surface of the Earth directly affects the boundary layer of the atmosphere and can affect the entire troposphere at longer times scales. Vegetation cover greatly regulates the exchange of heat, moisture and momentum between the surface and the atmosphere. The difference between the properties of ocean and land (with and without vegetation cover) further alter the energy distribution. The loop is closed by the circulation of the atmosphere, since it both responds to the energy gradient and regulates it by transporting energy and moisture. It is of critical importance to understand the interactions between these different climate components in order to address the issues of natural and anthropogenic climate change and climate predictability.

3.1.1 Hydrologic Cycle

Water is continually moving between the oceans, the atmosphere, the cryosphere, and land. Hydrology has been defined as the science of the hydrologic cycle (figure 3-1). The hydrologic cycle describes the flux of water among the reservoirs of the ocean, atmosphere and land (including the reservoirs of soil moisture, vegetation canopy and surface waters). The complete water cycle is global in nature. The total amount of water on Earth remains essentially constant on the time scale of millennia. The amount of water moved annually through

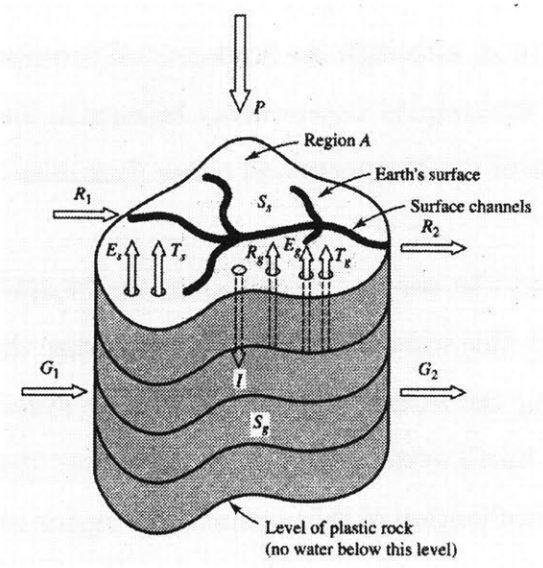

Figure 3-1: Regional hydrologic cycle representation as traditionally described. From Introduction to Hydrology by W. Viessman and G. Lewis ©HarperCollins College Publishers (1996)

the hydrologic cycle is roughly equivalent to 1-m depth of liquid water spread uniformly over the surface of the Earth. The equivalent liquid-water depth of the total water vapor in the atmosphere would be 2.5 cm. This suggests that the residence time of a water molecule in the atmosphere should be in the order of 8-9 days (Hartmann 1994). Since there is an equivalent 3-km depth of water near the surface in the ocean, cryosphere and land reservoirs, an average water molecule has to actually wait a very long time between brief excursions to the atmosphere. Therefore, changes in the land or ocean reservoir properties can seriously affect the supply of water vapor to the atmosphere.

In regional hydrologic studies, there has been a traditional frontier between meteorology and surface hydrology. The conceptual control volumes of both disciplines had a clear separation boundary that allowed progress in both fronts but preclude us from understanding Earth's hydrologic system as a whole. The land, biosphere, atmosphere and ocean systems are coupled in a wide range of space and time scales. This has promoted research in the planetary boundary layer from both the meteorology and surface hydrology communities. Recent efforts have pursued the study of a regional control volume that includes both the

atmosphere and land surface (figure 3-2). These efforts study the effects of vegetation in the exchange of heat and moisture between the land surface and the atmosphere. As widely recognized, vegetation affects the partitioning of precipitation into evapotranspiration, runoff and drainage. Furthermore, water changes between its liquid, solid and gas phase while it moves through the hydrologic system. Evapotranspiration requires a change from the liquid phase to the vapor phase, resulting in latent energy flux. This flux of energy couples the water cycle and the energy cycle through the principle of energy conservation. Finally, the vegetation canopy further alters the energy flux by regulating the momentum exchange at the boundary layer.

3.1.2 Energy Balance

This section presents the principle of energy balance following the discussion in Wallace and Hobbs (1977) and Hartman (1994). For any system in thermal equilibrium, the sources and sinks of heat must balance following the First Law of Thermodynamics. For an atmosphere near hydrostatic balance, the diabatic heating or cooling of an air parcel is related to the enthalpy and geopotential of the parcel by:

$$\frac{dq}{dt} = \frac{d(c_p T + \Phi)}{dt} \tag{3.1}$$

Where $\frac{dq}{dt}$ is the diabatic-heating rate in W/kg, c_p is the specific heat of air at constant pressure, T is air temperature and Φ is geopotential. The diabatic-heating rate accounts for the combined effect of net radiative heating rate (N_r), exchange of heat with the surroundings by conduction and convection (S_h), and the release of latent heat of condensation of water vapor (L_{hr}). This can be expressed in the following mathematical statement:

$$\frac{dq}{dt} = N_r + S_h + L_{hr} \tag{3.2}$$

The latent heat release of condensation of water vapor is the result of changes between vapor and liquid (or solid) phases. The rate of change of the mixing ratio of a parcel ($\frac{dw}{dt}$) can be divided into a component due to phase changes, $\left(\frac{dw}{dt}\right)_p$, and a component due to

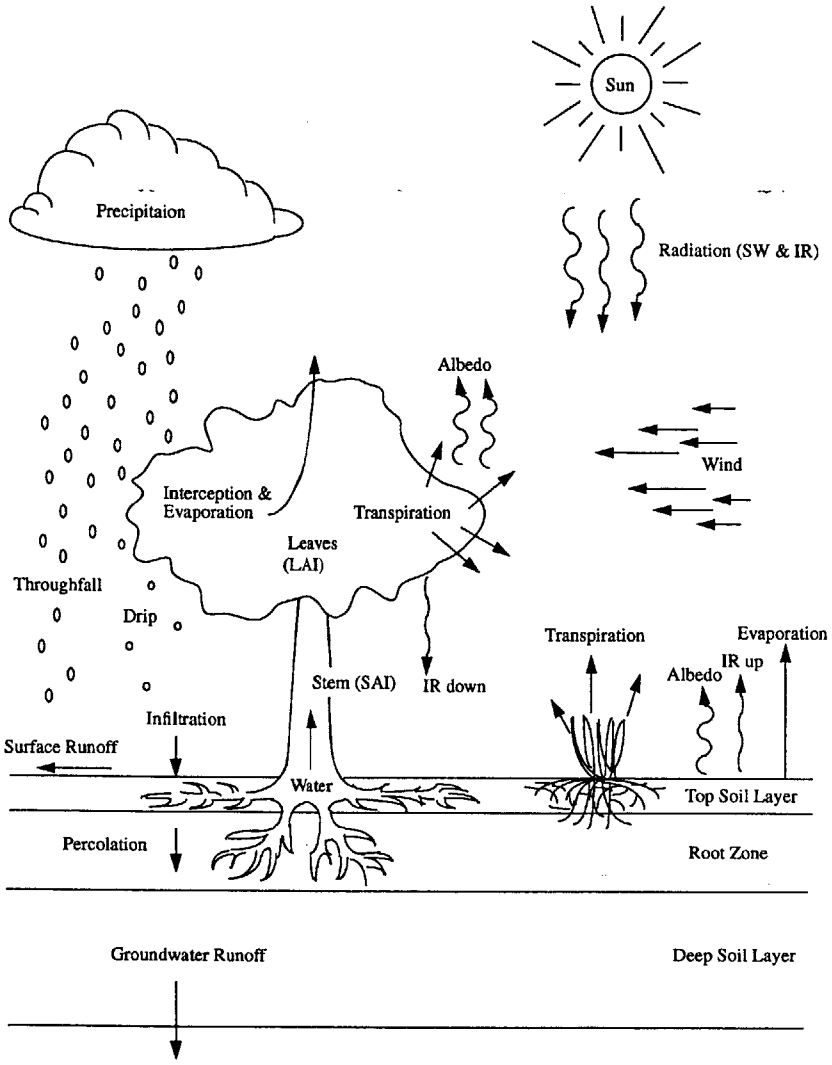

Figure 3-2: Biosphere-atmosphere interactions in the heat and hydrologic cycles, based on Dickinson et al., (1992). ©American Geophysical Union

exchanges of water vapor molecules with the surroundings by conduction and convection, $\left(\frac{dw}{dt}\right)_e$. Therefore, the latent heat release of condensation of water vapor is the remainder of the latent heat release due to absolute changes in the mixing ratio of the parcel and changes due to convection and conduction processes. This is a process in which heat is lost, therefore we use a negative sign for the absolute mixing ratio change. This can be express mathematically as:

$$L_{hr} = -L\left(\frac{dw}{dt}\right)_p = -L\left(\frac{dw}{dt}\right) + L\left(\frac{dw}{dt}\right)_e \tag{3.3}$$

Here, L is the latent heat of vaporization assumed to be constant with respect to temperature. It is convenient to express $L\left(\frac{dw}{dt}\right)_e$, the latent heat exchange with the environment as L_h. Therefore, combining equations 3.1, 3.2 and 3.3 and re-arranging we obtain:

$$\frac{d(MSE)}{dt} = N_r + S_h + L_h \tag{3.4}$$

where,

$$MSE = c_pT + \Phi + Lw \tag{3.5}$$

The left-hand side of equation 3.4 is the rate of change of moist static energy (MSE). Moist static energy is defined in equation 3.5 as the sum of the enthalpy (c_pT), geopotential (Φ) and latent heat content (Lw) of the parcel. The right-hand side of equation 3.4 represents the heat fluxes due to net radiation (N_r), sensible heat exchange by conduction and convection (S_h), and latent heat exchange with the environment (L_h). For systems in equilibrium (e.g. the atmosphere as a whole), the long term mean heat fluxes would be equal to zero. Therefore, we would expect that the globally averaged and annually averaged moist static energy would be constant. Nevertheless, the fact that net radiation is a function of solar radiation tells us that we are not dealing with a closed system. Furthermore, the conservation equations as depicted in equation 3.4 refers to the energy following the parcel motion. If the local rate of change of the state variable is desired it is necessary to modified such equation to account for advection (horizontal motion), convection (vertical motion) and other higher order terms. This is the main difference between the Lagrangian and Eulerian

control volumes framework. Since we are interested in regional (local) climate processes, our frame of reference will be of the Eulerian type. As mentioned at the beginning of this chapter, the geometric characteristics of the Earth and its motion in space predisposes an uneven distribution of energy in the atmosphere. Global observations have actually shown that, in general, there is more energy at the tropics than at the poles. In fact, this meridional gradient of energy feeds the large-scale circulation (e.g. Hadley Cell) that moves heat poleward up to the subtropics. Due to the difference in heat storage of seawater and ground, there are also differences in moist static energy between ocean and land. This ocean-land gradient drives thermally-direct circulations like the monsoon (Eltahir and Gong 1996). The West African Monsoon is therefore very sensitive to the meridional distribution of energy due to the geographic location of the ocean and land mass (Zheng and Eltahir 1997). As shown in figure 3-2, vegetation affect the exchange of sensible and latent forms of heat and the absorbed and reflected radiation. Therefore, the state of the biosphere can play a significant role in the determining the strength of the monsoon.

3.2 Climate Processes

Research on rainfall variability over West Africa has traditionally followed two main hypotheses with regard to the role of biosphere-atmosphere-ocean interactions. One group focuses in understanding the response of the atmosphere to local land forcing (mainly processes involving changes in vegetation, soil moisture, surface albedo and evaporation). Another group investigates the teleconnections with remote oceanic forcing (primarily sea surface temperature anomalies in the Atlantic, Indian and/or Pacific oceans). In the following sections, a review of both groups of studies is presented.

3.2.1 Ocean-Atmosphere Interactions

As Nicholson (1989) explains in her review of the casual theories for the Sahel drought at that time, scientists believed that the correspondence between the dominant time scales of rainfall variability and those of other tropical parameters such as regional and global SST's suggested

possible forcing mechanisms of rainfall variability. This is a common assumption in the scientific community, especially in fluid dynamics, since the detection of persistent oscillations within a series is considered particularly valuable because such regular variations could be associated with a physical phenomenon like the monsoon. Whereas a random process like turbulence will occur with no persistence or regular structure (Stull 1999). We agree in principle with this assumption, provided the verified existence of a physical mechanism, in particular for large-scale phenomena. It is important to underscore this last point, since by no means a statistical correlation by itself provides a physical description of a large-scale mechanism. On the other hand, it can be argued that it is good science to study in more detail a high correlation phenomenon to try to determine if the correlation is the result of coincidence or a physical phenomenon. In many studies, high or low correlation has been reported without establishing the forcing mechanisms. In the last decade, attempts to provide physical explanation of the observed relations have emerged with different degrees of success. This section will provide a general review of the development of the atmosphere-ocean interaction theory.

Lamb (1978a,b) presented a case study of sub-Saharan rainfall deficit (surplus) associated to warm (cold) SST anomalies during summer. In that case study, no evidence was found that the summer SST anomaly originates in spring. Lamb (1978b) found that several surface atmospheric-oceanic features in spring followed by opposite patterns in summer are associated a composite of dry years. This was later confirmed by other studies from Hastenrath (1984), Lough (1986) and Lamb and Peppler (1992) using individual years. Lamb and Peppler (1992) argue that atmospheric circulation displacements in the meridional direction need not be large due to the strong negative meridional gradient of rainfall over West Africa. Nevertheless, they found several years in which they could not trace the anomalies back to the previous season. They also reported that the SST anomaly lags surface pressure anomaly suggesting that the large-scale atmospheric forcing to SST is stronger than the opposite. This will be reviewed later in the context of air-sea interaction theory developed by Emanuel (1994).

Another subset of ocean-atmosphere studies considers the role of global SST distributions including El Niño-Southern Oscillation (ENSO) events over rainfall variability in West Africa

(e.g. Glantz et al. 1991, Semazzi et al. 1988). These studies try to explain why certain years with wet-like anomalies in the tropical Atlantic resulted in dry conditions instead (Lamb and Peppler 1992). Most of these statistical studies focused in the correlation between summer rainfall and summer SST (either globally or regionally), but fail to provide a physical mechanism of the observed relation. The main argument is that during ENSO years the west-east Walker circulation-type is enhanced providing a negative feedback to convection (Plumb 1998). General circulation models (GCMs) have been used to address the issue of global SST anomalies correlation with summer rainfall variability across the Sahel (e.g. Folland et al. 1986 and Rowell et al. 1992 and 1995). This last study was able to simulate the observed summer rainfall anomalies and show that SSTs anomalies where responsible for most of the precipitation variations. Caution must be taken when accepting this conclusion though, since the complexities inherent in a GCM do not allow to separate detail mechanisms relating SST and rainfall across tropical North Africa.

The role of spring SST over the SETA region in West African rainfall variability was studied by Zheng et al. 1999. They found that when a pattern of positive SST anomalies is superimposed in spring, there is a noticeable reduction in rainfall over land during spring. After the SST anomaly vanishes, enhanced rainfall occurs in the following summer and early autumn. They observed that the positive spring SST anomaly results in a positive moisture anomaly over the ocean that is advected inland by the large-scale circulation. The advected moisture over land increases greenhouse trapping of heat, raising air temperatures over land and therefore restoring the strength of the monsoon flow. At the same time the SST anomaly vanishes, resulting in a larger meridional gradient of boundary layer energy, which favors a stronger monsoon, producing more rainfall in summer. The interactive soil moisture-rainfall feedback was crucial for the duration of the rainfall anomaly, although not essential for the initial rainfall enhancement. They concluded that the three-way interactions between ocean, land and atmosphere are responsible for the connection between spring SST and summer rainfall. Again, this suggests that both local land forcing and remote oceanic forcing should be considered when studying West African rainfall variability.

3.2.2 Biosphere-Atmosphere Interactions

As mentioned in the introduction, evapotranspiration play a significant role in both the hydrological and energy cycles. Indeed, evapotranspiration provide a critical link between both cycles underscoring the role of vegetation in regulating the regional climate. Nevertheless, vegetation affects the energy cycle in other direct and indirect ways like increasing the amount of solar radiation absorbed at the surface due to a lower albedo relative to bare soil. Charney (1975) pioneered the subject of the role of biosphere-atmosphere interactions when he presented a hypothesis describing the mechanisms of droughts in semi-arid regions. The essence of this study is that the atmospheric circulation and therefore rainfall over West Africa may be very sensitive to desertification near the southern boundary of the Sahara. Charney (1975) proposed a biogeophysical feedback mechanism that suggest that albedo increase due to desertification has a cooling effect that enhances local subsidence, thus reducing rainfall which limits vegetation growth and makes the drought self-sustaining. Subsequent modeling studies (Charney et al. 1977; Cunnington and Rowntree 1986; Xue and Shukla 1993) supported the common conclusion that vegetation degradation at the desert border promotes a significantly drier climate over the Sahel region. Nevertheless, Gornitz and NASA (1985) found that replacement of moist tropical forest and grasslands by a combination of tree crops, field crops and secondary regrow could lead to a smaller albedo change than the one used in most of the previous studies. Other land-atmosphere interactions studies have supported the hypothesis that vegetation degradation over the forest area has a significant weakening effect over the monsoon circulation. Thus, vegetation degradation may have played an essential role in the current drought over the Sahel (Zheng and Eltahir 1997 1998a). Nevertheless, the initial conditions of soil moisture and atmospheric conditions were found important in numerical modeling of the climate over West Africa by Cunnington and Rowntree (1986). Eltahir (1998) proposed a soil moisture-rainfall-feedback mechanism based on energy considerations, rather than water balance or precipitation recycling (see figure 1 in the referenced paper). The proposed mechanism accounts for negative feedback of clouds on albedo and interaction between local convection and large-scale atmospheric motions.

The role of vegetation distribution in rainfall variability over West Africa is discussed in

Zheng and Eltahir (1997 1998). The results of the numerical experiments showed that rainfall distribution depend critically on the location of the vegetation perturbations. Since Zheng and Eltahir were interested in perpetual summer states under different vegetation patterns, the model had static vegetation distributions. The coupled biosphere-atmosphere system was investigated by Wang and Eltahir (1999a,b). It was found that vegetation dynamics enhances the low-frequency variability of the Sahel rainfall. The response of vegetation to initial external forcing is a critical process in the severity and persistence of the observed drought according to their study.

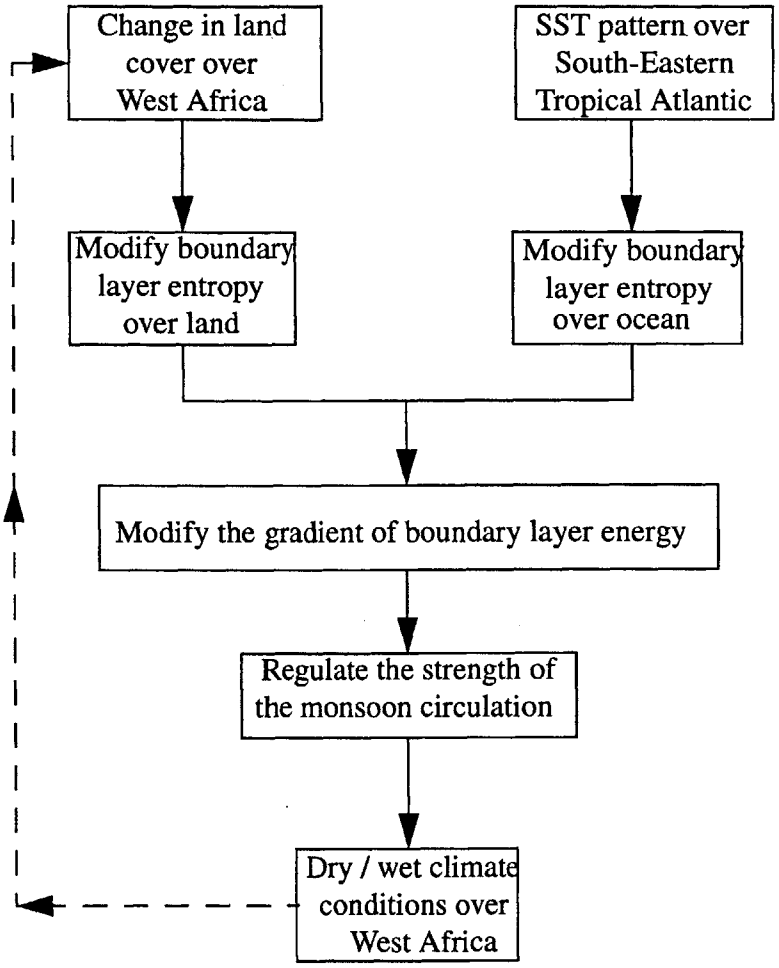

Figure 3-3: Biosphere-atmosphere-ocean interactions over West Africa (based on Eltahir and Gong, 1996)

Eltahir and Gong (1996) presented a hypothesis relating the meridional gradient of boundary layer energy or moist static energy in the boundary layer (BLMSE) to monsoon circulation and rainfall over West Africa (figure 3.2.2). According to this theory, a large meridional gradient of MSE in the boundary layer between ocean and land would favor an angular momentum conserving regime in a tropical atmosphere resulting in a strong meridional circulation. A healthy monsoon circulation provides a large-scale forcing that enhances precipitation. In addition to strengthening of the monsoon circulation, an augmentation in moist static energy increases the frequency and magnitude of local convection. Therefore, it provides an additional mechanism to enhance rainfall. In the other hand, a small meridional gradient of BLMSE would favor a radiative-convective equilibrium regime, resulting in a weak meridional circulation. Such weakening in the monsoon circulation would result in a precipitation decrease over the land region.

In the proposed hypothesis land and ocean processes control the meridional gradient of BLMSE by regulating the amount of BLMSE over land and ocean. Energy transfer processes controlling BLMSE over land are radiative cooling of the boundary layer (N_r), the total flux of heat from the surface, entrainment at the top of the boundary layer, and convective downdrafts (S_h and L_h components). All these processes are regulated by several land-atmosphere mechanism such as soil moisture-rainfall feedback in the daily and seasonal scales (Eltahir 1998) and vegetation dynamics in the seasonal and multi-year scales (Eltahir 1996; Wang and Eltahir 1999a,b). The surface energy balance requires that net radiation ($N_r = N_s + N_t$) and heat fluxes ($F = L_h + S_h$) be in equilibrium. Since we are considering only the land surface, we can neglect the contributions of convective downdrafts and entrainment to the heat fluxes at this moment. Therefore, L_h and S_h represent the latent heat flux and sensible heat flux from the surface. As derived in Eltahir (1996), we can show that a perturbation in net radiation (dN_r) due to vegetation degradation or soil moisture depletion must be balance by an equal perturbation in the heat fluxes (dF):

$$N_r + dN_r = F + dF \tag{3.6}$$

The change in net radiation is composed of changes in net solar radiation (dN_s) and

net terrestrial radiation (dN_t). Net solar radiation changes can be caused by surface albedo changes, cloud albedo changes, or by changes in atmospheric absorption from water vapor concentration changes. The change in N_t could be the result of changes in temperature of the surface and the boundary layer, changes in absorption and emission of the atmosphere from changes in water vapor content, and changes in cloud's absorptivity and reflectivity. Vegetation degradation and dry soil moisture conditions increases surface albedo but a decrease of water vapor and cloudiness due to the increase in Bowen ratio and drier boundary layer would counteract this effect. Therefore, the net solar radiation change (dN_s) is expected to be small. At the same time, the decrease in Bowen ratio would increase the air temperature close to surface and ground temperature. This would enhance upward terrestrial radiation, thus reducing net terrestrial radiation at the surface. The reduction of water vapor content and cloudiness reduces the corresponding greenhouse effect and results in further reduction of N_t at the surface. Therefore, it is expected that changes in N_r at the land surface be dominated by net terrestrial radiation change.

3.3 Biosphere-Atmosphere-Ocean Interactions

In the first chapters of this thesis, we argued that large-scale motions act as a forcing for precipitation without giving the specific details of the physical mechanism. This section will present certain misconceptions in the underlying mechanism of the interaction between large-scale flow and rainfall. Furthermore, it is possible to identify a major source of error and account for the underestimation of rainfall in most mesoscale models if one analyze in more detail the physical processes responsible of atmospheric motion in different scales. First, we will present the general theory of moist atmosphere flow as traditionally depicted. Then we will present a new way of thinking about the interactions between large-scale motion and convection over the tropical oceans proposed by Emanuel (1994). Then the extension of this theory over the ocean-biosphere surface as presented in Eltahir and Gong (1996) will be reviewed. Finally, the framework of the biosphere-atmosphere-ocean interaction theory

will be used to explain the regional climate of West Africa and identify most probable causes of discrepancies in previous studies regarding the importance of two different forcing mechanisms.

Previous climate studies assumed that radiative-convective equilibrium was a dynamic equilibrium in which large-scale motion initiates the flow and it is then maintained by convection. The general view on the interaction of large-scale motions and convection can be summarized in the following discussion from Gill, (1982; pp. 11-12):

> "To see how fluid motion can affect the balance, consider an atmosphere that, at some initial time, contained no water vapor, but was in radiative equilibrium. If the atmosphere absorbed no radiation at all, the ground would warm up as in the absence of an atmosphere, but the air above would remain cold. Although the system will be in radiative equilibrium, it would not be in dynamic equilibrium because the air warmed by contact with the surface could not remain below the cold air above without convection occurring, as it does in a kettle full of water that is heated from below. The vigorous motion produced carries not only heat up into the atmosphere, but also water vapor produced by evaporation at the surface. The water vapor then affects the radiative balance because of its radiation-absorbing properties, so the final equilibrium depends on a balance between radiative and convective effects and is called radiative-convective equilibrium.
>
> Whether or not convection will occur depends on the "lapse" rate, i.e., the rate at which temperature of the atmosphere decreases with height. Convection will only occur when the lapse rate exceeds a certain value. ... Another way of expressing the same ideas is in terms of potential energy. When the lapse rate exceeds the adiabatic value, the potential energy can be reduced by moving parcels adiabatically to different levels. Thus energy is released and is used to drive convection.
>
> If the atmosphere contained only small amounts of water vapor, convection would only occur if the dry adiabatic lapse rate were exceeded. In practice,

this situation is complicated by the fact that air at a given temperature and pressure can only hold a certain amount of water vapor. ... The condensed water ultimately returns to the earth's surface as precipitation.

This hydrological cycle affects the energy balance of the atmosphere in a number of important ways. First, clouds have an important effect on the total amount of energy absorbed by the atmosphere because they reflect and scatter a significant amount of the incoming radiation... Second, the radiation-absorbing properties of water vapor are important in determining the temperature of the lower atmosphere... Third, cooling takes place upon evaporation because of the latent heat required. This heat is released back into the atmosphere when condensation takes place in clouds. The heat transferred by this means is on average, about 75% of the convective transport."

Then goes on defining the moist adiabatic lapse rate (the modified adiabatic rate due to the presence of water vapor in the atmosphere). The important thermodynamic consideration, incredibly overlook by almost all climate models (e.g. "in the sake of computational efficiency") is included in the following paragraph of the same explanation:

"The moist adiabatic lapse rate is appropriate for ascending air, but for descending air the story is different. The amount of water vapor a parcel can hold increases as the parcel descends, so the parcel is always unsaturated and the dry adiabatic lapse rate is appropriate. Thus in a convective atmosphere, potential energy may be released where the air is ascending, whereas work is being done against gravity where the air is descending...

A problem in modeling the atmosphere is to find a satisfactory way to represent the effects of convection without modeling the details of the ascending and descending parcels of air. Radiative-convective equilibrium models represent the effects of convection in a very simple way."

There is when most climate models fail when trying to simulate the tropical atmosphere. The statement that "a tropical atmospheric model should be characterized by its relevance

to the essential climate dynamics, high computational efficiency, and capability of realistic simulations of the key variables of the coupled climate system" is desirable goal, but not a reality just yet. Such statement presumes the knowledge of the fundamental climate coupled dynamics and the capability of reproducing them from simplified physics. The deficiencies (e.g. temperature and precipitation biases) and discrepancies (e.g. different results with similar forcings) in the climate reproduction and prediction of different models is indisputable proof that we are still incapable of representing the essential climate processes of the system assuming no other trivial sources of errors.

This is not a new argument, nor it implies that climate prediction is not a reachable goal. All that we are saying is that there is still need for better physical representation of the different processes in order to reproduce and later predict the climate of a region. Furthermore, sensitivity studies of the climate to different forcing can be miss represented partially or even completely by the simplifying assumptions made in most climate models, as we shall see later.

Another example of the misconception in the role of large-scale flow on convection can be taken from one of the most popular books in dynamic meteorology by Holton (1992). In all fairness, he identifies the misconception and even provides the views of two alternative theories when discussing the development of hurricanes:

> "Observations indicate, moreover, that the mean tropical atmosphere is not saturated, even in the planetary boundary layer. Thus, a parcel must undergo a considerable amount of ascent before it reaches its LFC and becomes positively buoyant. ... In the tropics it is difficult to initialize deep convection unless the boundary layer is brought toward saturation and destabilized, which may occur if there is large-scale (or mesoscale) ascent in the boundary layer. Thus, convection tends to be concentrated in regions of large-scale low-level convergence. This concentration arises not because the large-scale convergence directly "forces" the convection but rather because it preconditions the environment to be favorable for parcel ascent to the LFC (level of free convection)."

It is then argued that cumulus convection and the large-scale environmental motion may

thus be viewed as cooperatively interacting. The idea of boundary layer pumping is then introduced together with the two competing theories of conditional instability of the second kind (CISK) and the air-sea interaction theory. The discussion ends explaining that sea-air interaction theory seem to be verified by observations whereas CISK theory fails to be observed. According to Emanuel et al., (1994), the original view of convection as a heat source for an otherwise dry circulation has precluded the understanding and representation of large-scale flow and convection in numerical models. Furthermore, emergence of CISK theory by Charney and Eliassen (1964) is attributed to the desire to account for the finite scale of ascent regions in developing tropical cyclones. Unfortunately, it had the undesirable effect of adding to the conceptualization of convection as a heat source of an otherwise dry atmosphere. This misconception was incorporated to numerical models in the Kuo-type convection scheme. An improvement to the "external" convection view was presented by Arakawa and Schubert (1974) in the "quasi-equilibrium" closure hypothesis for moist convection. They argued that the difference in time-scales between convective motions and large-scale flow do not allow significant conversion of available potential energy to kinetic energy of large-scale disturbances, a requirement in CISK. Fortunately, research on this area has advanced during the last decades. In particular, the explanation provided by Emanuel et al., (1994) seems to be the most accurate description of the problem. In their own words:

> "In the tropics, large scale upward motion is certainly associated with latent-heat release, but the latent heating is nearly balanced by a combination of radiative and adiabatic cooling. Whether or not this heating is positively correlated with temperature is a far more difficult question to answer. ... For now, we simply wish to point out that small errors in the determination of cumulus heating may lead to large errors in temperature, and thus to large errors in the dynamics of circulations in the convecting atmosphere."

After comparing the mathematical formulation requirements of the Kuo-type parameterization with observations of the tropical atmosphere, Emanuel et al., (1994) concludes that this CISK-type convection largely ignores that vertical motion is a response to instability. Which bring us to the original problem, e.g. how does large-scale motions and convection

interacts with each other in a moist atmosphere in radiative-convective equilibrium? To answer this question it is necessary to review the theories of thermally direct, zonally symmetrical circulations discussed in Held and Hou (1980), Emanuel et al. (1994), and Eltahir and Gong (1996). The thermal wind relation for a zonally symmetrical circulation in pressure coordinates can be written as:

$$\frac{\partial u}{\partial p} = \frac{1}{f}\frac{\partial \alpha}{\partial y} \tag{3.7}$$

With the aid of the Maxwell's relations, as explained in Emanuel (1994), the thermal wind equation can be rewritten in terms of the meridional gradient of saturation entropy:

$$\begin{aligned} \left(\frac{\partial \alpha}{\partial y}\right)_p &= \left(\frac{\partial \alpha}{\partial s^*}\right)_p \frac{\partial s^*}{\partial y} \\ &= \left(\frac{\partial T}{\partial p}\right)_{s^*} \frac{\partial s^*}{\partial y} \end{aligned} \tag{3.8}$$

In radiative-convective equilibrium, the neutrality condition for moist convection requires that the saturation moist entropy of the free atmosphere be almost equal to the actual boundary layer entropy ($s^* \approx s_b$). Therefore, it is possible to get the following solution for the troposheric-level zonal wind in terms of saturation entropy and temperature difference between the surface and the troposphere:

$$u_t = -\frac{1}{f}(T_0 - T_t)\frac{\partial s_b}{\partial y} \tag{3.9}$$

The absolute vorticity (η_t) at the tropopause can be obtained from the above equation 3-9 as in Emanuel (1994) and Eltahir and Gong (1996). Plumb and Hou (1992) provided a solution for equation 3-10. Emanuel (1994) developed a similar expression assuming geostrophic balance (relation 3-11).

$$\eta_t = f - \left(\frac{\partial u_t}{\partial y}\right)$$

$$= f + \frac{\partial}{\partial y}\left(\frac{1}{f}(T_0 - T_t)\frac{\partial s_b}{\partial y}\right) \tag{3.10}$$

$$1 + \frac{1}{f^2}\frac{\partial}{\partial y}\left((T_0 - T_t)\frac{\partial s_b}{\partial y}\right) - \frac{\beta}{f^3}(T_0 - T_t)\frac{\partial s_b}{\partial y} > 0 \tag{3.11}$$

For an atmosphere in radiative-convective equilibrium, relation 3-11 holds. On the other hand, conservation of absolute vorticity requires that regions with positive Coriolis parameter (f) must be balanced by negative relative vorticity $\left(\frac{\partial u_t}{\partial y}\right)$ in equation 3-10. If relation 3-11 does not holds true, an angular momentum conserving regime is obtained. Such regime results in a circulation like the monsoon. Therefore, it is expected that relation 3-11 be close to zero during any given time during the year. The onset of the monsoon can be represented by the time that relation 3-11 is violated. Eltahir and Gong (1996) performed a sensitivity analisys of the components of the the necessary conditions for the development of an angular conserving regime. Due to the geographic location of West Africa, the dominance of a conserving momentum regime is regulated by the meridional gradient of boundary layer energy. First, the temperature difference between the tropopause and the surface is fairly constant over the tropics ~100K, as stated in Emanuel (1994 1995). Second, the coriolis parameter f is $+2.48\text{x}10^{-5}$ sec^{-1} for a region located at 10°N like West Africa (Eltahir and Gong 1996). This implies that the factor $\frac{1}{f^2}$ is $16.3\text{x}10^{8}$ sec^2 and that $\frac{\beta}{f^3}$ is $55.8\text{x}10^{2}$ sec^3 m^{-1}. Therefore, the signs of $\left(\frac{\partial s_b}{\partial y}\right)$ and $\frac{\partial}{\partial y}\left(\frac{\partial s_b}{\partial y}\right)$ ultimately determine if the radiative-convective equilibrium is violated and an angular conserving regime is established.

Chapter 4

Observational and Reanalysis Datasets

In the following sections, a brief description of the main datasets used for the analysis of the regional climate over West Africa is presented. It is important to recognize the limitations and implied assumptions of the datasets used in order to evaluate the significance of any conclusions. References to in-depth review articles are included where appropriate. We start by describing the NCEP/NCAR Reanalysis as our primary climate data source. Then we proceed to describe other specialized datasets that complement the information provided in the NCEP/NCAR Reanalysis.

4.1 NCEP/NCAR Reanalysis

A complete description of the reanalysis project is given by Kalnay et al. (1996). The NCEP/NCAR Reanalysis is a cooperative effort between the National Center for Environmental Prediction (NCEP) and the National Center for Atmospheric Research (NCAR). They have produced a 50+years record of atmospheric fields over the world by assimilating data from land surface stations, rawinsondes, pibals, aircraft, ships, satellite and other sources. The period covered in the last release of the dataset is from January 1948 to present. It is the only dataset to have a 6-hr time-resolution of multiple climate variables for such

Class	Source	Climate Variable
A	Data from observations only	temperature, horizontal wind, geopotential height, pressure
B	Observations and model tendencies	specific humidity and vertical velocity
C	Input from model only	precipitation, heat fluxes, net radiation, soil moisture
D	Fixed values	land-sea mask, plant resistance surface roughness

Table 4.1: NCEP-NCAR Reanalysis data fields classification based on Kalnay et al., (1996)

a long period. The other comparable datasets have shorter time coverage, e.g. ECMWF (1979-93) and NASA/DAO (1985-93). The vertical resolution of the NCEP/NCAR Reanalysis is 17 pressure levels from 1000 hPa up to 10 hPa for most atmospheric variables. Specific humidity is defined in eight levels (1000 hPa to 100 hPa only) and pressure vertical velocity is defined in 12 levels (1000 hPa to 300 hPa only). Horizontal resolution varies depending on which climatic variables are considered. All pressure level variables are defined in a 2.5° x 2.5° grid with 144 x 73 points. All surface flux data are defined in a T62 Gaussian grid with 192 x 94 points (~ 1.9° x 1.9°). The classification of the variables depends on the relative influence of the observational data and the model on the gridded variable. Table 4.1 summarizes this information for the variables used in this study. As shown in table 4.1, the class A analysis variable is the most reliable class since it is strongly influenced by observed data. The analysis variable designated as class B corresponds to a value that is strongly influenced by both observational data and model output. The class C variable is derived from the model only with no observations affecting the variable in a direct manner. Nevertheless, the model is forced by the data assimilation module to remain close to real atmospheric values. Climatological fields are designed as class D. The model used in the Reanalysis solves the primitive-equations with vorticity, divergence, logarithm of surface pressure, specific humidity, and virtual temperature as prognostic variables (Philips 1995).

As previously mentioned, the NCEP/NCAR Reanalysis assimilated data from a variety sources. Rawisondes (raobs) usually report height, temperature, moisture, winds and pressure. Pibals report wind data only. Pibal observations are usually made by tracking a

Continent	Observation	1973	1976	1980	1990	1998
Africa	Number of raobs and pibals	257	235	243	225	131
	Reports per day	0.7	1.1	1.2	1.2	1.3
North America	Number of raobs and pibals	221	198	195	192	177
	Reports per day	1.4	1.6	1.6	1.5	1.5

Table 4.2: NCEP-NCAR Reanalysis data counts for Africa and North America based on Jenne (1999)

balloon with radar at the surface. In Table 4.2 we present selected years of the number of stations reporting data and the average reports per day per station for the North America and Africa. Two trends are noticed in the table. The declining number of raobs and pibal reporting after the 1980 decade (243 to 131 in Africa) is noticed. In addition, the stable amount of 1.2 reports per day, per station for Africa and 1.5 per day, per station for North America is evident. Similar trends are observed in the NCEP decode of the Global Telecommunication System (GTS) data according to Jenne (1999). The report states that during 1977-1990 the number of reports reaching NCEP was around 280 reports per day, falling to 173 in 1998. While the data density of raobs and pibals has decreased, the satellite available data has increased in the last two decades. The monthly radiosondes observations were increasing from 1962 to 1975, then were stabilized for the 1975-1995 period and finally start declining after 1997. The number of land stations remained almost constant from 1967-1997, although only the savanna region had observations from 1957-67. The available land stations and radiosondes before 1962 are quite limited except for the 1949-53 period. The advantage of the NCEP/NCAR Reanalysis database over other observational datasets is that it incorporates the largest amount of valid observations into an operational spectral model that has an advanced quality control. The classification of variables presented in this section must be recalled when making comparison between different variables. The 3-D variational spectral interpolation scheme and the availability of observations since the 1950's give us reassurance in the quality of the dataset. The data at the daily time scale is expected to have larger uncertainties than the correspondly data at the monthly scale due to incomplete records, and the effects of small scale atmospheric motions (e.g. the hydrostatic assumption is not valid in short time scales, especially in convective regions).

4.2 Global Precipitation Climatology Project (GPCP)

Due to the limitations of the precipitation field of the NCEP/NCAR Reanalysis given that it includes modeled precipitation rather than observed, it is necessary to look for additional sources of precipitation data. One such dataset is the Global Precipitation Climatology Project (GPCP) established by the World Climate Research Programme (WCRP) under the Global Energy and Water Cycle Experiment (GEWEX). The GPCP dataset provides spatial and time averaged precipitation estimates based on infrared and microwave satellite observations together with ground station measurements. The monthly-mean data is available in a 2.5° x 2.5° grid for the July 1987-December 1995 period. The primary satellite data sources are the Geostationary Operational Environmental Satellite (GOES, United States), Geostationary Meteorological Satellite (GMS, Japan), Meteosat geostationary satellites (European Community), the operational NOAA polar-orbiting satellites and observations from the Special Sensor Microwave/Imager (SSM/I) of the U.S. Defense Meteorological Satellite Program. Ground station data is obtained from the WMO network and local radar measurements. Arkin and Xie (1994) provide an in-depth description of the algorithm used to produce the GPCP dataset.

4.3 Global Land Precipitation Dataset (Hulme's Dataset)

Algorithms to derive precipitation rates from satellite-based observations are still under development, so we also use a ground station-only dataset for analysis and comparison with modeled precipitation. Dr. Mike Hulme of the Climatic Research Unit in the University of East Anglia in England produced one of the most extensive global land precipitation datasets available. The station dataset is an extension of the CRU/US DoE data described by Eischeid et al. (1991). The data is available in 2.5° latitude by 3.75° longitude grid. It includes monthly and yearly precipitation, together with the number of stations used in each grid-box

to estimate the precipitation value. The data for each gridbox was obtained using Thiessen polygon weights to average the data from the gauges within the gridbox. Missing station values were estimated from the anomalies of surrounding stations. Gross outliers and typographical errors from all stations were screened out by various semi-automated techniques. Although no topographic weighting was incorporated to the interpolation scheme, no major effect is expected due to the small dependence of precipitation anomalies on topography. The proper selection of a representative reference period to compute the climatology average is by far the most constraining factor. Hulme (1992), and Hulme and New (1997) provide a more complete description of the land precipitation dataset and the algorithm used to interpolate the station data to the selected grid.

The Global Land Precipitation dataset from Prof. Mike Hulme of the University of East Anglia (UK) provides a great temporal coverage of station measurements for the 1900-98 period. Nevertheless, the spatial coverage over our region of study is not complete. There are 184 stations over the forest region (5°N-10°N, 15°W-15°E), 140 over the Sahel-savanna region (10°N-17.5°N, 15°W-15°E), and only 27 over the Sahara desert. The lack of stations over the desert region is not significant in terms of classic surface hydrology. Nevertheless, it limits the ability of testing the interactions between land and atmosphere over the region since it makes difficult to determine changes in the northward extension of the summer rainfall. Fortunately, the spatial coverage over the forest and savanna regions is sufficient to trace rainfall fluctuations over the last century. The forest region has 96% area coverage and the savanna has 92% area coverage, using the ratio of actual to maximum number of contributing pixels over the defined regions. It should be pointed out that there is no data for July 1997 over the savanna region. Since the extent of the dataset is so large, such missing data should not alter the results of the analysis performed.

4.4 International Satellite Cloud Climatology Project/ Surface Radiation Budget (ISCCP/SRB)

The International Satellite Cloud Climatology Project (ISCCP) was established as the first project of the WCRP. It was designed to collect and analyze satellite radiance measurements in order to determine the global distribution of cloud radiative properties. The radiance measurements are obtained from four major satellite programs GOES (5-10), GMS (1-5), METEOSAT (2-7) and NOAA (7-14). The C2 data series provides monthly global atmospheric data for the July 1983-June 1991 period. A complete description of the ISCCP project is provided by Rossow et al. (1991), and Bishop et al., (1997). The C-products are described in another paper by Rossow and Walker (1991). The D-series are described in Rossow and Schiffer (1999). They provide cloud radiative properties for the period of January 1986 to December 1993 (except for an operational interruption from February-June 1987). The Surface Radiation Budget project by NASA-Langley Laboratory (Gupta et al. 1999) used data from the ISCCP/C-series and the Earth Radiation Budget Experiment (ERBE: Barkstrom 1984) to compute radiance under clear-sky and cloudy conditions for shortwave and longwave radiation. The data was sampled from 30-km pixels and then averaged over 280-km pixels and finally converted to a 2.5°x2.5° equal area grid. Pal (1999, personal communication) converted the databases to a 2.5° latitude x 2.5° longitude grid in order to facilitate the comparison with other datasets.

4.5 Global Sea-Ice, Sea-Surface Temperature Dataset (UKMO GISST)

The Hadley Centre of the United Kingdom Meteorological Office produced the most extensive sea-ice, sea surface temperature dataset available for research. The dataset was created using a variety of techniques including the computation of anomalies from a climatology derived for the 1961-90 period. Empirical orthogonal functions analysis (EOF) of the anomalies were used to fill voids from the in-situ and satellite-derived measurements. The developers

of the dataset took into account the different types of biases associated with the different observational platforms (e.g. ships, buoys or satellites). The latest version of the dataset covers the period of 1900-1999 in a 1°x1° global grid. Parker et al. (1995) and Rayner et al., (1996) provide a detailed description of the GISST dataset.

4.6 Normalized Difference Vegetation Index from Goddard Space Flight Center (NDVI GSFC)

The Normalized Vegetation Index was obtained thanks to the Distributed Active Archive Center at the Goddard Space Flight Center. The NDVI GSFC dataset has a resolution of 1 degree by 1 degree (Chan 1998). It provides monthly global coverage for the period between July 1981 to October 1994. The NDVI is calculated by taking advantage of the the difference in reflectivity of clorophyll over the visible and near infrared regions. The index is computed using channels 1 (0.58-0.68 μm) and 2 (0.73-1.10 μm) of the Advanced Very High Resolution Radiometer on board in the NOAA-series satellite in the following formula:

$$NDVI = \frac{\alpha_2 - \alpha_1}{\alpha_2 + \alpha_1} \tag{4.1}$$

Where α_1 and α_2 are the reflectivities of channels 1 and 2. This type of ratio reduces significantly the variations from surface topography and Sun elevation angle. Justice et al. (1985) showed that NDVI is highly correlated to vegetations parameters as the leaf area index (LAI), and green-leaf biomass.

Chapter 5

Biosphere-Atmosphere-Ocean Interactions over West Africa

This chapter presents the results of analysis of the regional climate over West Africa. We present a comprehensive analysis using datasets from many sources and covering different time-scales mostly in the low frequency range (monthly to decades). The objective of this chapter is to physically explain the spatio-temporal characteristics found by empirical data analysis in the context of the biosphere-atmosphere-ocean interactions theory presented in Gong and Eltahir (1996). The main assumptions made for a first approximation of the large-scale flow in the atmosphere is that mesoscale and planetary motions are in hydrostatic, radiative-convective equilibrium. This is an assumption readily verified by observations. Furthermore, it is assumed that the boundary layer can be represented by the layer below 925 hPa in such spatio-temporal scales. This may seem a crude representation of the boundary layer, since it is one of the most heterogeneous, transient atmospheric phenomena. Nevertheless, it is important to recall that we are interested in the large-scale processes regulating the regional climate. Furthermore, the state of the boundary layer under consideration is moist static energy as defined in 3.5. Thus, any change in depth would be registered in the geopotential component at the time scales studied (Emanuel 1995). It is considered that the micro-scale effects are integrated over time and space into the large-scale field. These assumptions prevent us from getting into discontinuity problems often encountered in

the smaller spatio-temporal scales. On the other hand, a thorough physical analysis of the boundary layer processes will require the study of micro-scale processes and their interaction with large-scale motion.

During the last four decades, technological advances in information technology, remote sensing techniques and observational networks have produced an enormous quantity of climate data. Improvements in all these technologies are still in progress and optimally will result in larger-coverage, smaller spatial and temporal resolution, and better quality datasets. A brief description of the datasets analyzed in this chapter was presented in Chapter 4. The following sections present the results of a spatio-temporal analysis performed to the most important climatic variables in the biosphere-atmosphere-ocean interactions theory.

5.1 Long-Term Climatology

In order to simplify the analysis of the regional climate over West Africa it is desirable to identify different regions with similar climatic properties (homogeneous regions). A first approximation can be made by determining the annual mean and variance of different climate variables. The climatology was determined by calculating the average from all the monthly values in the 1958-97 period. The interannual variability was obtained by calculating the variance for the whole period. The use of climatological values in this section would be restricted to the determination of spatial patterns that will assist in the subdivision of the region under study.

In this study, we are interested in the regional circulations (motion systems with horizontal scales in the order of 10^3 km) regulating the climate of West Africa during the recent drought. Our first approach is to characterize the temporal mean and variance of different climate variables. This will allow us to make certain simplifications in the analysis of climate feedback processes. The climatology for the 1958-97 period of the monthly 1000-hPa surface temperature, specific humidity, wind and moist static energy is presented in figure 5-1. The interannual variance of the same variables is shown in figure 5-2. All this values are derived from the NCEP/NCAR Reanalysis as identified in the figure. The first remarkable feature is the almost-zonal homogeneity over the region. The contours of the climate variables "follow"

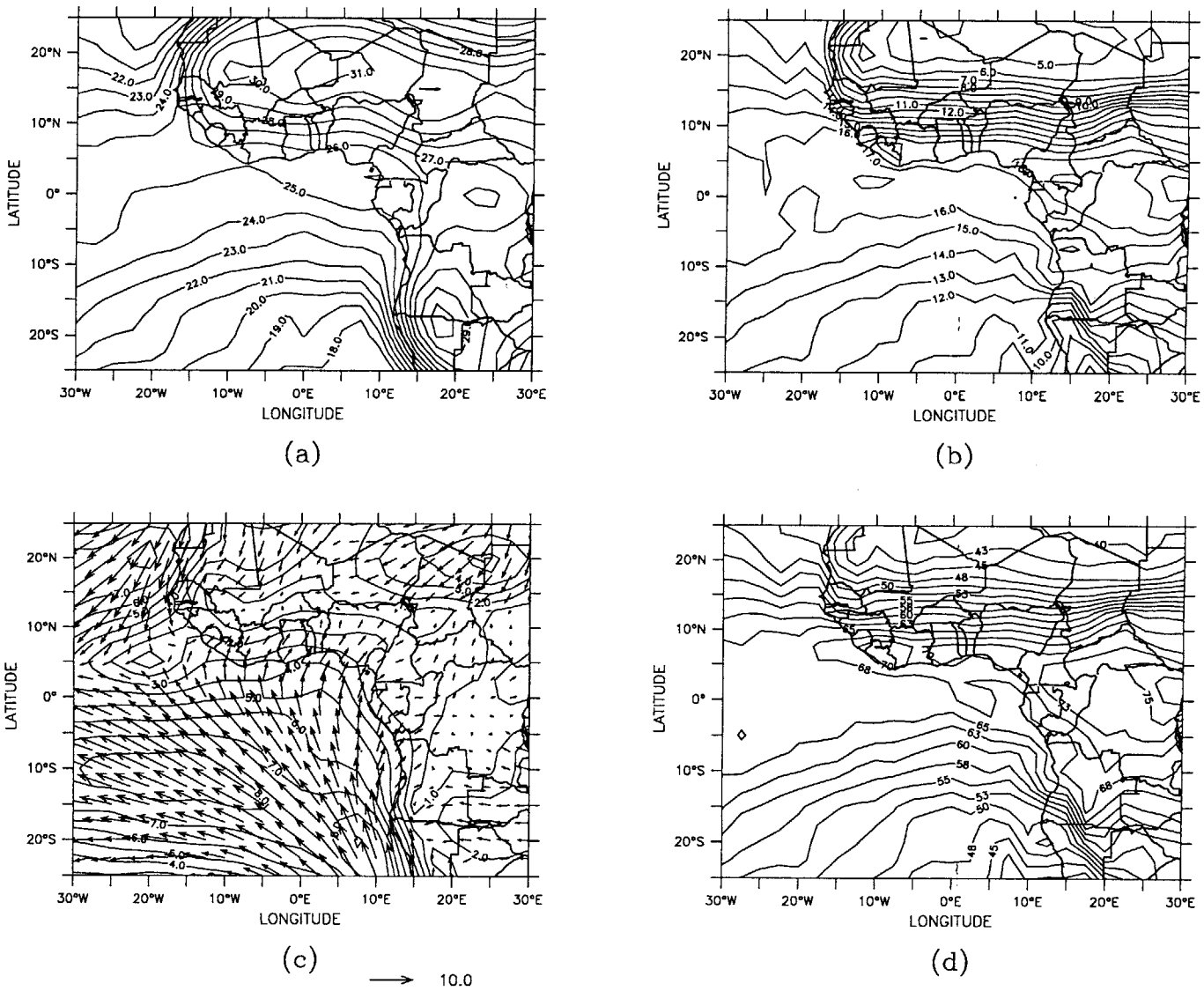

Figure 5-1: Climatology of selected NCEP/NCAR Reanalysis fields over the West African region. Fields are (a) surface temperature [$°C$], (b) specific humidity [kg/kg], (c) surface wind and [m/s] (d) moist static energy in the boundary layer [$°C$]

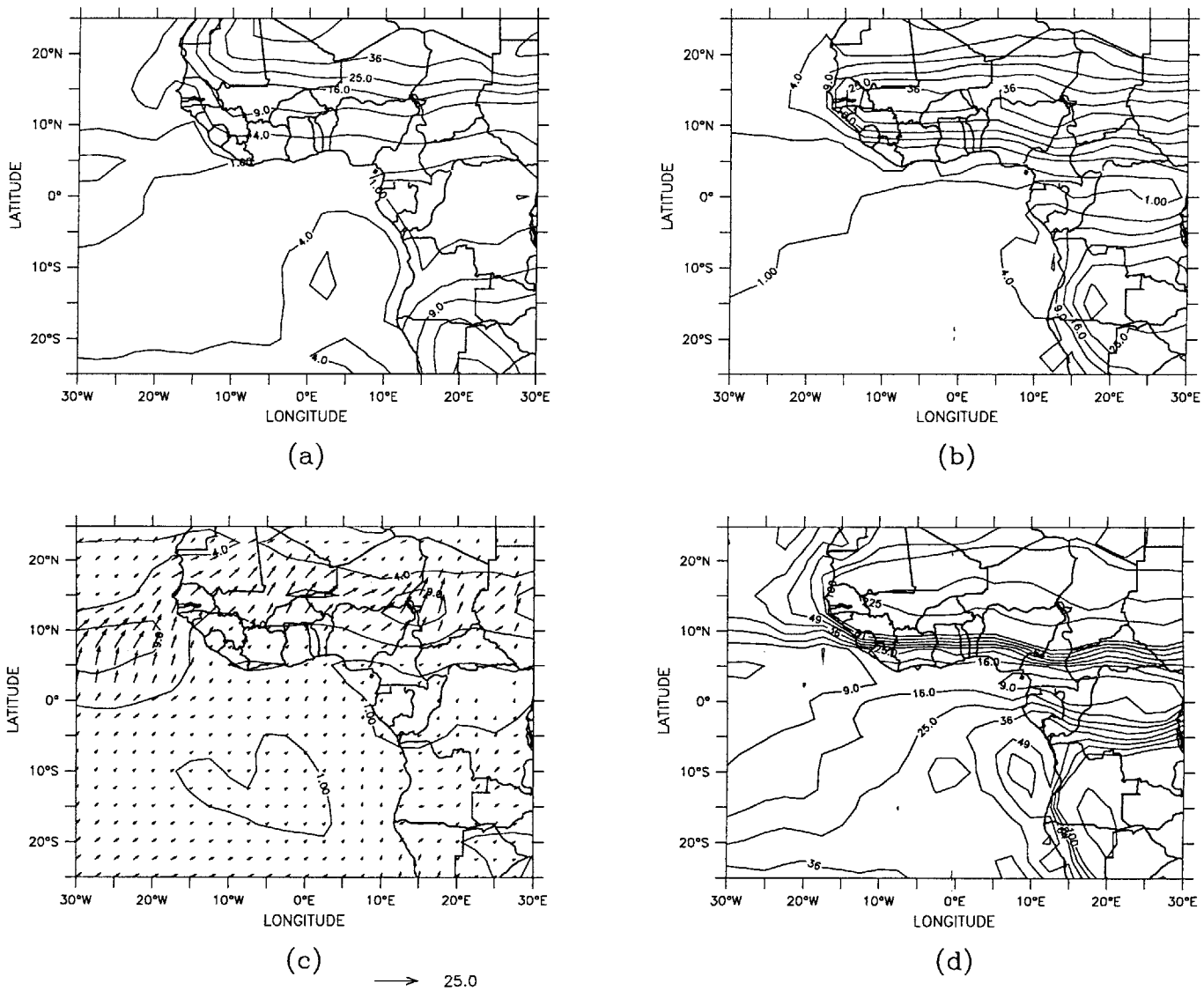

Figure 5-2: Total Variance of selected NCEP/NCAR Reanalysis fields over the West African region. Fields are (a) surface temperature $[°C]^2$, (b) specific humidity $[kg/kg]^2$, (c) surface wind $[m/s]^2$ and (d) moist static energy in the boundary layer $[°C]^2$

the coastline. Another significant feature is the low variability near the Equator, increasing poleward in both directions. This is consistent with temporal fluctuation of net radiation. Perhaps more interesting is the low mean and high variance of winds and moist static energy concentrated over the Sahel. This large-scale feature agrees with the theory presented in the previous chapter. The energy state of this region is critical for the occurrence of large-scale convergence and local convection (through the interactions between local convection and large-scale flow). This feature underscores the importance of the biosphere state over a region, since vegetation plays a significant role in regulating the exchange of heat, moisture and momentum, therefore regulating the energy state over a region.

Similar plots for net radiation, cloud cover, net shortwave and net longwave radiation are presented in figures 5-3 and 5-4. These plots are derived from the ISCCP/SRB project, C2 dataset for the June/1983-July/1991 period. The climatology for the period from 01/86 to 12/93 of the low cloud amount, medium-level cloud amount high-level cloud amount and deep convective cloud amount are shown in figures 5-5 and 5-6. These variables are obtained from the ISCCP-D2 database.

The climatology of sea surface temperature over the South Eastern Tropical Atlantic (SETA) region derived from the Global sea-Ice, Sea Surface Temperature (GISST) dataset is presented in figure 5-7. There is zonal symmetry above the 5°S latitude between the 15°W and 15°E (defined hereafter as UPSETA region). A northwest gradient can be observed with warmer temperatures in the imaginary triangle with vertices in (5°S, 35°W), (5°S, 10°E) and (25°S, 35°W). In addition, colder temperatures in a triangle reflected along the diagonal described are evident. There is no significant difference in temporal variability between the upwelling South Eastern Tropical Atlantic (UPSETA) and the SETA region as readily observed in figure 5-7, despite of the different physical processes that are believed to control the SST over those regions. The Guinea Coast (UPSETA region) is considered an upwelling zone, whereas the rest of the SETA region is dominated by wind-stress dynamics. Both zones have a remarkable low variability as expected from the high thermal capacity of oceans and small variations in radiative forcing over the Tropics. The upwelling dynamics don't seem to dominate the annually averaged variability.

Finally, rainfall from Global Precipitation Climatology Project (GPCP) and NCEP/NCAR

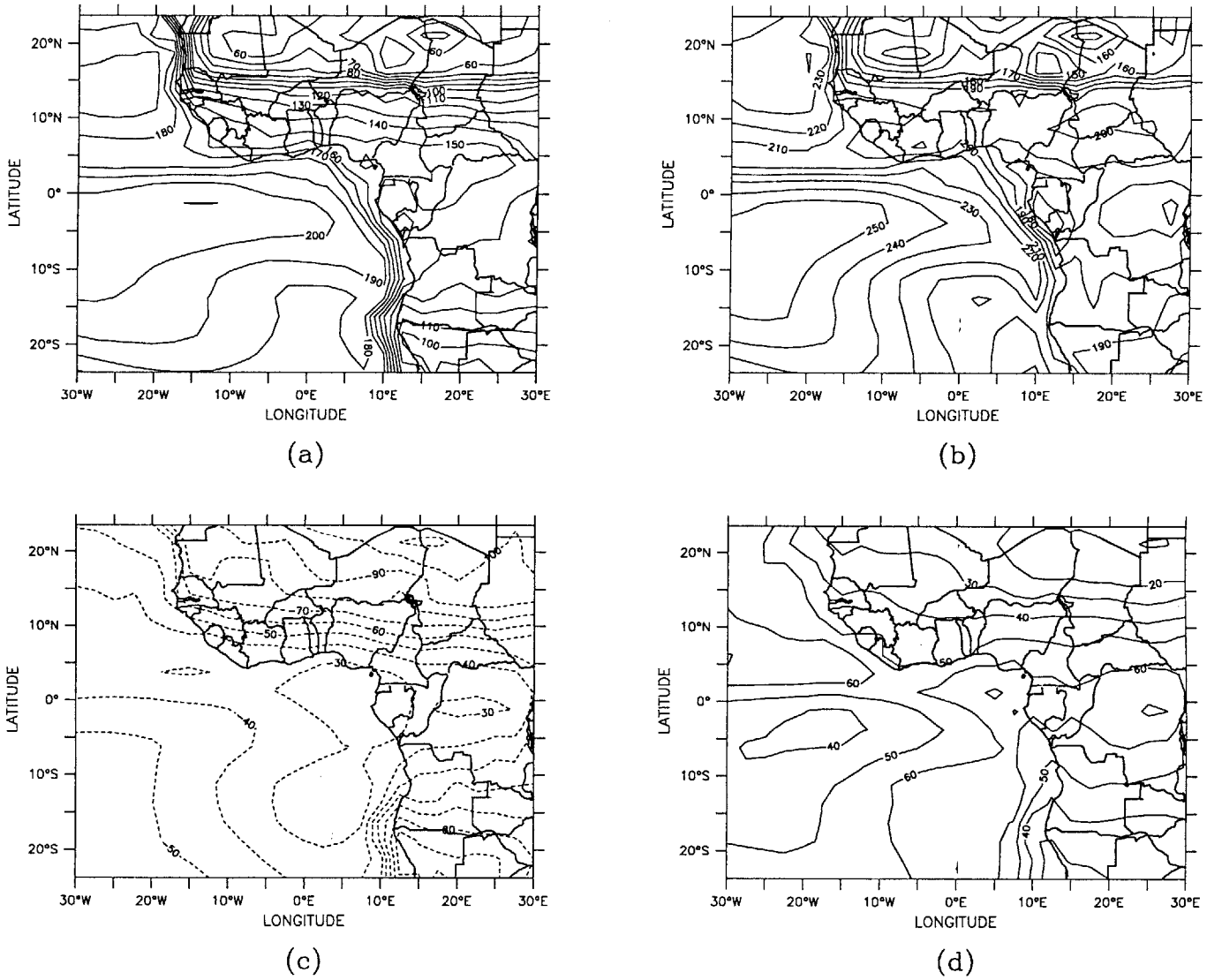

Figure 5-3: Climatology of selected ISCCP/SRB variables over the West African region. Variables are (a) net radiation $[W/m^2]$, (b) net shortwave radiation $[W/m^2]$, (c) net longwave radiation $[W/m^2]$ and (d) cloud cover [%]

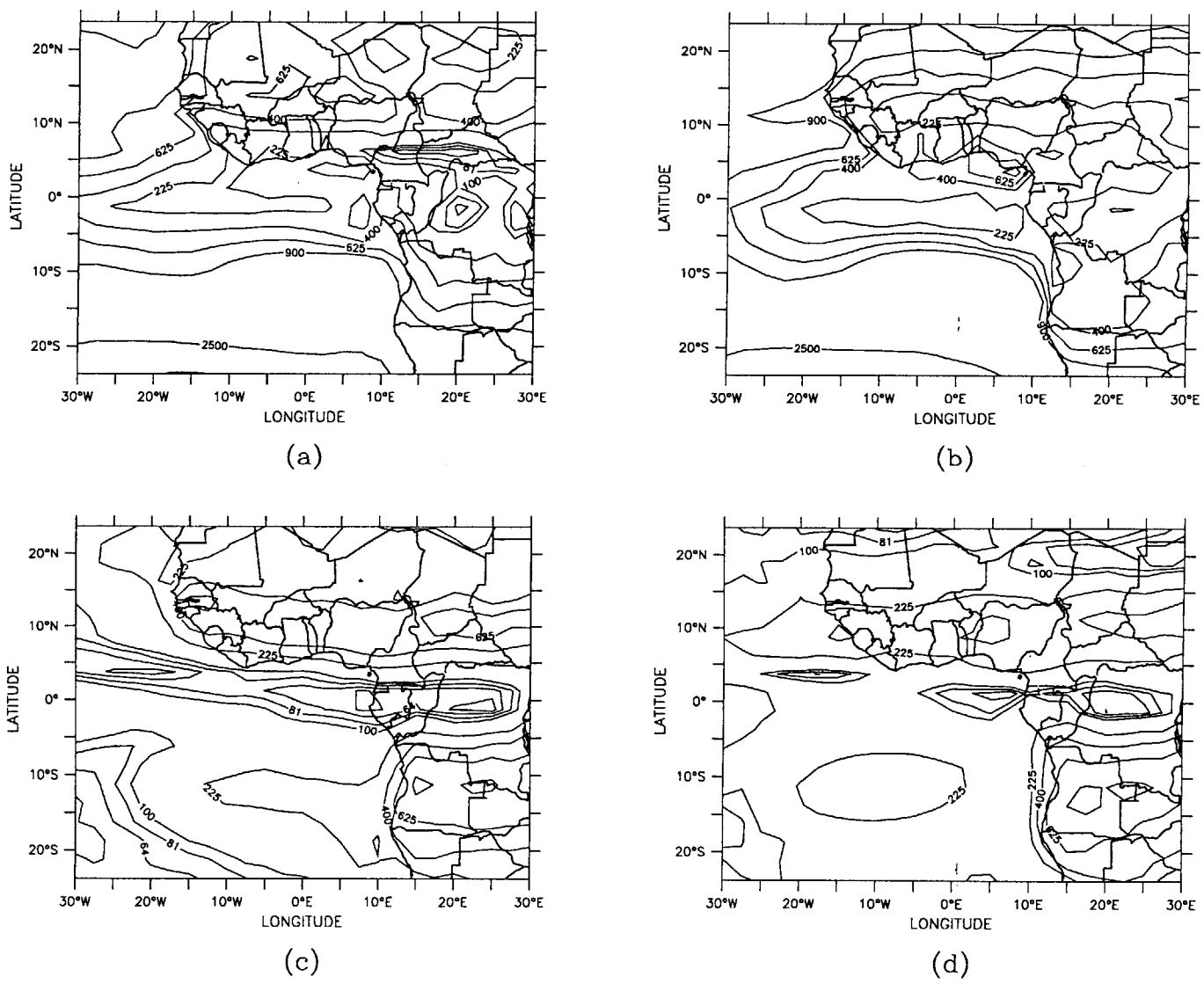

Figure 5-4: Variance of selected ISCCP/SRB variables over the West African region. (a) net radiation $[W/m^2]^2$, (b) net shortwave radiation $[W/m^2]^2$, (c) net longwave radiation $[W/m^2]^2$ and (d) cloud cover $[\%]^2$

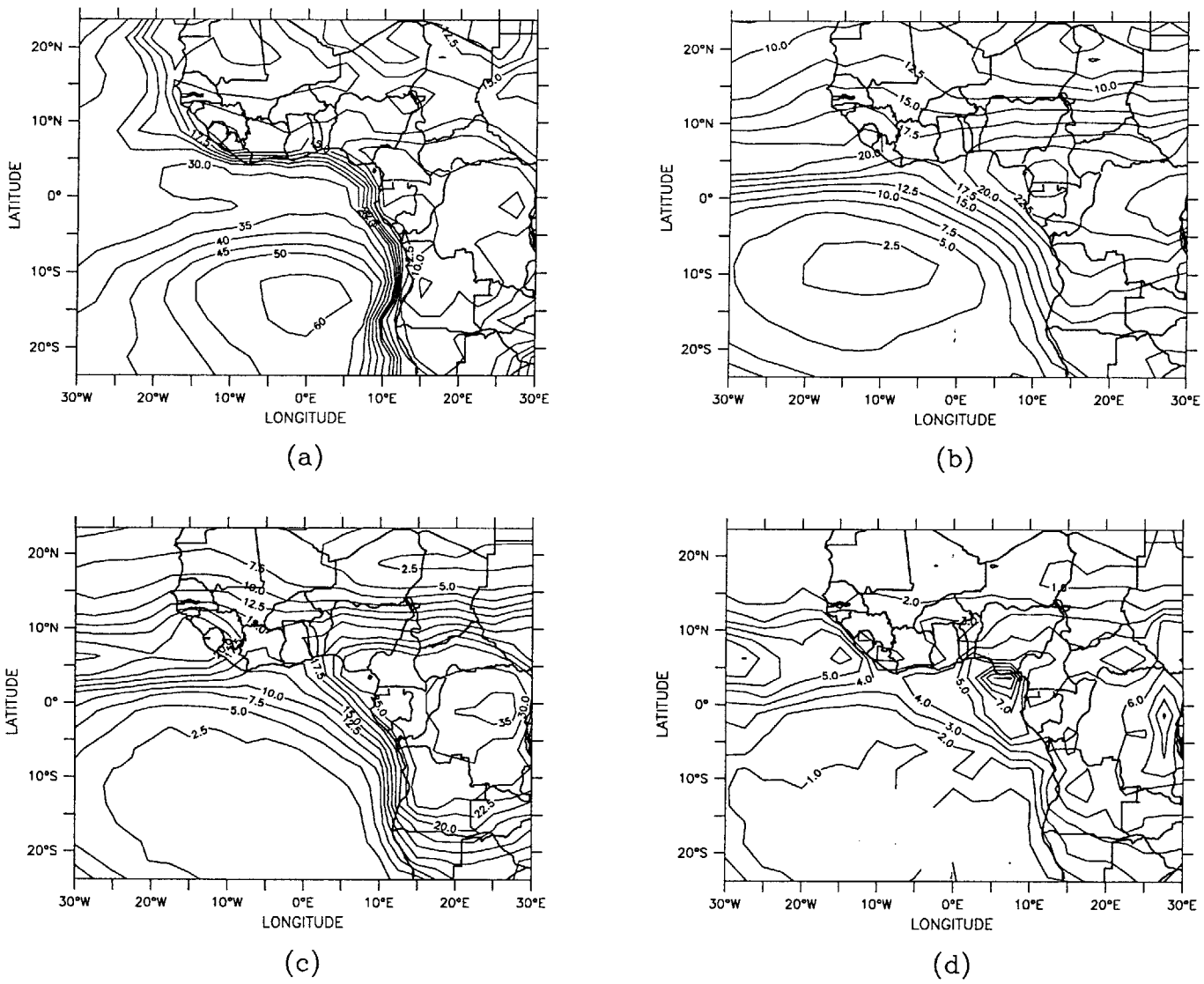

Figure 5-5: Climatology of selected ISCCP-D2 variables over the West African region. Variables are (a) low cloud amount [%], (b) middle cloud amount [%], (c) high cloud amount [%] and (d) deep convective cloud amount [%]

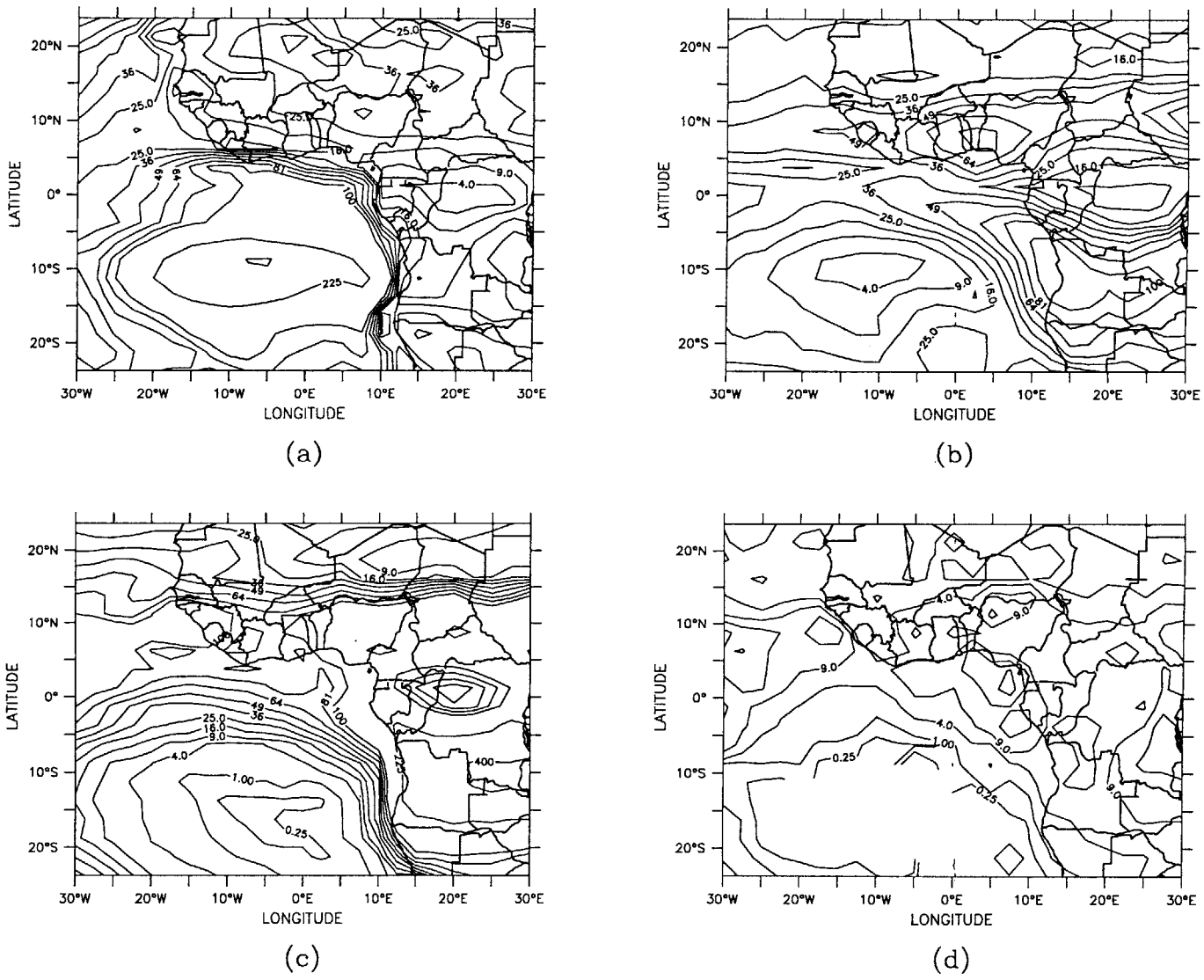

Figure 5-6: Variance of selected ISCCP-D2 variables over the West African region. Variables are (a) low cloud amount $[\%]^2$, (b) middle cloud amount $[\%]^2$, (c) high cloud amount $[\%]^2$ and (d) deep convective cloud amount $[\%]^2$

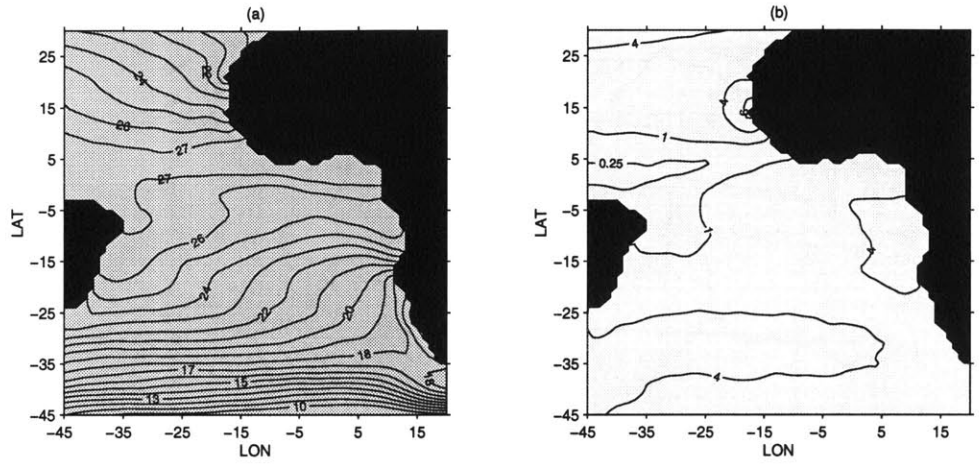

Figure 5-7: Climatology of sea surface temperature over the SETA region, based on UKMO GISST (1900-97) (a) long term mean [$°C$], (b) long term variance [$°C]^2$

Reanalysis are presented in figure 5-8. Although the mean values of the different sources don't agree, the meridional structure and variability are remarkably similar. This is an interesting result since the precipitation field in the NCEP/NCAR Reanalysis is a simulated field. It seems that the operational model is capable of reproducing the variability of rainfall over the region even when the mean value is underestimated.

These plots of climate variables suggest the existence of distinct climatic homogenous regions. In general, it can be observed that over land, regions with deep convection coincide with high moist static energy regions and atmospheric convergence. Over the ocean, high moist static energy regions coincide with high net radiation regions and predominant low level clouds. It was mentioned in section 2.3 that mesoscale motions like the Intertropical Convergence Zone (ITCZ) and the monsoon provide a large-scale forcing to precipitation in the tropical atmosphere (Emanuel 1994; Eltahir and Gong 1996). Therefore, it is desirable to study the variability of the mechanisms driving these atmospheric motions and compared it to rainfall variability.

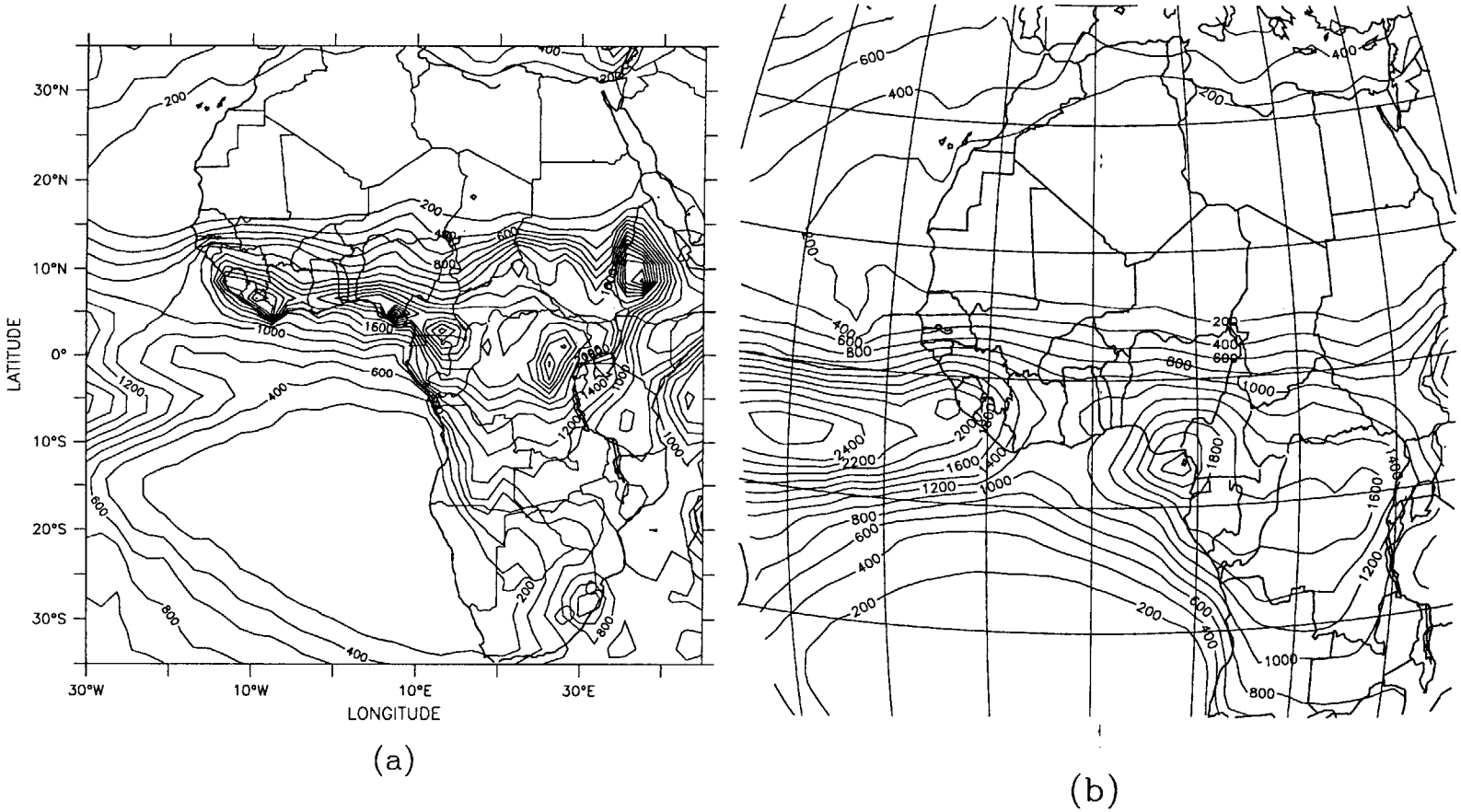

Figure 5-8: Climatology of rainfall over the West African region. Fields are (a) NCEP/NCAR Reanalysis simulated precipitation (1958-97) and (b) Global Precipitation Climatology Project (July 1987 - December 1995) [*mm/year*]

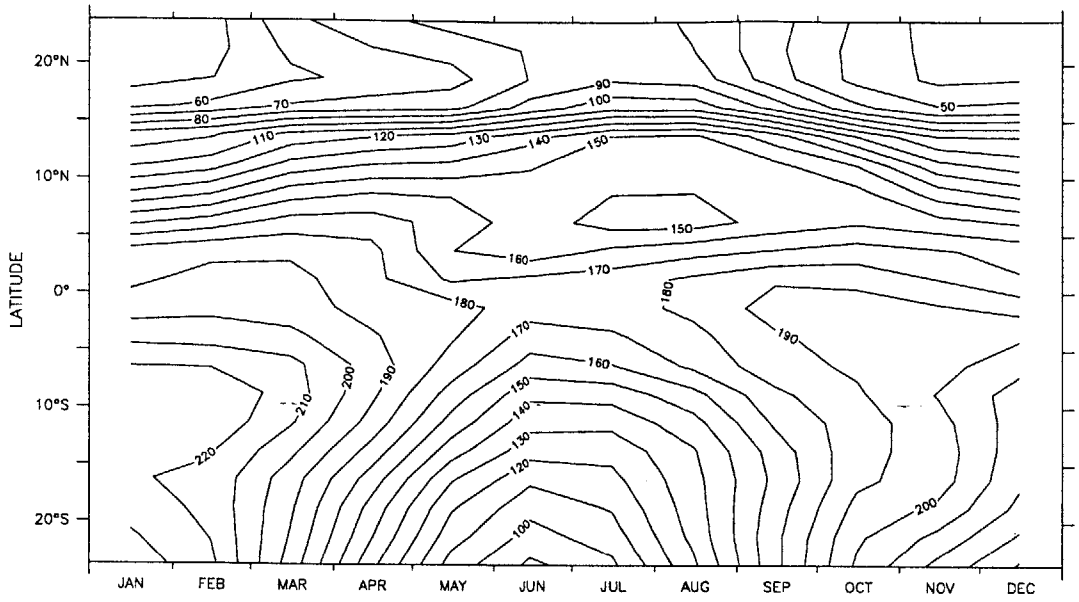

Figure 5-9: Zonally averaged seasonal cycle of net radiation $[W/m^2]$ as a function of latitude derived from ISCCP/SRB

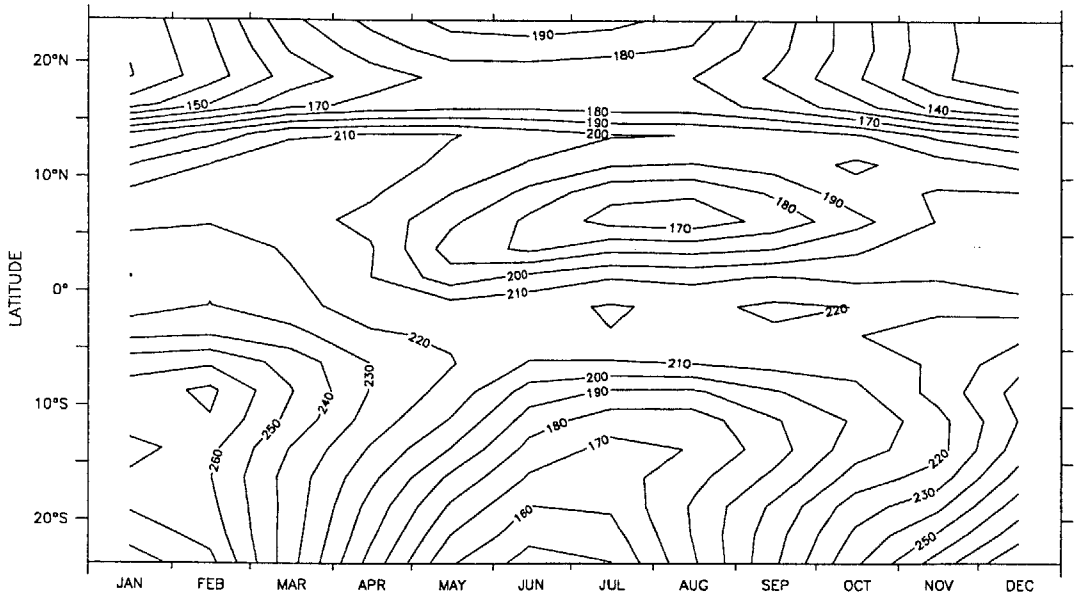

Figure 5-10: Zonally averaged seasonal cycle of net short wave radiation $[W/m^2]$ as a function of latitude derived from ISCCP/SRB

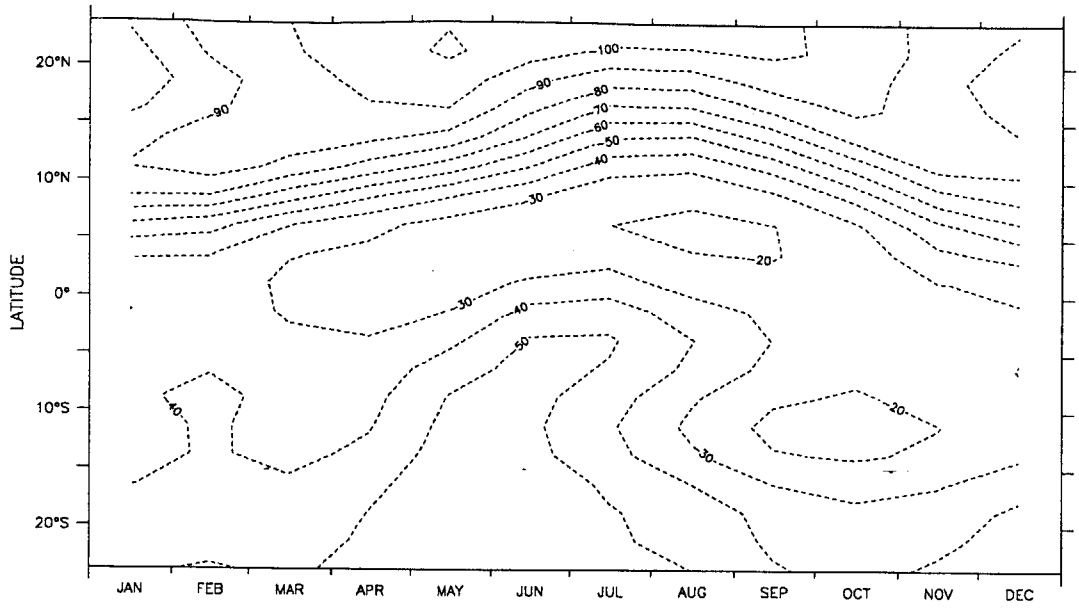

Figure 5-11: Zonally averaged seasonal cycle of net terrestrial radiation $[W/m^2]$ as a function of latitude derived from ISCCP/SRB

5.2 Inter-Seasonal Variability

This section presents a seasonal analysis performed to the most significant variables in the boundary layer energy theory. The geographical distribution of the mean and variance of several essential climate variables were presented in the above paragraphs. We will now study in more detail, the temporal variability of the state-properties presented in an effort to detect fluctuations and/or changes in the biosphere-atmosphere-ocean system. We aim to decompose the observed variance into multi-period cycles and trends.

It has being recognized for a long time that the non-stationarity of climate obscures the accurate recognition of seasonal and yearly fluctuations. Seasonal and yearly climate fluctuations are a direct consequence of the radiative forcing on the hydrological cycle. It should be recalled that the hydrological cycle is a global process in nature. Seasonal variations in the top of the atmosphere radiance (incoming solar radiation) are due to the tilt of the Earth's polar axis and to the ellipticity of the earth's orbit. The variance in the maximum incident radiation on the Earth is estimated to vary seasonally by $\pm 3.5\%$ due to earth's elliptical orbit. The amplitude of seasonal variations in the incident radiation is estimated to change between $0 - 15\%$ in the 10^1-10^2 millennium time scale. Nevertheless, the annual

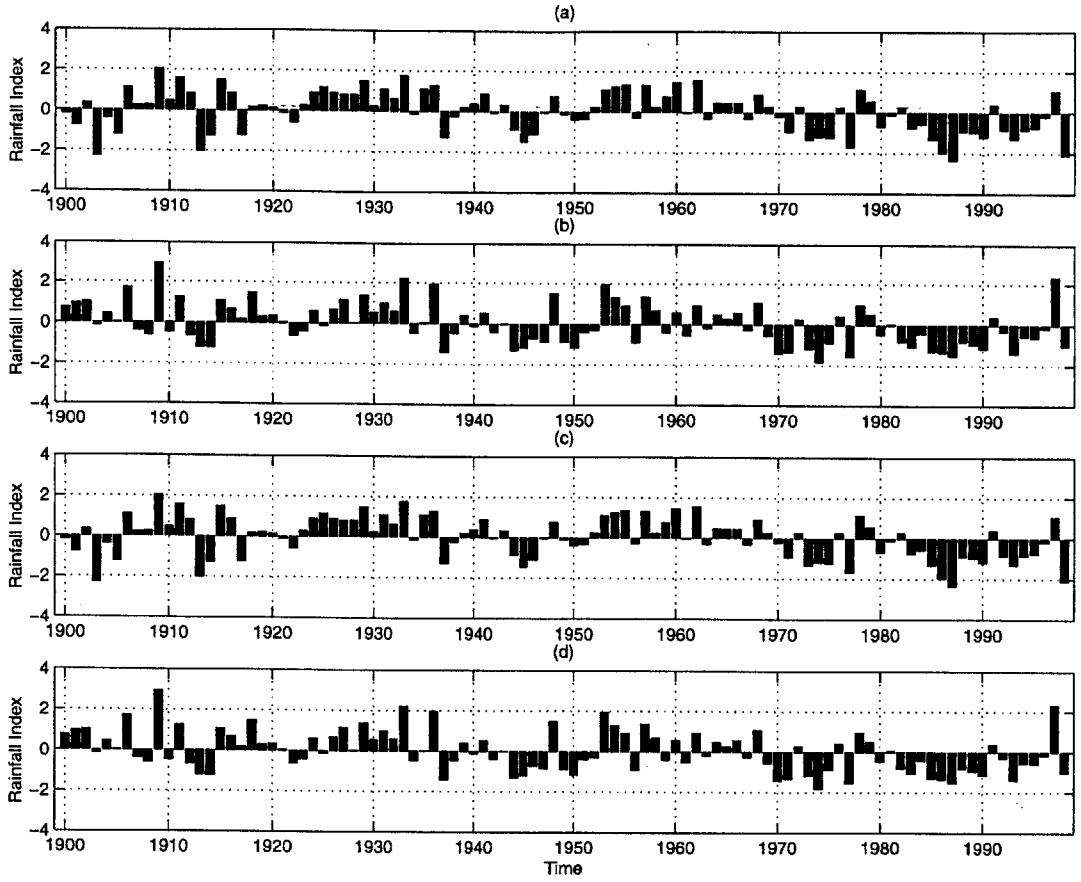

Figure 5-12: Normalized rainfall index [ ], for (a) spring, forest region, (b) spring, savanna region, (c) summer, forest region and (d) summer, savanna region.

integrated variation is very little (Gill 1982). However, it is less clear how the Earth system and its components (e.g. biosphere, atmosphere, and ocean) responds to variations in radiative forcing since there are non-linear internal processes at the same time. In this section, we aim to study the spring and summer seasons in higher detail to verify the proposed theory of biosphere-atmosphere-ocean interactions. Therefore, analysis of seasonal series of rainfall and moist static energy is presented to further study these interactions. First, we start by showing the net radiation seasonal cycle derived from the ISCCP-C2 data figure 5-9. The maximum net radiation occurs during austral summer over the South Eastern Tropical Atlantic (SETA). For latitudes above the Equator and below 10°N, the maximum net radiation occurs in early spring and late summer. Finally, the maximum net radiation for latitudes above 10°N occurs during northern summer. The net radiation components are presented in figures 5-10 and 5-11. The maximum net shortwave radiation over West Africa occurs during spring, while the maximum net longwave radiation occurs in late summer.

The difference between seasons can be appreciated in figures 5-13- 5-15. The establishment of the monsoon circulation during summer over land can be readily observed in figure 5-15 (c). The relative vorticity turns negative over land up to the troposphere. Furthermore, the location of the negative relative vorticity coincides with the maximum moist static energy and the low-level wind convergence (figures 5-13- 5-14). The maximum boundary layer moist static energy is located where the meridional gradient is zero and the meridional rate of change of this gradient is negative. This observations are consistent with the monsoon dynamics theory presented in Chapter 3.

5.3 Interannual Variability

Using a monthly time-scale allow us to study the integrated effects of boundary layer processes over the regional climate (e.g. gives enough time to reach a certain state in terms of dynamic equilibrium). As mentioned earlier, an additional advantage of using a monthly time scale is the fact that is long enough to avoid discontinuity in the record and short enough to detect changes in the medium and low frequencies.

Although clouds are very infrequent over desert regions, they have to be considered over

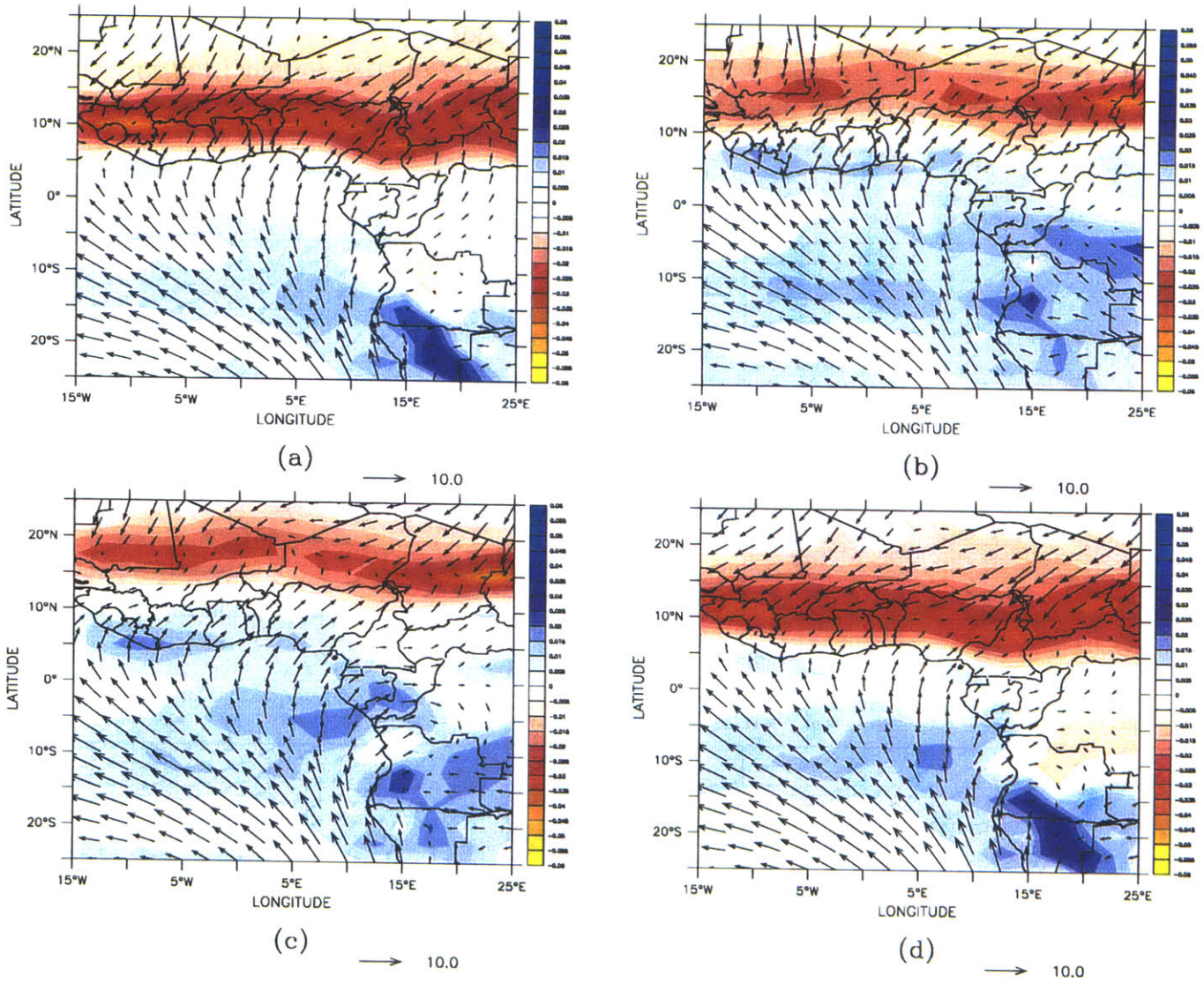

Figure 5-13: Meridional gradient of boundary layer moist static energy $[°C/km]$ and low-level wind $[m/s]$ over West Africa. 1958-97 Climatology for (a) Winter (b) Spring (c) Summer (d) Autumn

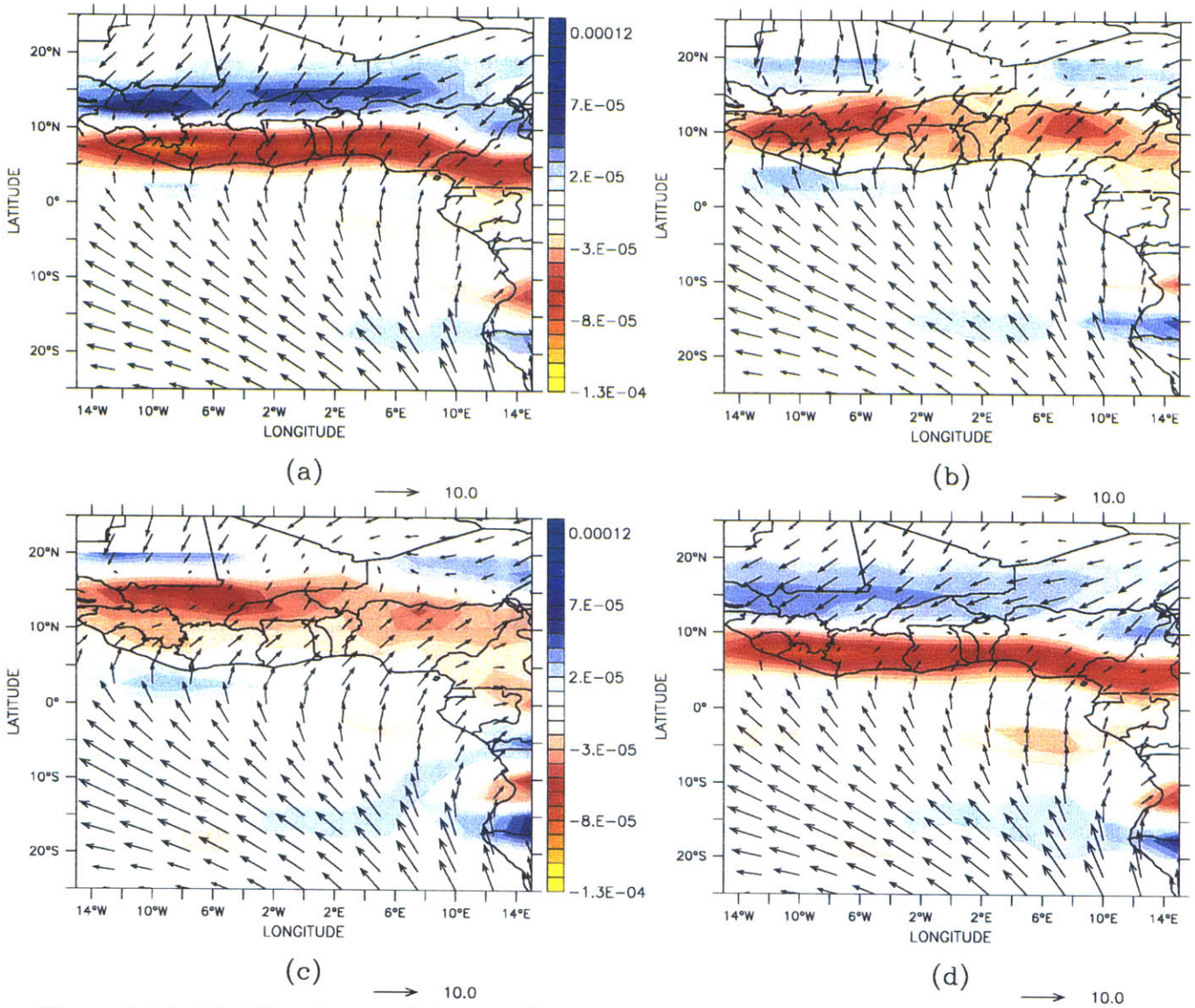

Figure 5-14: Meridional rate of change of meridional gradient of boundary layer moist static energy [$°C/km^2$] and low-level [m/s] wind over West Africa. 1958-97 Climatology for (a) Winter (b) Spring (c) Summer (d) Autumn

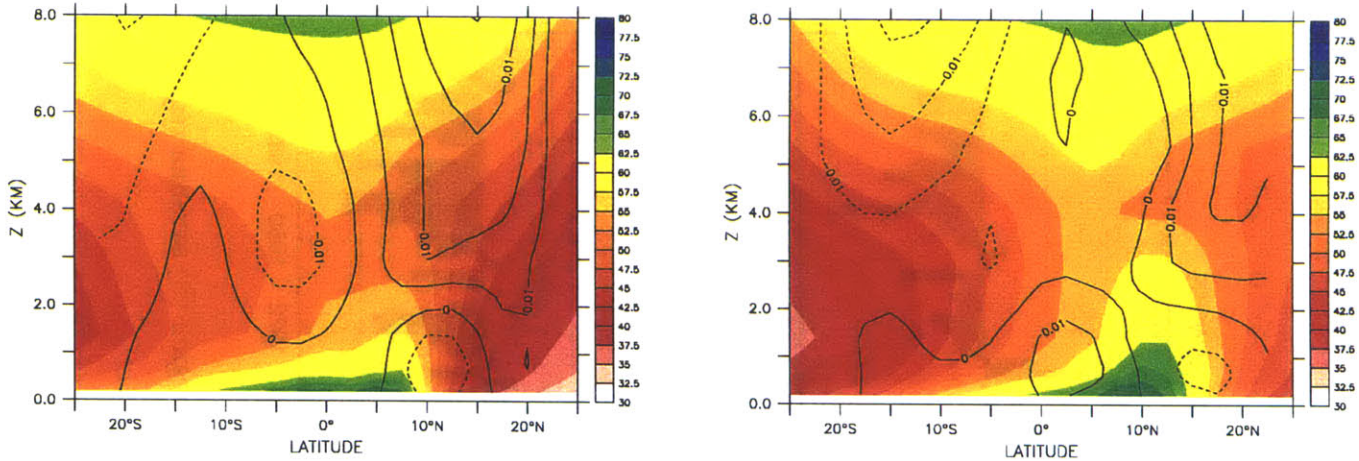

(a) JFM

(b) AMJ

(c) JAS

(d) OND

Figure 5-15: Zonally averaged boundary layer moist static energy [$°C$] and potential vorticity [$sec^{-1}x10^3$] over West Africa. 1958-97 Climatology for (a) Winter (b) Spring (c) Summer (d) Autumn

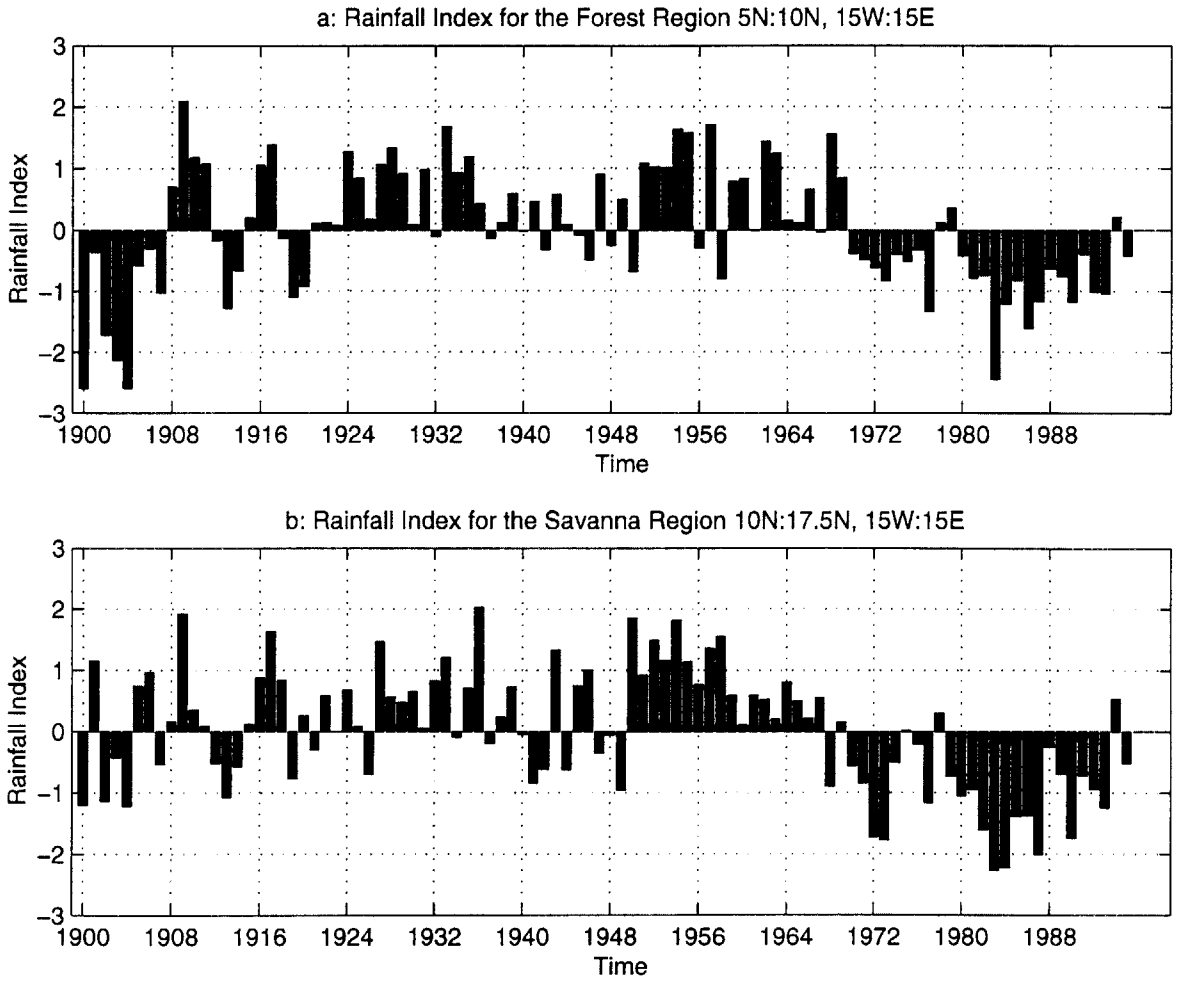

Figure 5-16: Normalized rainfall index [ ] for (a) forest region (b) savanna region

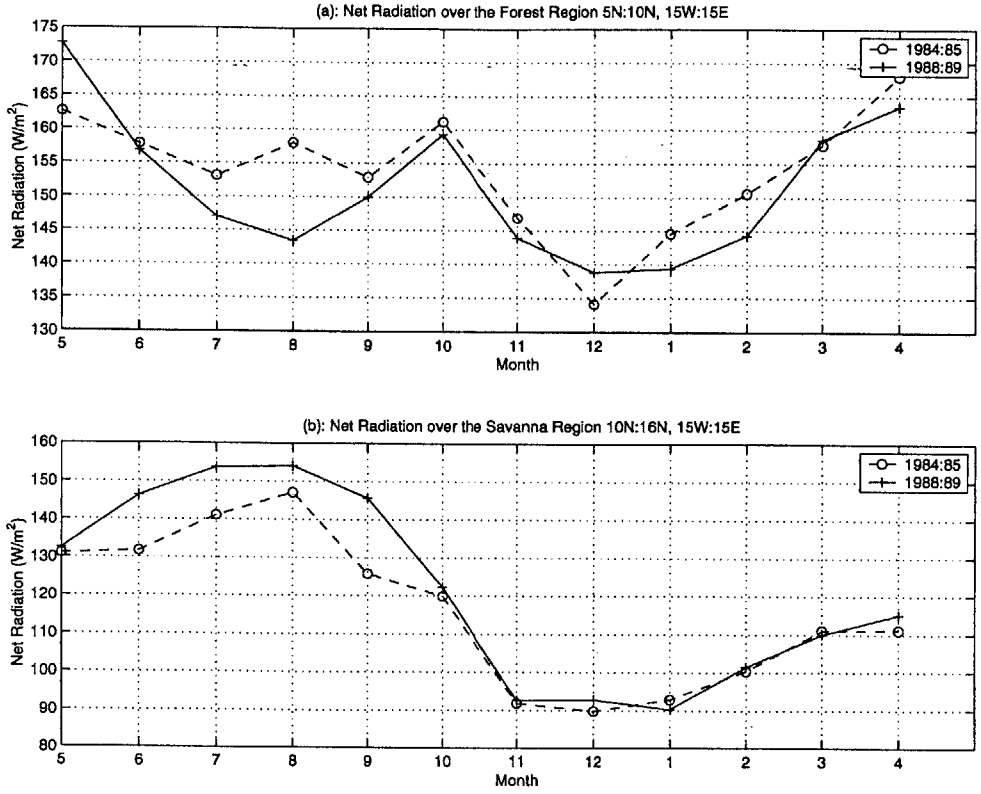

Figure 5-17: Time series of radiation components $[W/m^2]$ over (a) forest region (b) Sahel region

forest and semi-arid regions. The effect of clouds over the deforested regions would be to change the contributions of net long wave and net short wave radiation by canceling the albedo effect and enhancing the reduction of terrestrial radiation (Eltahir 1996). Therefore, the net radiation reduction would be mostly due to the net terrestrial radiation decrease. Still, we would get a net radiation reduction that must be balanced by a reduction in surface heat fluxes that would result in a decrease of BLMSE over land. Observations of radiation fluxes during the dry years of 1983-1991 are available from the International Satellite Cloud Climatology Project/Surface Radiation Budget study (ISCCP/SRB). In addition, the ISCCP/D2 study provides data of fractional cloud cover for the 1986-1993 period (see section 4.4 for a brief description of the datasets). Although there is no strong interannual variability, the difference between a relatively wet and a dry year is evident (figure 5.3). In 1988, the wettest year of that dry period, net radiation was ~20 W/m^2 higher than in the driest year of the covered period (1984). The inhibition of interannual variability could be explained as a result of the dry state persistence of the system. Modeling studies are required in order to verify the proposed mechanism, in particular to address the conditions prior to the onset of the drought. We would expect higher radiation fluxes in accordance to the observed higher moist static energy for the wet period of 1958-67 to satisfy energy balance considerations.

In order to eliminate the seasonal cycle and study in greater depth the relationship between energy and precipitation, we normalized the zonally-averaged moist static energy and precipitation field by substracting the monthly mean and dividing by the monthly variance. It is clear from figures 5-18 and 5-19, that there was a transition from wet conditions towards dry conditions during the late sixties. This conditions persisted during the whole year as it can be observed in the January and July zonally-averaged moist static energy anomaly shown in figures 5-21 and 5-20. The greatest change $[-10°C]$ occurred in the region between 10°N and 17.5°N. As presented in Chapter 2, this corresponds to the savanna region. On the other hand, the forest region $(5°N - 10°N)$ suffered a similar degradation during the dry-winter season.

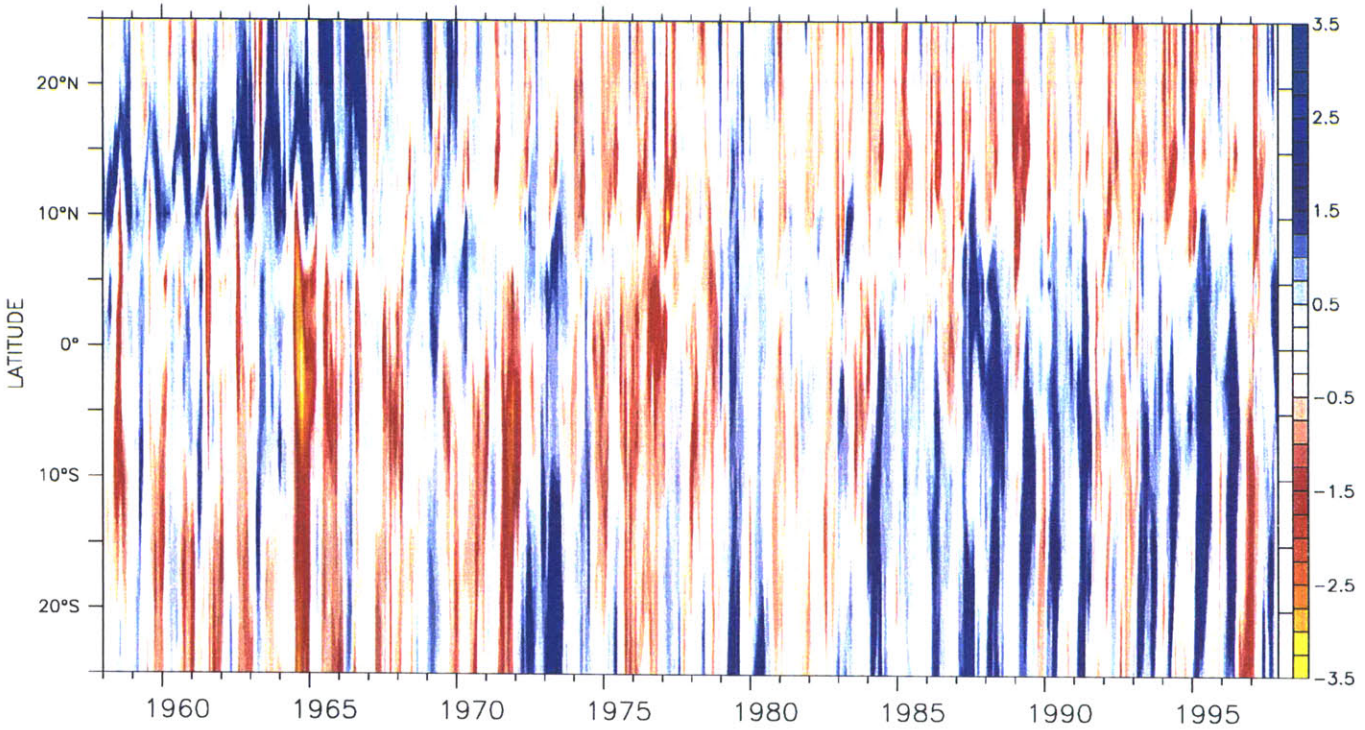

Figure 5-18: Normalized anomaly of moist static energy over the West African region [ ]. The values are zonally-averaged over the 15°W-15°E longitudes.

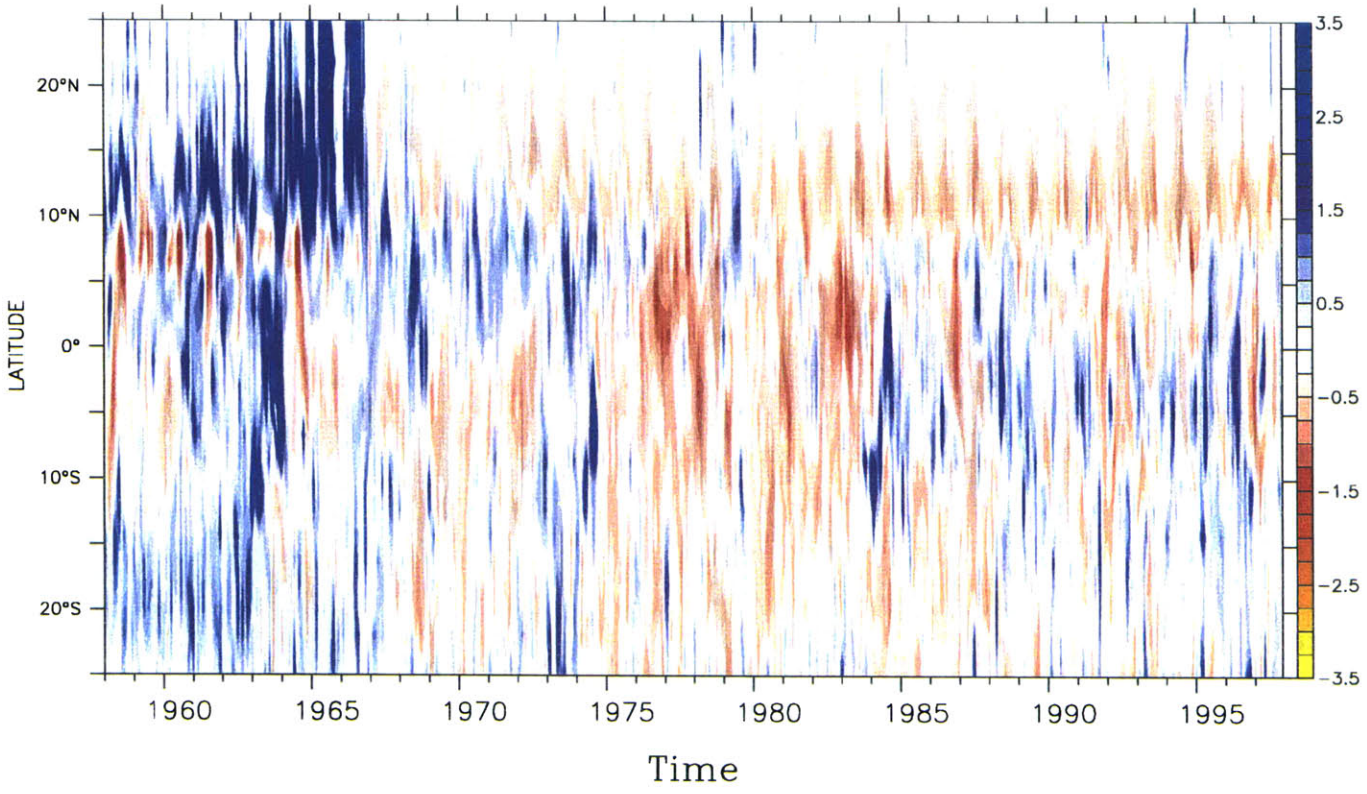

Figure 5-19: Normalized anomaly of precipitation over the West African region [ ]. The values are zonally-averaged over the 15°W-15°E longitudes.

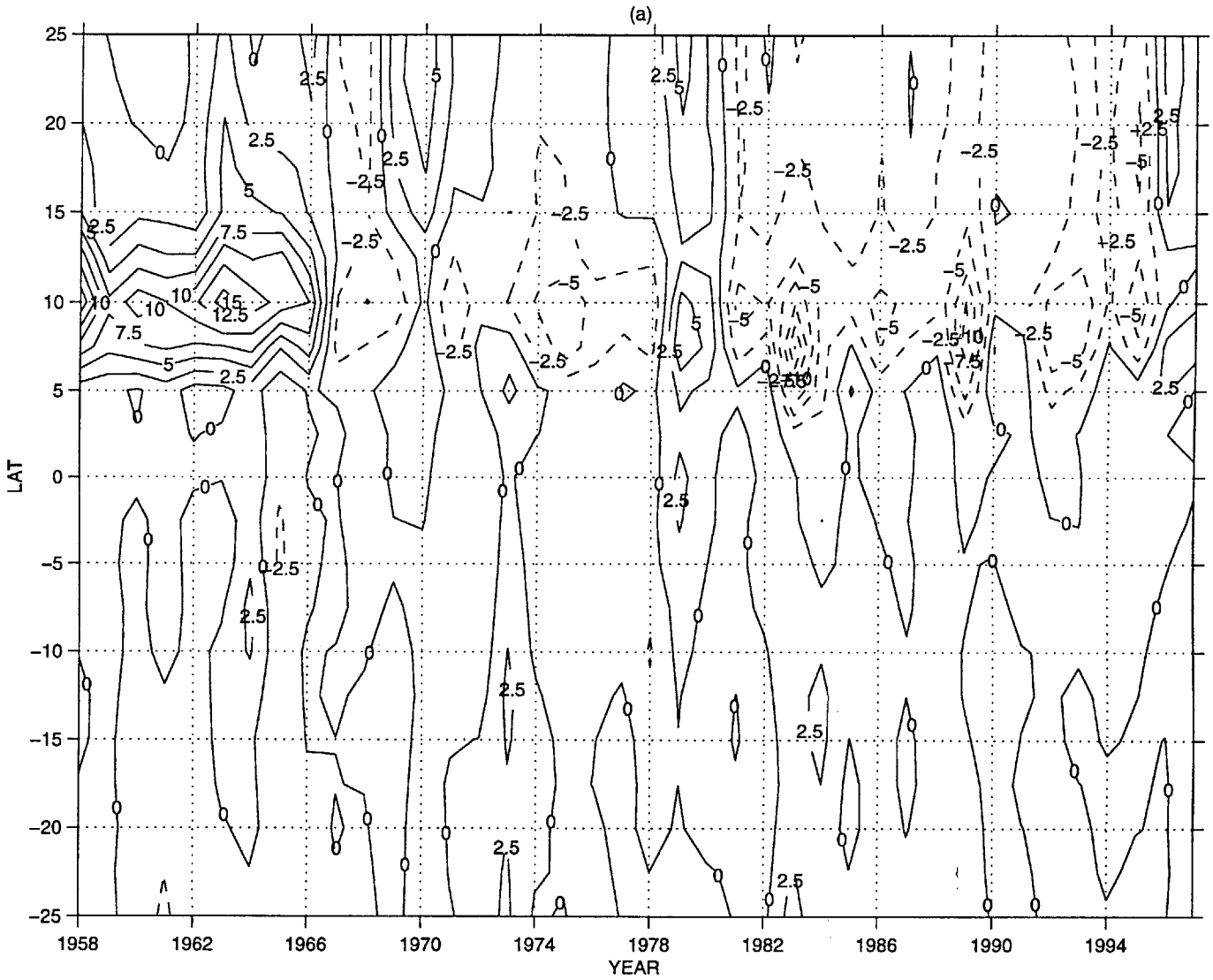

Figure 5-20: Zonally averaged moist static energy anomaly in the boundary layer [$^{\circ}C$] for (a) January (1958-97).

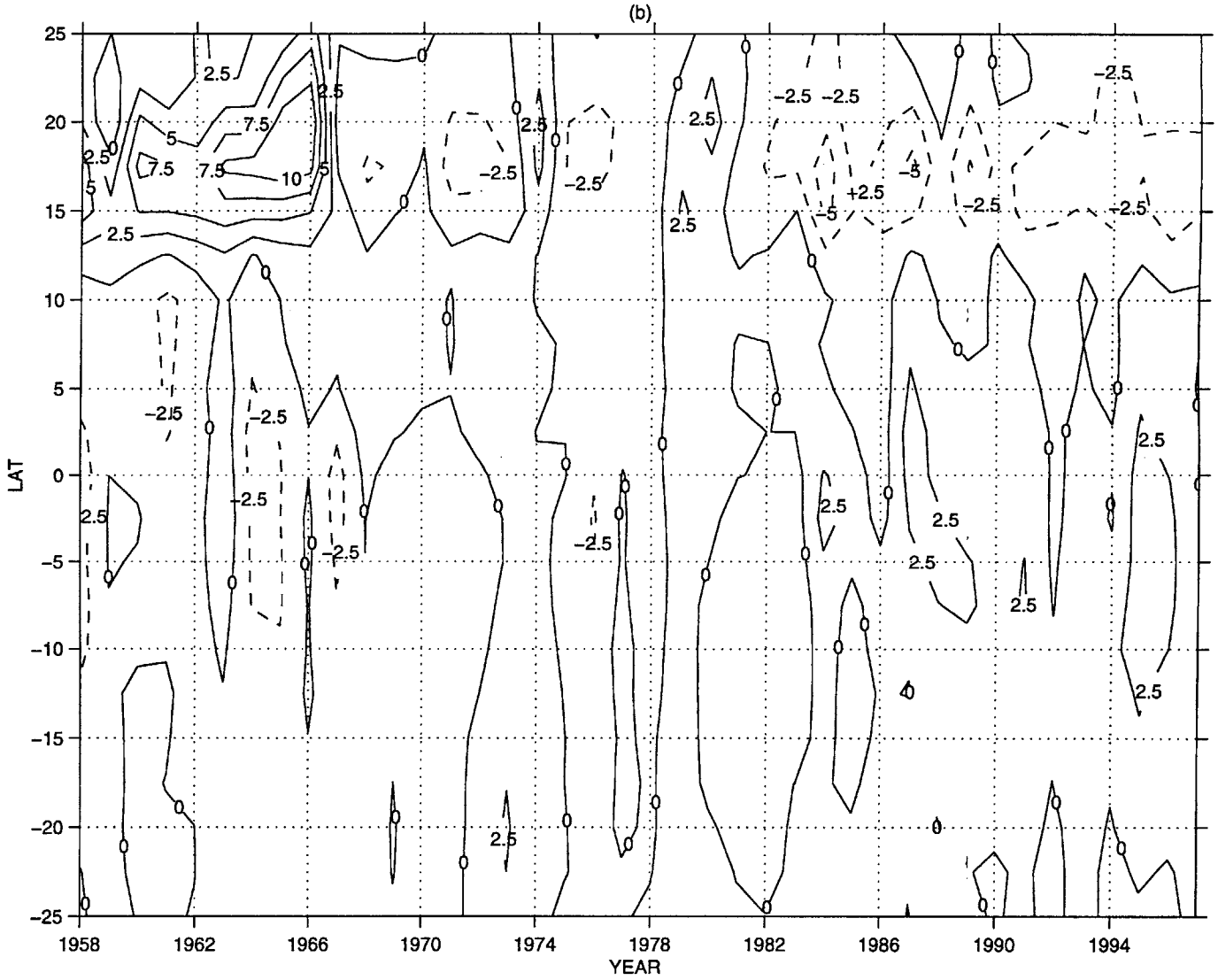

Figure 5-21: Zonally averaged moist static energy anomaly in the boundary layer [$°C$] for (b) July (1958-97).

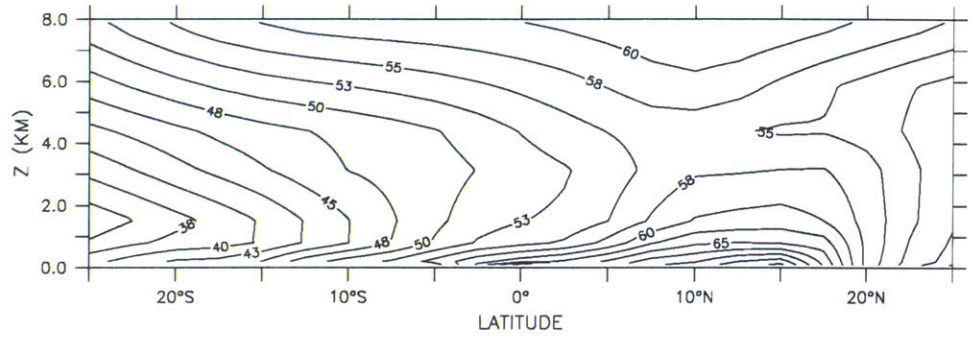

(a)

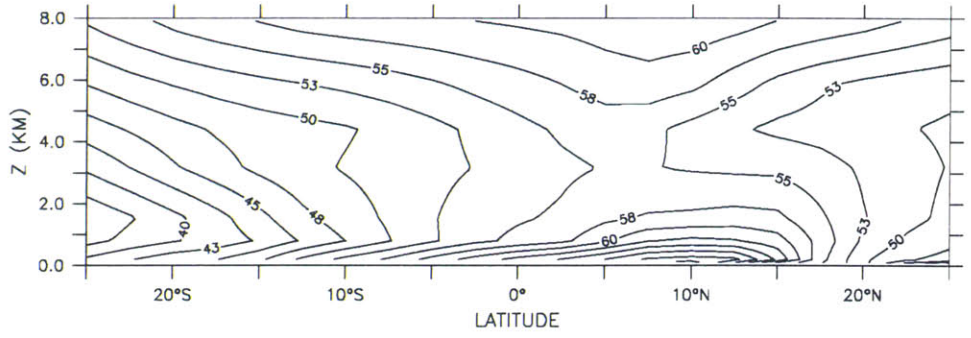

(b)

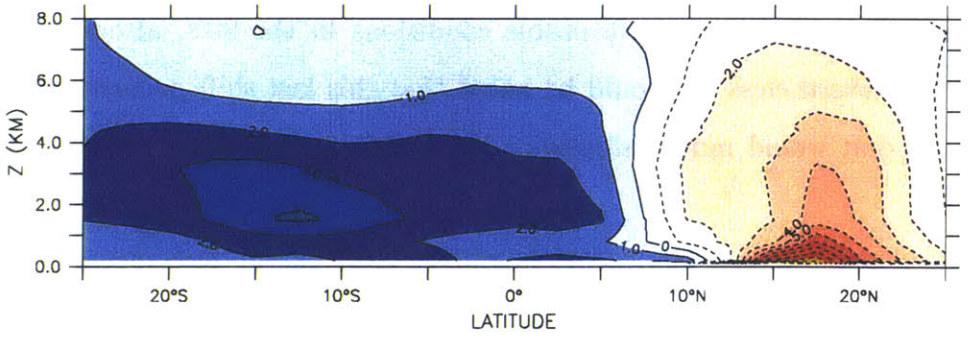

(c)

Figure 5-22: Zonally averaged moist static energy in the boundary layer [$°C$] for (a) wet period (1958-67) (b) dry period (1988-97) (c) difference.

5.4 Inter-decadal Variability

Boundary layer moist static energy (BLMSE) over land is lower during the dry decade of 1988-97 compared to the wet ten-year period of 1958-67 (figure 5-22). This is consistent with vegetation degradation between the two periods. It should be noticed that the decrease in BLMSE over the savanna region is larger than over forest, suggesting that summer distribution of boundary layer energy is more sensitive to vegetation degradation over that region. Another way of viewing this is that the forest-type vegetation has a stronger resilience than savanna-type vegetation in accordance to Wang and Eltahir (1999b).

The other mechanism regulating the meridional gradient of BLMSE is the pattern of SST distribution over the SETA Region. Sea surface temperature over the SETA region has become warmer in the last three decades (figure 5-23). Summer moist static energy over the ocean has actually increased when the wet and dry periods are compared, in support of a flatter gradient of boundary layer energy (figure 5-22). According to Lamb (1978a,b), relatively cold (warm) SST episodes in spring followed by relatively warm (cold) episodes in summer would favor dry (wet) states. This can be observed by plotting the normalized difference of summer and spring SST over the SETA region (figure 5-23). There was a clear shift between favorable conditions for a wet-state before the 70's to dry-state favorable conditions after the 70's, consistent with the onset of the drought. On the other hand, there was shift towards wet-state favorable conditions in the 90's, although the drought has continued. Nevertheless, it should be noted that this last shift occurred during a weak monsoon state that would indeed slowdown the northward advection of heat over the sea surface.

Therefore, a simultaneous increase in boundary layer energy over ocean and a decrease over land results in a flat meridional gradient of moist static energy in the boundary layer. In addition, the location of the maximum moist static energy is displaced southward. These conditions result in a weakening of the monsoon. Figures 5-26 to 5-29 show the boundary layer moist static energy meridional gradient and its meridional rate of change for the period before the drought and the difference between the dry and wet periods. The plots correspond to (a) winter (b) spring (c) summer and (d) autumn seasons. The location of the merid-

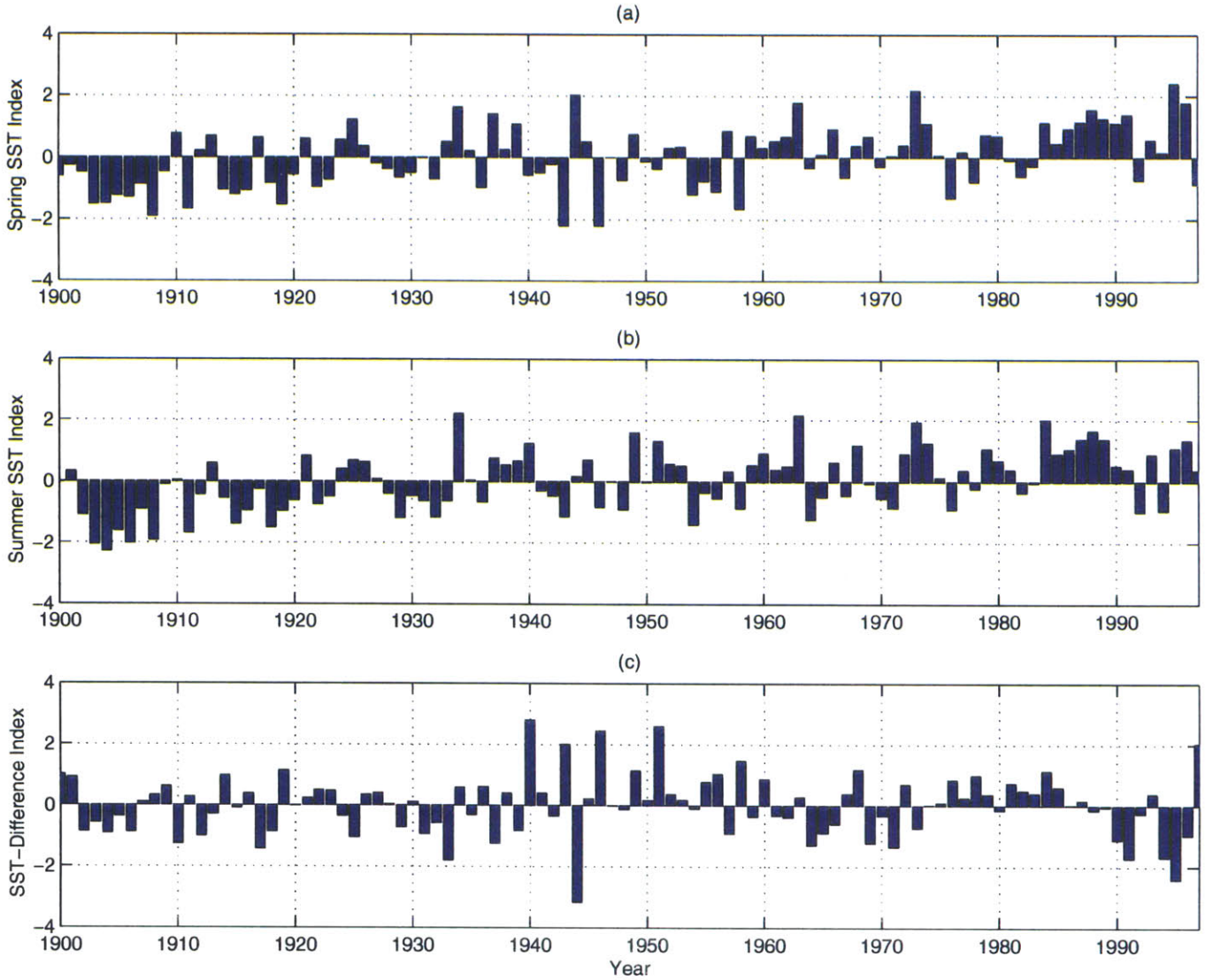

Figure 5-23: Normalized sea surface temperature [ ] over the SETA region for (a) Spring (AMJ), (b) Summer (JAS), and (c) difference between spring and summer.

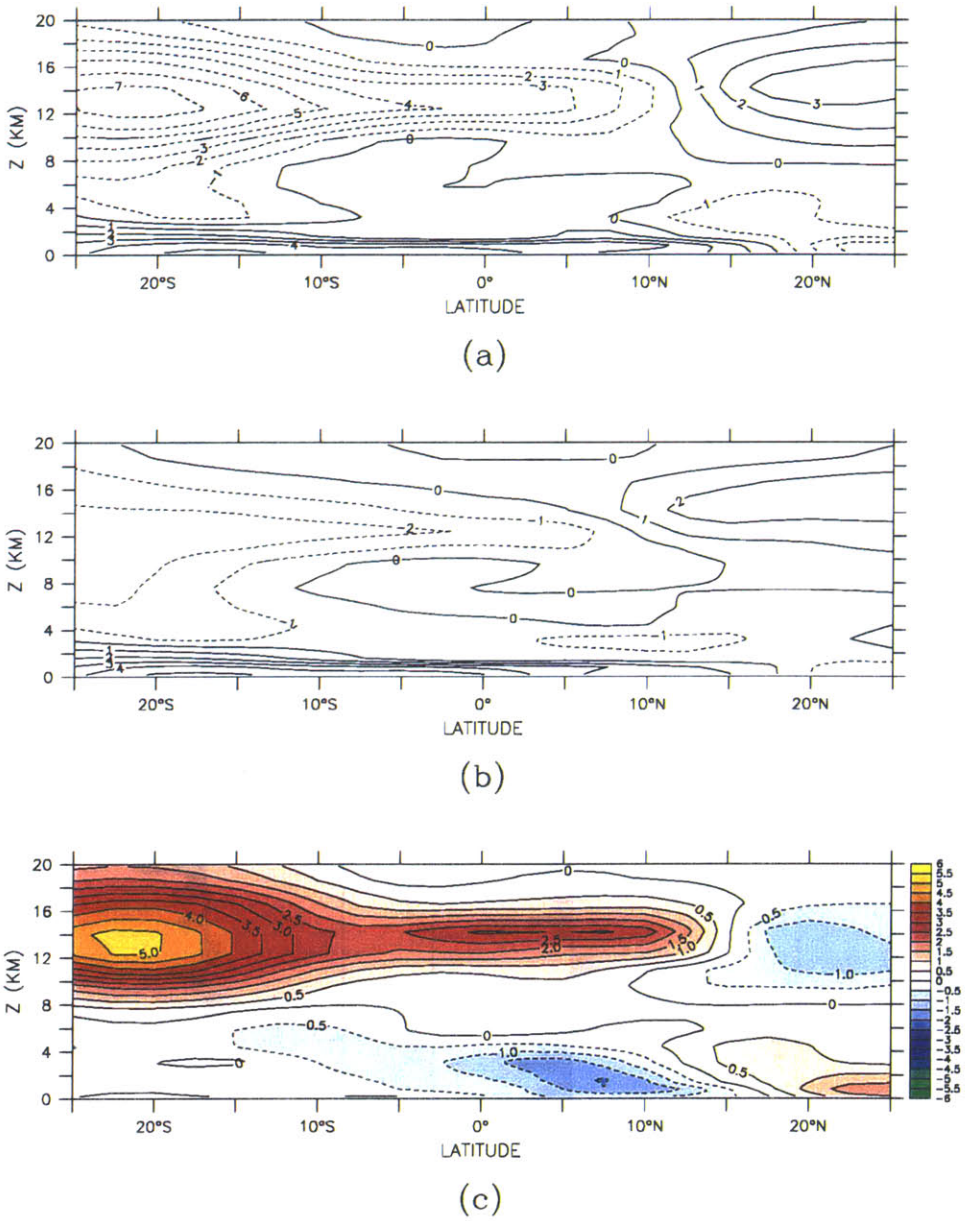

Figure 5-24: Meridional section of meridional wind $[m/s]$ for the (a) wet period (1958-67), (b) dry period (1988-97) and (c) difference between the two periods.

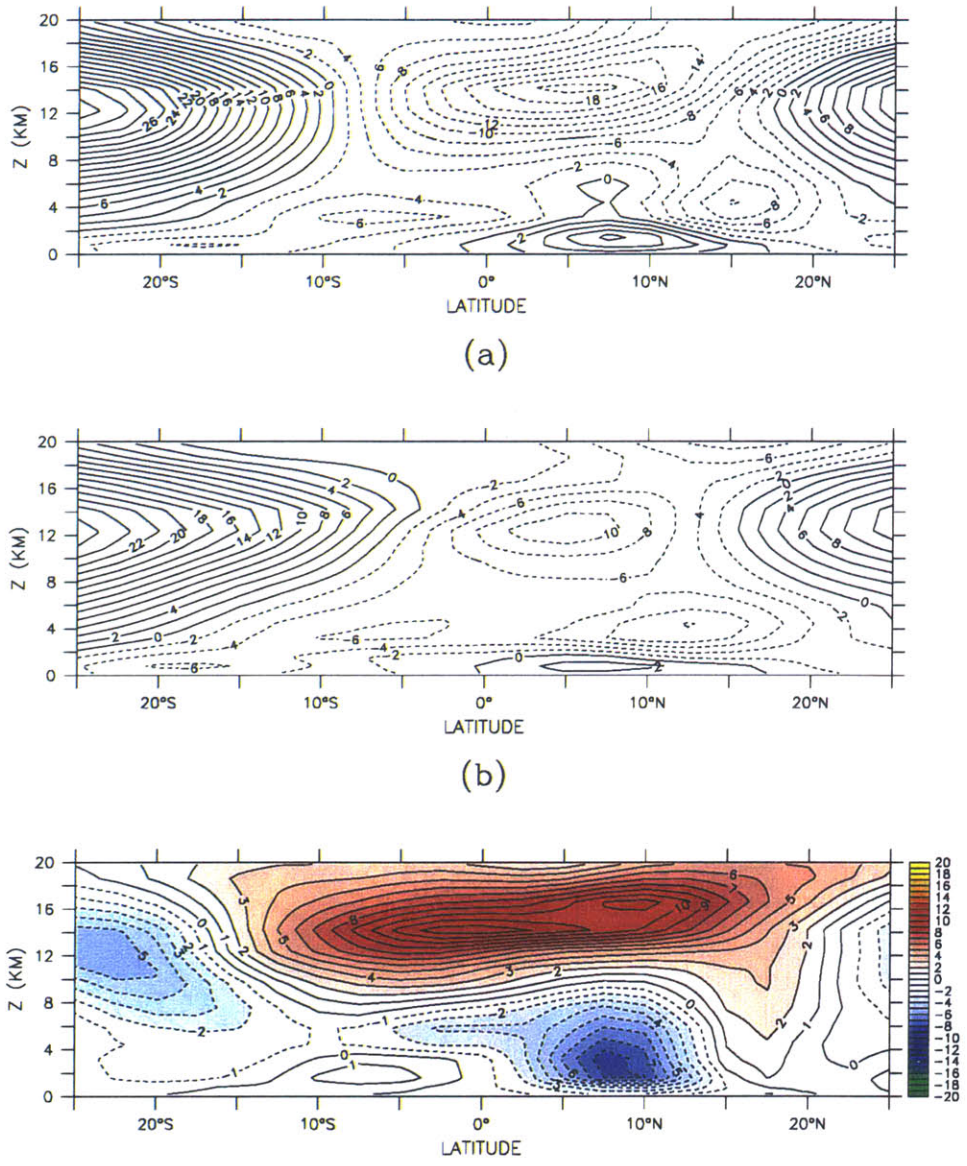

Figure 5-25: Meridional section of zonal wind $[m/s]$ for the (a) wet period (1958-67), (b) dry period (1988-97) and (c) difference between the two periods.
9in

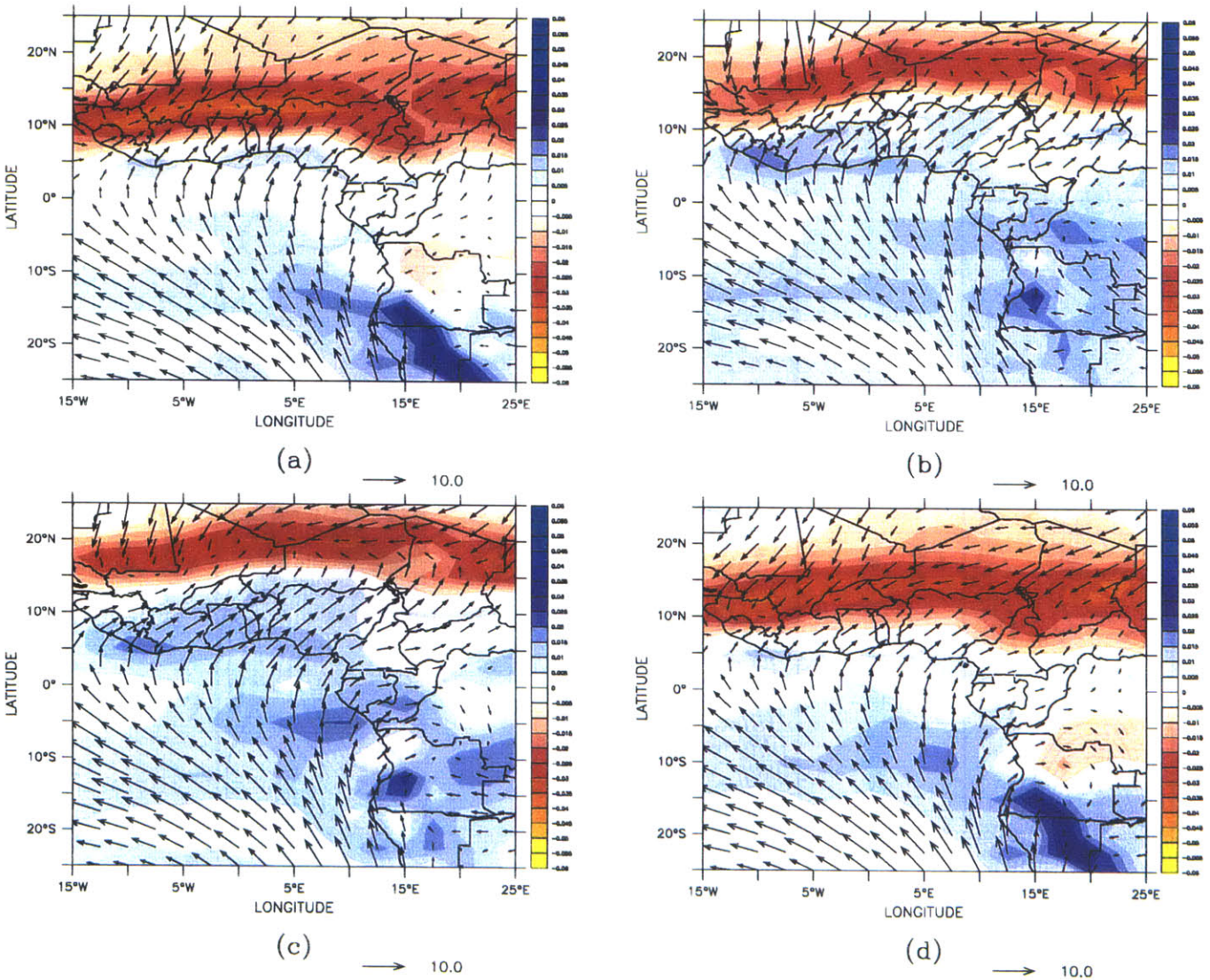

Figure 5-26: Meridional gradient of boundary layer moist static energy $[°C/km]$ and low-level wind $[m/s]$ over West Africa. Wet Period (1958-67) Climatology for (a) Winter (b) Spring (c) Summer(d) Autumn

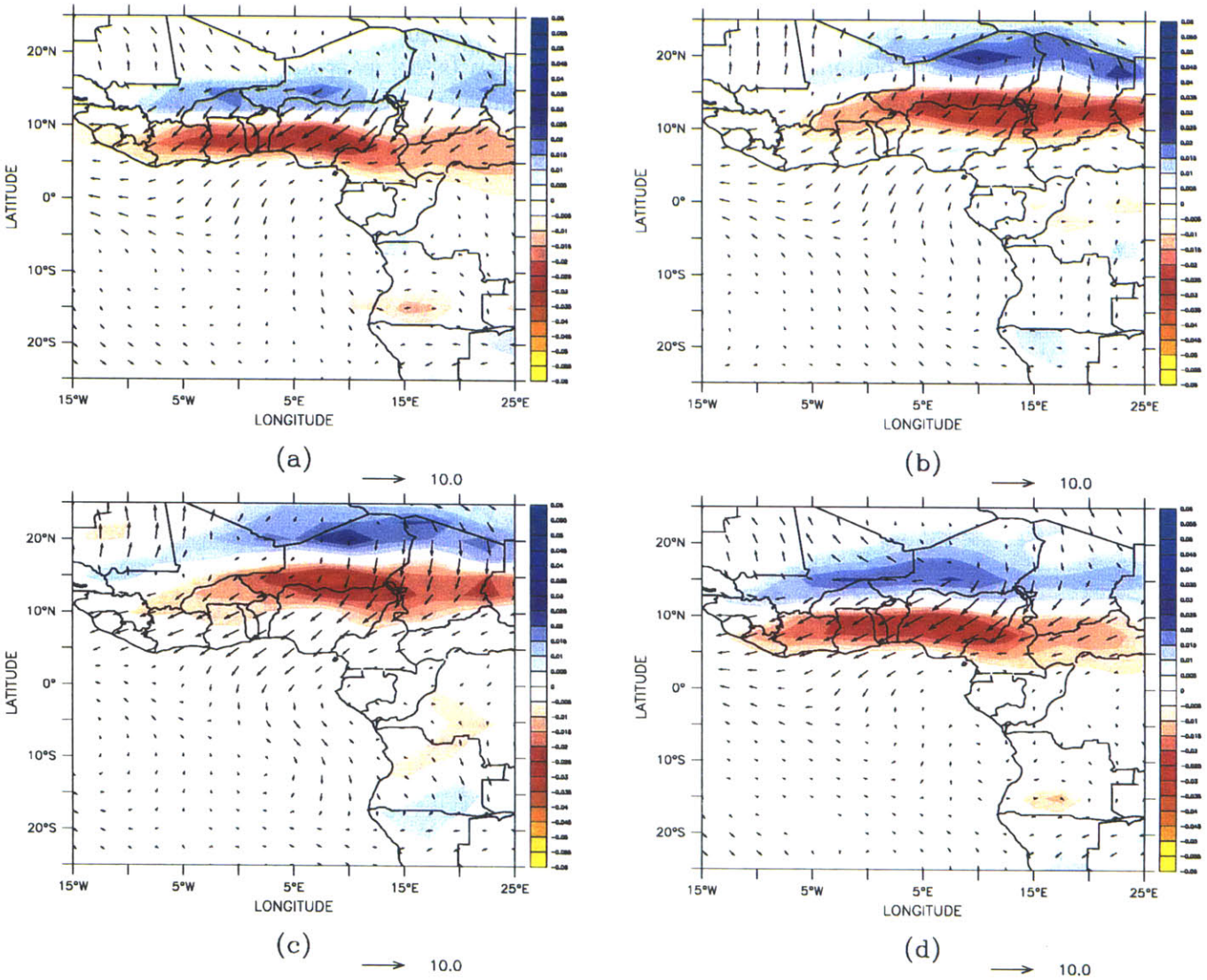

Figure 5-27: Meridional gradient of boundary layer moist static energy $[°C/km]$ and low-level wind $[m/s]$ over West Africa. Difference between dry period (1988-97) and wet period (1958-67) climatology for (a) Winter (b) Spring (c) Summer(d) Autumn

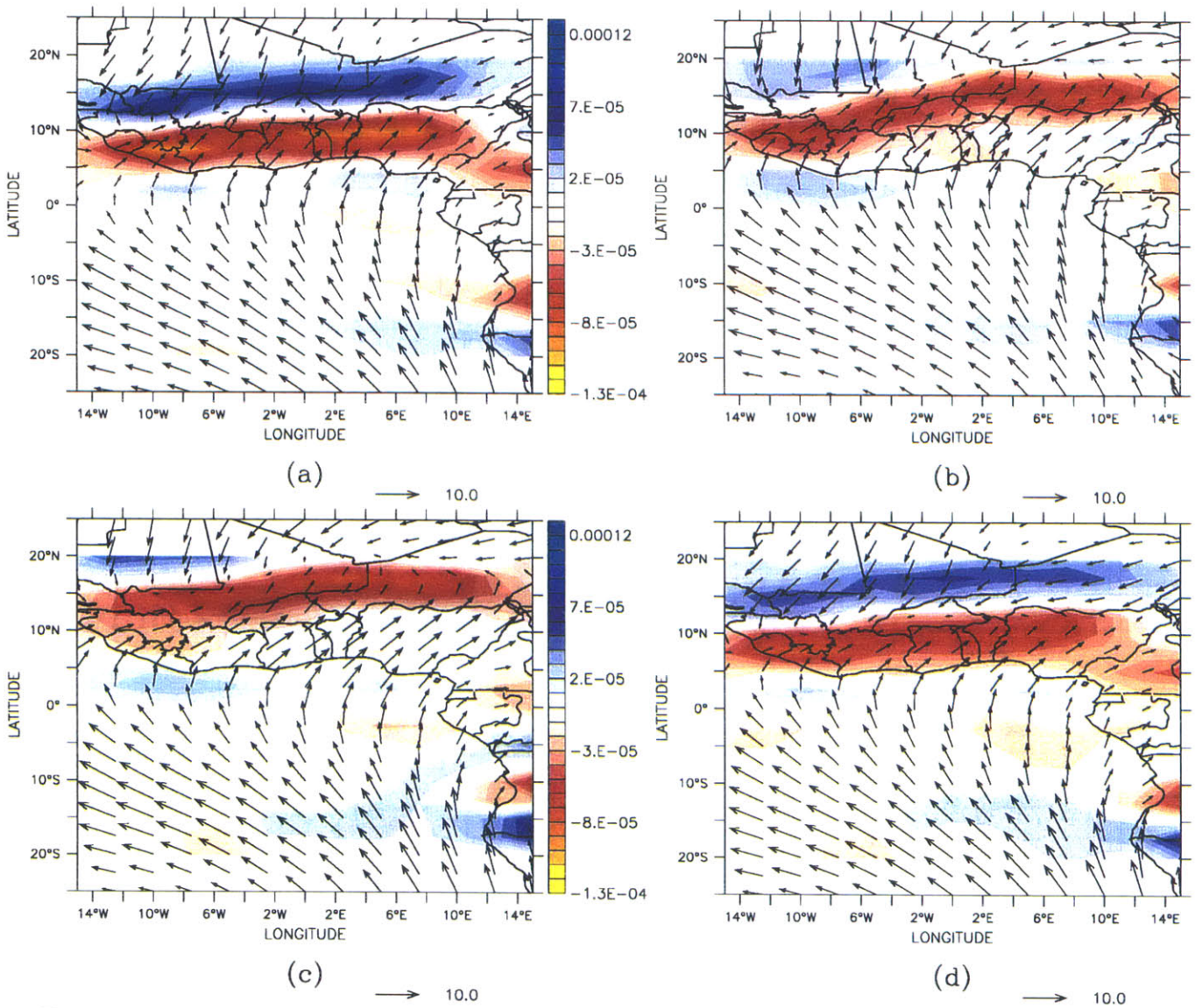

Figure 5-28: Meridional rate of change of meridional gradient of boundary layer moist static energy $[°C/km^2]$ and low-level $[m/s]$ wind over West Africa. Wet period (1958-67) climatology for (a) Winter (b) Spring (c) Summer (d) Autumn

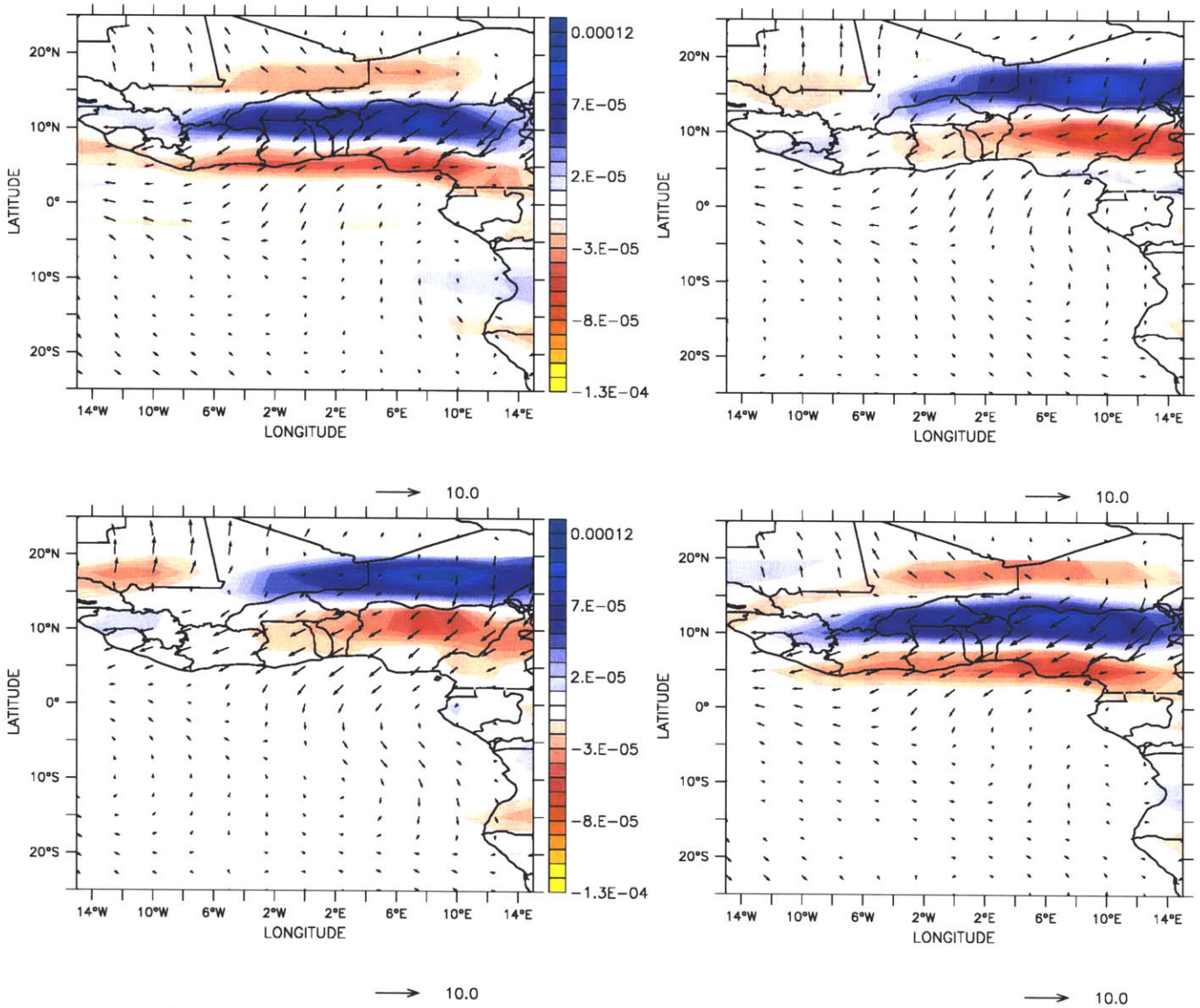

Figure 5-29: Meridional rate of change of meridional gradient of boundary layer moist static energy $[°C/km^2]$ and low-level $[m/s]$ wind over West Africa. Difference between dry period (1988-97) and wet period (1958-67) climatology for (a) Winter (b) Spring (c) Summer (d) Autumn

ional boundary layer MSE zero-gradient (and negative second derivative) shifted southward between the two periods. This is observed by the change of sign in the meridional gradient of boudary layer moist static energy. The Inter-Tropical Convergence Zone also shifted southward as expected from relations 3-10 and 3-11. This is observed in figure 5-29 by the southward pointing vectors of the low level winds. Similar observations of the meridional gradient of energy in the boundary layer and monsoon strength were reported by Eltahir and Gong (1996). They studied the inter-annual variability by comparing a relative wet year (1958) to a relative dry year (1960) before the onset of the current drought. Observations of meridional wind for the 1958-67 and 1988-97 periods show a decrease in magnitude (~1-2 m/s) of the low-level northward winds (figure 5-24). At the same time, there is a magnitude decrease (~2.5-5 m/s) in the southward winds in the mid-upper troposphere for the 1988-97 period. An interesting feature of the West African summer monsoon is the formation of the African Easterly Jet (AEJ) centered at 16°N and 650 hPa (~5 km) for the 1958-67 period. It can be observed that its center shifted southward by 3.5° and sank by ~0.5 km during the dry period (figure 5-25). In addition, the Tropical Easterly Jet (TEJ) is weaker by as much as 10.0 m/s during the dry period. The height of the TEJ decreased by approximately 1.5 km. Finally, the low-level westerlies over the Guinea Coast forest region (5°N-10°N) decreased by ~4.0 m/s. These observations are consistent with a weaker monsoon circulation between the two studied periods.

5.5 Summary

There is a strong meridional gradient of annual precipitation ranging from 2500 mm near the Guinea Coast to less than 200 mm over the Sahara (figure 5-8). Other important ecosystem variables show a strong meridional structure as well (figures 5-1 to 5-8), like surface air temperature, specific humidity and vegetation distribution. We were interested in relating these observed gradients in a comprehensive theory that considers the role of biosphere-atmosphere-ocean interactions in shaping the climate over the region.

In this chapter, we used the theoretical framework described in Chapter 3 to explain observations of different climate variables during the 1958-1997 period over West Africa and

the South Eastern Tropical Atlantic (SETA) region. According to the hypothesis presented, changes in surface conditions (land and ocean) have a significant impact over rainfall variability through several feedback mechanisms (see section 3.2). The origin of these changes could be either natural or anthropogenic, especially over land. Vegetation degradation over the tropical region induced a reduction of net radiation that must be balanced by a decrease of heat fluxes in the boundary layer (Eltahir 1996). This resulted in a reduction of Boundary Layer Moist Static Energy (BLMSE) over land promoting a flatter gradient of BLMSE between ocean and land. Although observations of vegetation cover, radiation and heat fluxes are scarce, there are long periods of frequent observations of temperature, humidity and geopotential height that were used to estimate the boundary layer energy over the region. This observations showed a decrease in boundary layer moist static energy between the period before the drought and after the drought. The maximum BLMSE was located by the zero-gradient and negative first derivative of the meridional gradient of boundary layer moist static energy. The location of the maximum BLMSE shifted southward between the two periods. This is consistent with a displacement of the Inter-Tropical Convergence Zone. The strenght of the monsoon circulation decreased between the two periods as verified by the decrease in speed of the zonal and meridional wind components.

Chapter 6

Summary and Conclusions

The meridional gradient of moist static energy in the boundary layer over ocean and land provides an important link in the biosphere-atmosphere-ocean system over West Africa. It constitutes the backbone of a general theoretical framework describing the role of biosphere-atmosphere-ocean interactions in shaping the regional climate. The energy distribution between land and ocean provides a physical mechanism to address rainfall variability in terms of three-way interactions of the biosphere-atmosphere-ocean system. Although sometimes scarce, observations of the period before and during the drought are consistent with the proposed theory. We performed an analysis of the inter-annual and intrannual variability of different climatic variables (e.g. moist static energy, wind, relative vorticity, precipitation, sea surface temperature and radiation components) that confirms the proposed physical theory of biosphere-atmosphere-ocean interactions. A wet state characterized the climate conditions up to the late 1960's. Higher than climatology rainfall has been reported from various studies for the period between 1958-67. Here we presented evidence of a stronger monsoon circulation during that same period. The monsoon circulation is a large-scale forcing for rainfall over the region. The theory presented by Eltahir and Gong (1996) related the monsoon circulation strength to the distribution of boundary layer energy between ocean and land. We showed here that the distribution of moist static energy in the boundary layer between ocean and land changed significantly between 1958-67 and 1988-97. A flatter meridional gradient of energy resulted from the increase in moist static energy over the South

Eastern Tropical Atlantic (SETA) region and a decrease of energy over land. These ocean conditions were not favorable for high precipitation rates. Such changes are consistent with increase SST over the Atlantic Ocean and vegetation degradation over West Africa. The changes in energy distribution resulted in a weaker monsoon circulation and a reduction in the frequency and magnitude of convective events is expected. The ocean conditions represented by the difference between summer and spring sea surface temperatures became favorable for high precipitation rates during the last decade of the 20^{th} century. On the other hand, the biosphere conditions remained unfavorable. This is consistent with the reduction in rainfall observed for the last thirty years. The persistence of the moist energy anomaly feedbacks into the biosphere-atmosphere-ocean system perpetuating the current dry climate condition.

The consistency between the physically based theory and observations is an encouraging factor to perform further studies of the biosphere-atmosphere-ocean system. In order to quantify the contributions of each climate component it is necessary to perform a sensitivity analysis. Since regional scale field experiments can be disregarded as technologically infeasible, scientists have turned their efforts towards numerical experiments. Recent advances in information technology and the previously mentioned progress in theoretical physics provide a fertile ground for the development of the hydroclimatology field. Future research includes sensitivity experiments on deforestation, desertification and sea surface temperature variations using a state of the art regional climate model. Recent enhancements on the large-scale precipitation scheme, sub-grid spatial variability and the surface-vegetation-atmosphere transfer scheme will be included in these future studies. Numerical modeling would be use to further study the proposed mechanisms in order to get insights of the causes of the drought.

Bibliography

Arkin and Xie 1994, The Global Precipitation Climatology Project: First Algorithm Intercomparison Project, *Bulletin of the American Meteorological Society*, American Meteorological Society, Volume 75

Barkstrom 1984, The Earth Radiation Budget Experiment (ERBE), *Bulletin of the American Meteorological Society*, American Meteorological Society, Volume 67

Chan 1998, The AVHHR Land Pathfinder One Degree Monthly Composite Global Data Set, *EOS Distributed Active Archive Center (DAAC)* NASA Goddard Space Flight Center, Maryland

Charney 1975, Dynamics of deserts and drought in the Sahel, *Quarterly Journal of the Royal Meteorological Society*, 101

Cook 1999, Generation of the African Easterly Jet and Its Role in Determining West African Precipitation, *Journal of Climate*, American Meteorological Society, Volume 12

Cunnington and Rowntree 1986, Simulations of the Saharan atmosphere-dependence on moisture and albedo, *Quarterly Journal of the Royal Meteorological Society*, 112

Deichmann 1996, African Population Database Documentation, *National Center for Geographic Information and Analysis*, University of California, Santa Barbara, California

Eischeid et al. 1991, A comprehensive precipitation data set for global land areas. US Department of Energy Report No. DOE/ER-69017T-H1, Washington DC

Emanuel 1994, Atmospheric Convection, Oxford University Press

Emanuel et al. 1994, On large-scale circulations in convecting atmospheres, *Quarterly Journal of the Royal Meteorological Society*, 120

Emanuel 1995, On Thermally Direct Circulations in Moist Atmospheres, *Journal of the Atmospheric Sciences*, American Meteorological Society, Volume 52, No. 9

Eltahir and Gong 1996, Dynamics of Wet and Dry Years in West Africa, *Journal of Climate*, American Meteorological Society, Volume 9

Eltahir 1998, A soil moisture-rainfall feedback mechanism, 1.Theory and observations, *Water Resources Research*, American Geophysical Union, Volume 34, No. 4

Folland et al. 1986, Sahel rainfall and worldwide sea temperatures, 1901-85, *Nature*, 320

Gill 1982, Atmosphere-Ocean Dynamics, Academic Press, San Diego, California

Gornitz 1985, A survey of anthropogenic vegetation changes in West Africa during the last century-Climate implications, *Climate Change*, No.7

Gupta et al. 1999, A Climatology of Surface Radiation Budget Derived from Satellite Data, *Journal of Climate*, American Meteorological Society, Volume 12

Hartmann 1994, Global Physical Climatology, Academic Press, San Diego, California

Higgins et al. 1996, Intercomparison of the NCEP/NCAR and the NASA/DAO Reanalysis (1985-1993), *NCEP Climate Prediction Center*, Boulder, Colorado

Holton 1992, An Introduction to Dynamic Meteorology, Academic Press, San Diego, California

Hulme 1997, A 1951-80 global land precipitation climatology for the evaluation of general circulation models, *Climate Dynamics*, Volume 7

Hulme and New 1997, Dependence of Large-Scale Precipitation Climatologies on Temporal and Spatial Sampling, *Journal of Climate*, American Meteorological Society, Volume 10

Janowiak et al. 1998, A Comparison of the NCEP-NCAR Reanalysis Precipitation and the GPCP Rain Gauge-Satellite Combined Dataset with Observational Error Considerations, *Journal of Climate*, American Meteorological Society, Volume 11

Jenne 1999, Data Counts of NCEP Data from GTS (and other datasets), 1962-98, *NCAR Scientific Computing Division*, Boulder, Colorado

Kalnay et al. 1996, The NCEP/NCAR 40-Year Reanalysis Project, *Bulletin of the American Meteorological Society*, American Meteorological Society, Volume 77, No. 3

Lamb 1978a, Case studies of tropical Atlantic surface circulation patterns during recent sub-Saharan weather anomalies: 1967 and 1958, *Monthly Weather Review*, 106

Lamb 1978b, Large-scale tropical Atlantic surface circulation patterns associated with sub-Saharan weather anomalies, *Tellus*, 30

Lebel and Amani 1999, Rainfall Estimation in the Sahel: What is the Ground Truth?, *Journal of Applied Meteorology*, American Meteorological Society, Volume 38

Lough 1986, Tropical sea surface temperature and rainfall variations in sub-Saharan Africa, *Monthly Weather Review*, 114

Nicholson 1989, African Drought: Characteristics, Casual Theories and Global Teleconnections, *Geophysical Monogram 52*, American Geophysical Union, IUGG Volume 7

Nicholson 1994, Century-scale series of standardized annual departures of African rainfall, Pp.952-962, In T.A. Boden, D.P. Kaiser, R.J. Sepanski, and F.W. Stoss, *Trends '93: A Compendium of Data on Global Change*, ORNL/CDIAC-65. Oak Ridge, Tennessee

Parker et al. 1995, The 1961-1990 GISST2.2 Sea Surface Temperature and Sea-Ice Climatology, *Hadley Centre for Climate Prediction and Research*, United Kingdom Meteorological Office, London

Phillips 1995, Reanalysis Model status as of Jan. 10, 1995., ftp: // wesley.wwb.noaa.gov / pub / reanal / random_notes / model

Rayner et al. 1996, Version 2.2 of the Global sea-Ice and Sea Surface Temperature data set, 1903-1994, *Hadley Centre for Climate Prediction and Research*, United Kingdom Meteorological Office, London

Rossow et al. 1991, International Satellite Cloud Climatology Project (ISCCP) Documentation of Cloud Data, *World Meteorological Organization* New York

Rossow and Schiffer 1999, Advances in Understanding Clouds from ISCCP, *Bulletin of the American Meteorological Society*, American Meteorological Society, Volume 80

Rossow and Walker 1991, International Satellite Cloud Climatology Project (ISCCP) Description of Monthly Mean Cloud Data (Stage C2), *World Meteorological Organization*, New York

Stull 1999, An Introduction to boundary layer meteorology, Kluwer Academic Publishers, Massachusetts

Trenberth and Guillemot 1998, Evaluation of the atmospheric moisture and hydrological cycle in the NCEP/NCAR reanalyses, *Climate Dynamics*, Volume 14, Issue 3

Wallace and Hobbs 1977, Atmospheric Science: An Introductory Survey, Academic Press, Orlando, Florida

Wang and Eltahir 1999a, Biosphere-Atmosphere interactions over West Africa: 1.Development and validation of a coupled dynamic model, *Quarterly Journal of the Royal Meteorological Society* (accepted)

bibitemimpj Wang and Eltahir 1999b, The role of vegetation dynamics in enhancing the low-frequency variability of the Sahel rainfall, *Water Resources Research*, American Geophysical Union

Zheng and Eltahir 1997, The response to deforestation and desertification in a model of West African monsoons, *Geophysical Research Letters*, Volume 24, No.2

Zheng and Eltahir 1998a, A soil moisture-rainfall feedback mechanism, 2.Numerical experiments, *Water Resources Research*, American Geophysical Union, Volume 34, No. 4

Zheng and Eltahir 1998b, The Role of Vegetation in the Dynamics of West African Monsoons, *Journal of Climate*, American Meteorological Society, Volume 11

Zheng et al. 1999, A mechanism relating tropical Atlantic spring sea surface temperature and west African rainfall, *Quarterly Journal of the Royal Meteorological Society*, 125